AMBIDENTATE SALICYLALDIMINES N-(3-AMINOPROPYL) MORPHOLINE: COORDINATION BEHAVIOUR TOWARDS COPPER, NICKEL AND ZINC DIVALENT IONS AND BIOLOGICAL APPLICATIONS.

NURUL AZIMAH BINTI IKMAL HISHAM

FACULTY OF SCIENCE
UNIVERSITY OF MALAYA
KUALA LUMPUR

2013

AMBIDENTATE SALICYLALDIMINES N-(3-AMINOPROPYL) MORPHOLINE: COORDINATION BEHAVIOUR TOWARDS COPPER, NICKEL AND ZINC DIVALENT IONS AND BIOLOGICAL APPLICATIONS.

NURUL AZIMAH BINTI IKMAL HISHAM

DISSERTATION SUBMITTED IN FULFILLMENT OF
THE REQUIREMENT FOR THE DEGREE OF
MASTER OF SCIENCE

DEPARTMENT OF CHEMISTRY
FACULTY OF SCIENCE
UNIVERSITY OF MALAYA
KUALA LUMPUR

2013

Abstract

Two flexidentate Schiff-base ligands condensed from salicylaldehyde or 5-chlorosalicylaldehyde with N-(3-aminopropyl)morpholine were prepared *in situ* and reacted with zinc(II), copper(II) and nickel(II) salts. These compounds were characterised by elemental analyses and various physico-chemical techniques. Single crystal X-ray analyses were carried out on nine different complexes. Upon complexation, the Schiff bases underwent deprotonation at the hydroxyl to act as mono-anionic ligands. When a ligand:metal ratio of 2:1 was applied, the deprotonated Schiff bases coordinated metal ions through phenolate and imine groups in a square-planar or tetrahedral geometry. In contrast, 5-chlorosalicylaldimine reacted with the metal ions in a 1:1 ratio to form complexes wherein morpholine nitrogen also participates in an *N,N,O*-tridentate coordination mode. The structures of the complexes were characterized by spectroscopic methods and single crystal X-ray diffraction.

The Schiff bases and their metal complexes were evaluated for cytotoxic and antioxidant activity. Cytotoxic screening was carried out against human breast cancer cells with positive estrogen receptor (MCF-7), human breast cancer cells with negative estrogen receptor (MDA-MB-231), and colon cancer cell line (HT-29). This cytotoxicity also was tested on two normal cells, normal liver cells (WRL-68) and normal colon cell lines (CCD-841). The Schiff bases L^1H, was found to be very active against breast cancer with positive estrogen receptor cells and also colon cancer cells with the lowest IC_{50} values. Antioxidant screening was carried out by using ferric reducing antioxidant power (FRAP) assay. All compounds were found to have low activity except for L^1H ligand with FRAP value higher than the standard BTH and Trolox.

Abstrak

Dua bes Schiff ligan fleksibel yang disintesiskan daripada kondensasi di antara salisilaldehid atau 5-klorosalisilaldehid dengan N-morfolina(3-aminopropil) telah disediakan secara *in situ* dan bertindak balas dengan garam zink(II), kuprum(II) dan nikel(II). Semua sampel telah dicirikan dengan menggunakan pelbagai teknik kimia-fizik. Analisis sinar-X telah berjaya dilakukan terhadap sembilan kompleks hablur tunggal yang berbeza. Kompleks bes Schiff terhasil dengan pendeprotonan kumpulan hidroksil dan bertindak sebagai ligan mono-anionik. Apabila nisbah ligan:logam 2:1 digunakan, bes Schiff ternyah proton akan berkoordinat dengan ion logam melalui fenolat dan imina dan mempunyai geometri empat segi satah atau geometri tetrahedron. Sebaliknya, kompleks 5-klorosalisilaldehid bertindak balas dengan ion logam dengan nisbah 1:1, nitrogen morfolin akan mengambil bahagian berkoordinat melalui kaedah *N,N,O*. Struktur kompleks dicirikan menggunakan kaedah spektroskopi dan analisis sinar-X.

Bes Schiff dan kompleks logam masing-masing telah diuji untuk menilai aktiviti sitotoksik dan anti-oksida. Analisis sitotoksik telah dilakukan ke atas beberapa jenis sel barah iaitu sel barah payu dara manusia dengan penerima estrogen positif (MCF-7), sel barah payu dara manusia dengan penerima estrogen negatif (MDA-MB-231) and sel barah kolon (HT-29). Analisis sitotoksik ini juga telah diuji ke atas dua sel normal iaitu sel hati (WRL-68) dan sel kolon (CCD-841). Terdapat satu bes Schiff L^1H yang sangat aktif terhadap sel barah payu dara dengan penerima estrogen positif dan juga sel kanser kolon dengan nilai IC_{50} yang terendah. Saringan kereaktifan antioksida telah dijalankan dengan menggunakan keadah kuasa antioksida penurunan ferik (FRAP). Semua sebatian didapati mempunyai aktiviti yang rendah kecuali bagi ligan L^1H yang mempunyai nilai FRAP lebih tinggi daripada BTH and Trolox.

Acknowledgement

First of all, I would like to convey my sincere appreciation to my helpful supervisor, Professor Dr. Hapipah Mohd Ali for her guidance and encouragement throughout my research. Without her supervision, constructive idea and comment, this research would not be able to be completed. Second, special thanks to Dr Hamid Khaledi, for his assistance in solving the crystal structures of my compounds.

I would like to express my gratefulness also to my research collaborators, Prof. Dr. Mahmood Ameen Abdulla Hassan and his fellow researchers (Pouya), who unconditionally helped in conducting the biological activity for my compounds. My thanks are also extended to all my friends who are under Prof. Hapipah supervision for their support and to all staff and laboratory technician of Chemistry Department, Faculty of Science, University of Malaya.

My appreciation is also extended to my parents, all my families and friends for their unconditional support and continuous encouragement for me to finish my studies. I would also like to thank Mr. Mehran for his help in the preparation process of this thesis and motivation. Finally, I would like to convey my gratefulness to University of Malaya for the approved of graduate research assistantship scheme. This study was funded by University of Malaya research grants ER009/2011A and HIR-UM-MOHE:F000009-21001 (Prof Hapipah and Late Datuk Hamid).

TABLE OF CONTENTS

Content **Page**

LIST OF FIGURES

LIST OF TABLES

LIST OF SCHEMES

ABBREVIATIONS

°	Bond angles
Å	Angstrom
δ	Chemical shift in ppm
μM	Micromolar
ν	Wavenumber
B.Subtilis	*Bacillus subtilis*
C. albicans	*Candida albicans*
CAT	Catalase
CCD-841	Normal colon cells
CHN	Elemental analysis
CHNS	Carbon, Hydrogen, Nitrogen, Sulphur
$Cu(CH_3COO)_2 \cdot H_2O$	Copper(II) acetate monohydrate
$CuCl_2.2H_2O$	Copper(II) chloride dehydrate
DMSO	Dimethyl sulphoxide
DMSO-d_6	Deuterated DMSO
DNA	Deoxyribonucleic acid
DPPH	2,2-diphenyl-1-picrylhydrazyl free radical
E. coli	*Escherichia coli*
EAC	*Ehrlich ascites carcinoma*
FRAP	Ferric Reducing Antioxidant Power
FT-IR	Fourier Transform-Infrared
GPx	Glutathione peroxidase enzyme
H_2O_2	Hydrogen peroxide
HT-29	Human colon adenocarcinoma cells
IC_{50}	Half maximal inhibitory concentration
JURKAT	Leukaemia cell line

K_3 [Fe $(CN)_6$]	Potassium ferricyanide
KBr	Potassium bromide
L^1H	(E)-2-((3-morpholinopropylimino)methyl)phenol
L^2H	(E)-4-chloro-2-((3-morpholinopropylimino)methyl)phenol
LMCT	Ligand to metal charge transfer
LNCaP	Prostate cancer cells
M	Micro molar
MCF-7	Human breast cancer cells with positive estrogen receptor
MDA-MB-231	Human breast cancer cells with negative estrogen receptor
MTT	3-(4,5-dimethylthiazol-2-yl)-2,5-diphenyl tetrazolium bromide
N, S, O	Nitrogen, Sulphur, Oxygen
NaOH	Sodium hydroxide
$Ni(CH_3COO)_2 \cdot 4H_2O$	Nickel(II) acetate tetrahydrate
$NiCl_2$	Nickel(II) chloride
NMR	Nuclear Magnetic Resonance
P. fluorescens	*Pseudomonas fluorescens*
ppm	Part per million
quin	Quintet
S. aureus	*Staphylococcus aureus*
SOD	Superoxide dismutase
THF	Tetrahydrofuran
TPTZ- Fe^{3+}	Ferric tripyridyltriazine (complex
UV-vis	UV-visible
WRL-68	Normal liver cells
$Zn(CH_3COO)_2 \cdot 2H_2O$	Zinc(II) acetate dehydrate
$ZnCl_2$	Zinc(II) chloride

LIST OF APPENDICES

1.0 INTRODUCTION

1.1 *Schiff bases*

The coordination chemistry of Schiff base ligands and transition metal ions has developed rapidly in the past decade. The ligand named after the researcher, Hugo Schiff reported his synthesis over hundred years ago (Wilkinson *et. al.*, 1987). The attention on these ligands arose mainly due to their capability of producing the Schiff bases metal complexes with a variety of coordination modes. In addition, the resulting complexes have been under investigation for many years due to numerous applications, essentially in the treatment of cancer (Osowole *et. al.*, 2012), as antimicrobial agents (Aminabhavi *et. al.*, 1985; Prasad *et. al.*, 2010), fungicide agents (Mishra & Soni, 2008), antiviral agents (Wang *et. al.*, 1990) and potential applications in other fields such as catalysts for many reactions (Rezaeifard *et. al.*, 2010) and also electrochemistry (Tai *et. al.*, 2003). The general structure of the Schiff base is portrayed in Figure 1.1.

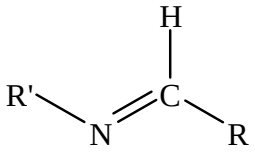

Figure 1.1: General structure of Schiff base.

1.2 *Chemistry of Schiff bases*

Schiff bases containing an azomethine or imine group (–C=N–) are commonly synthesized via the condensation of primary amines and active carbonyl compounds (Casellato & Vigato, 1977; Dey *et. al.*, 1981). Condensation of these compounds is carried out in different reaction conditions and using common solvent such as methanol or ethanol. The general formation of azomethine group is shown according to Scheme 1.1.

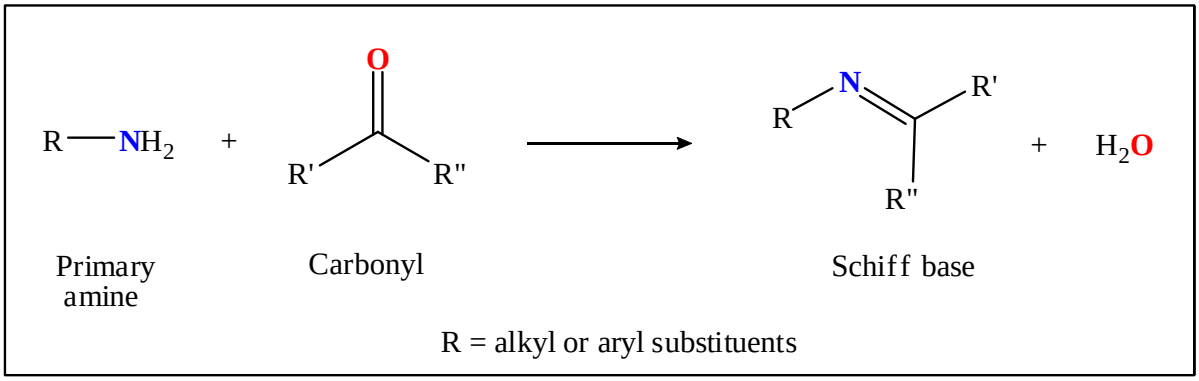

Scheme 1.1: General formation of Schiff base.

Schiff bases ligands that contain aryl substituent or aromatic aldehydes are substantially more stable and more readily synthesized. Whereby, the ligands containing alkyl substituents or aliphatic aldehydes are rather unstable and readily polymerizable (Hine & Yeh, 1967). Generally, Schiff bases with ketone are formed less readily than those with aldehydes, due to the extra carbon of ketone that donates electron density to the azomethine carbon. Hence, making the ketone less electrophilic compared to aldehyde (Fessenden & Fessenden, 1998).

Normally, formation of Schiff base occurs either at room temperature, upon heating, in the presence of acid catalyst or base catalyst. Formation of an imine involves two steps. Firstly, the amine nitrogen acts as a nucleophile, attacking the carbonyl carbon, resulting in a normally unstable carbinolamine intermediate. Upon deprotonation of nitrogen and elimination of the hydroxyl group formed C=N (imine) and also displaced water molecule. The mechanism is depicted in Scheme 1.2.

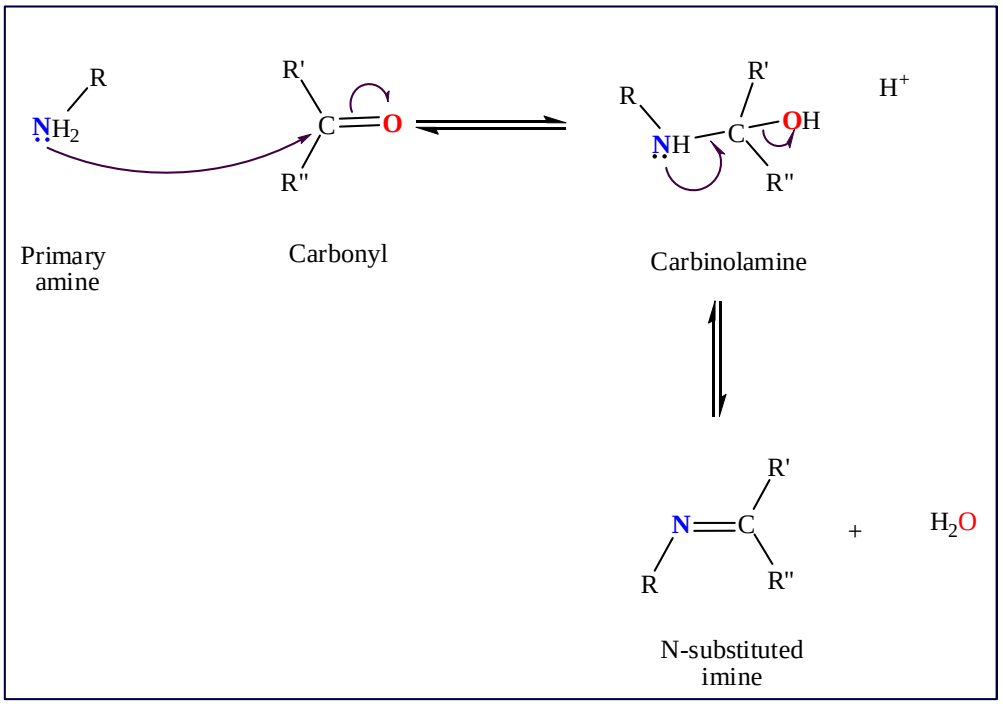

Scheme 1.2: Mechanism formation of Schiff base.

Futhermore, the carbinolamine loses water by either acid or base catalysed conditions. Since the carbinolamine is alcohol, it undergoes acid catalysed dehydration as shown in Scheme 1.3.

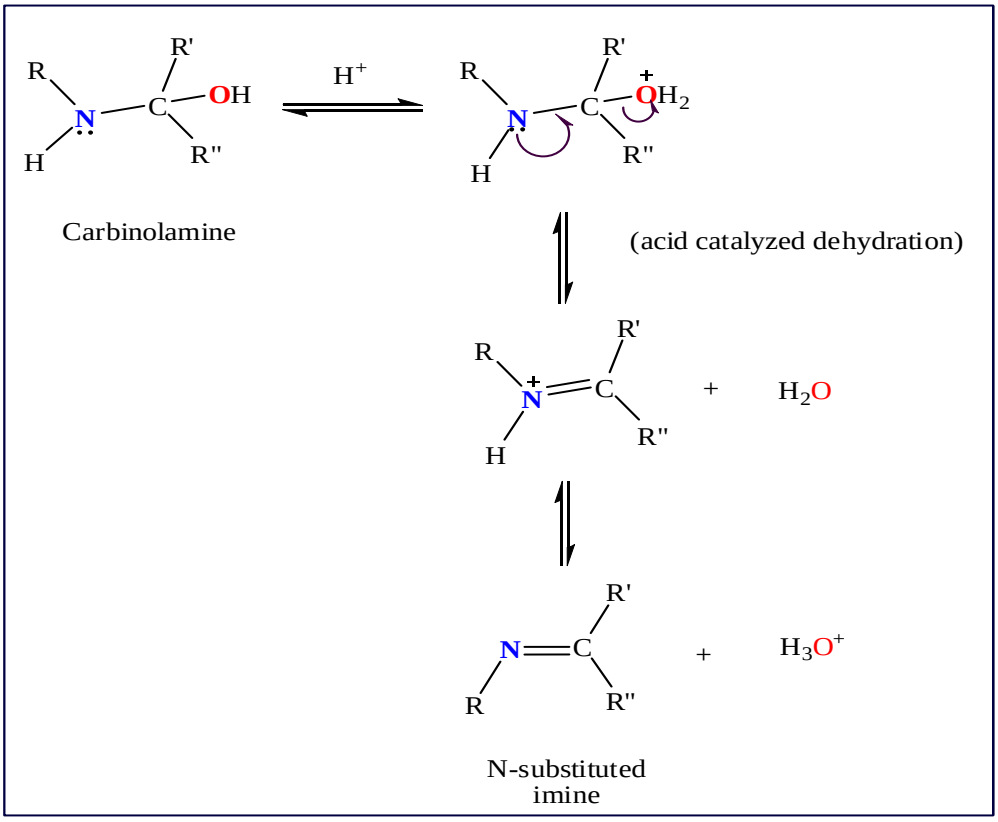

Scheme 1.3: Formation of Schiff base *via* acid catalysed dehydration.

1.3 *Schiff base complexes*

Since the nineteenth century discoveries, a wide range of complexes derived from Schiff base ligands have been studied. Especially the transition metal complexes have played an important role in the development of modern coordination chemistry, due to various coordination modes. Transition metals have a different tendency to form complexes because of the presence of empty *d* orbitals to accept lone pairs of electrons from the ligand (Zumdahl & Zumdahl, 2008). Schiff base complexes also have a diverse biological functions, such as the haem group and vitamin B_{12} coenzyme which contain transition metal (Woollins, 2010).

Metal complexes with chelating ligands containing N, S and O donor atoms have interesting versatility in coordination modes. For example, Schiff bases formed by condensation of salicylaldehyde with a primary amine are capable of coordinating metal ions. Metal coordination modes in these complexes involve phenolate oxygen and imine nitrogen to form six-membered chelate rings. If the amine fragment contains other donors located for coordination to metal, the Schiff base can act as a polydentate ligand or, depending on flexibility of the amine fragment, may show ambidentate behaviour. The Figure 1.2 shows some examples of tridentate and ambidentate Schiff base ligand.

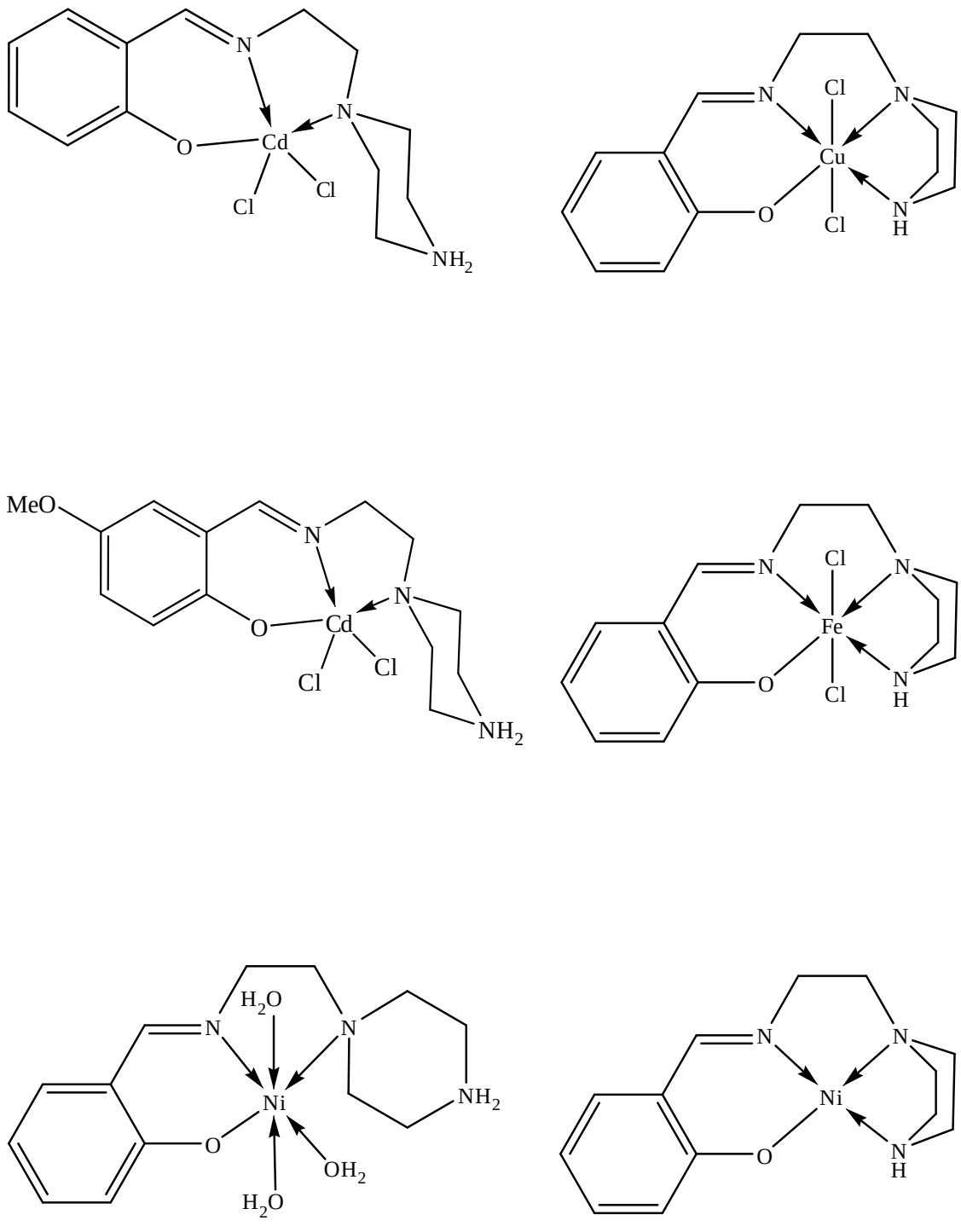

Figure 1.2: Tridentate and ambidentate Schiff base ligands.

1.4 *Cancer and cancer drugs*

Cancer remains a major cause of mortality worldwide. This disease is characterized by the uncontrolled multiplication of abnormal cells in the body (Gupta, 1994). Due to this disease, researchers all over the world are trying to find anticancer drugs that have fewer side effects to the human body. Since the 1940s, anticancer drugs have been developed and commercialized in the United State, Europe and Japan. However, every anticancer drug that has been developed to kill cancer cells will have affects prompting the normal cell division because cancer exhibits no biochemical differences to the healthy normal cells (Rang *et. al.*, 1995).

The inorganic metal complexes are used as chemotherapeutic agents although organic, non-metal containing agents are most widely employed. Complexes of transition metals are exploited as anticancer drugs due to their cytoxicity properties. Platinum drugs, such as carboplatin and cisplatin as shown in Figure 1.3 are proving effective against cancer cells. In addition, cisplatin are effective against ovarian cancers, testes cancers and other solid tumors (Howard-Lock & Lock, 1987).

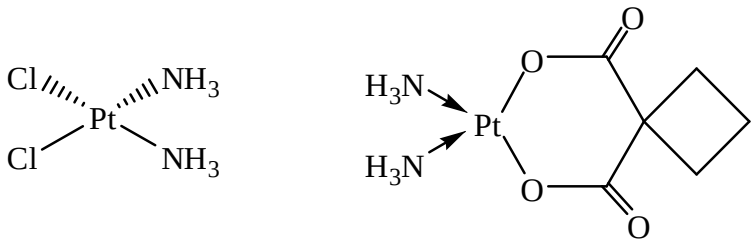

Figure 1.3: Structure of cisplatin and carboplatin.

1.4.1 **Breast cancer**

According to the World Health Organization, more than 1.2 million people are diagnosed with breast cancer annually. This cancer initiated by various environmental and/or hereditary factors. Some of the usual symptoms of breast cancer are swelling at part of the breast, lump in the underarm area, skin irritation around the breast, nipple pain and

nipple discharge. The Malaysian Cancer Registry in 2003 had reported that breast cancer is the most commonly diagnosed cancer (31 %) in women (Lim and Halimah, 2004). Nevertheless, breast cancer death rates have been gradually decreasing due to better detection and easily treatments available. Recent studies reveal that breast cancer risk is dependent on several factors including genetic predisposition and menopause (Vogel, 2008). Breast cancer is less common in younger females (<30 years old) but is generally more aggressive compared to older women. Therefore, the survival rates for younger breast cancer patients are lower.

1.5 *Antioxidants*

Antioxidants are compounds that inhibit the oxidation process through numerous mechanisms, such as by preventing the formation of reactive radical species or by scavenging them. Free radicals are chemical fragments of molecules that possess an unpaired electron and are continuously produced in cells during normal metabolism. Free radicals can cause extensive damage to macromolecular components like DNA, carbohydrates, lipids and protein if allowed to react uncontrollably. The levels of antioxidants and oxidants in the body are continuously maintained in homeostasis by dietary antioxidants and antioxidant enzymatic systems in the body. The imbalance of these systems has been claimed to cause chronic diseases over a sustained period, including cancer (Galli *et. al.*, 2005) and coronary heart disease (Adams *et. al.*, 1999).

A free radical is very reactive and can be defined as element or compound that needs an electron to fill an unfilled molecular valence orbital. They often "attack" and remove electrons from the molecule in closest proximity which can be neutral, positively or negatively charged (Hughes *et al.*, 1999). Oxygen can become a reactive molecule when oxygen is visible to a source of high energy, the energy is transferred to shape singlet oxygen (Ardestani *et al.*, 2007).

$$O_2 \quad + \quad \text{Energy} \longrightarrow O_2\bullet$$

Normally, over 95% of the oxygen reduced to H_2O by the electron transport system in the mitochondria:

$$O_2\bullet + 4e^- + 4H^+ \longrightarrow 2H_2O$$

When molecule oxygen is reduced by one electron, superoxide radical is produced:

$$O_2 + e^- \longrightarrow O_2\bullet^-$$

After the second electron is added at physiologic pH, the two products of hydrogen peroxide (H_2O_2) and hydrogen peroxide are formed:

$$2\ O_2\bullet^- + 2H^+ \longrightarrow O_2 + H_2O_2$$

$$O_2\bullet^- + H_2O_2 + 4H^+ \longrightarrow O_2 + H_2O + HO\bullet$$

The formation of HO• from H_2O_2 is catalyzed by transition metals such as iron and copper. $O_2\bullet^-$, H_2O_2 and HO• are known as reactive oxygen species (ROS) and are continuously produced by aerobically growing cells (Castro & Hermandez-Aaron *et al.*, 2002).

Dietary antioxidants (or non-enzymatic antioxidants) can be evaluated by several established techniques. Although the reagents and chemistry involved may differ in these procedures but the theory is based on redox chemistry and free radical discoloration. For instances, the ferric reducing antioxidant power (FRAP) assay (Benzie & Strain, 1996) is based on redox chemistry and the 2,2-diphenyl-1-picrylhydrazyl (DPPH) radical scavenging method (Oki *et. al.*, 2002) was established on free radical discoloration.

Associated to dietary antioxidants, enzymatic antioxidant systems are natural mechanisms in our body that provide an endogenous method to overcome oxidative stress. For example, the glutathione peroxidase (GPx) enzyme, which is found in virtually all mammalian tissues, protects the body against the accumulation of free endogenous hydrogen peroxide. The GPx enzyme catalyzed the reaction by converting it to water to produce a non-toxic product. The oxidized glutathione molecule is stimulated by reduction, catalyzed by glutathione reductase. Functioning mutually, these two systems complement each other in maintaining homeostasis (Mills, 1957). Other examples of antioxidant enzymes particularly in the human liver are superoxide dismutase (SOD) and catalase (CAT) which catalyze the dismutation of superoxide into oxygen and hydrogen peroxide and also decomposition of hydrogen peroxide to water and oxygen, respectively (Greenwald, 1990; Muzykantov, 2001).

Oxidation is a chemical reaction that transfers electrons from a substance to an oxidizing agent. Stray oxidation reactions can produce free radicals. These free radicals trigger chain reactions that could produce additional radical species that damage cells. Without the presence of antioxidants to sequester them, biomolecules are exposed to further radical oxidation. Hence, these lead to macromolecule alterations such as lipid peroxidation, enzymatic damage and DNA mutation. Accumulation of the yields of oxidative damage gives rise to oxidative stress which has been allied with the pathogenesis of many human diseases, such as Alzheimer's disease, Parkinson's disease, cancer, and aging (Valko *et. al.*, 2007).

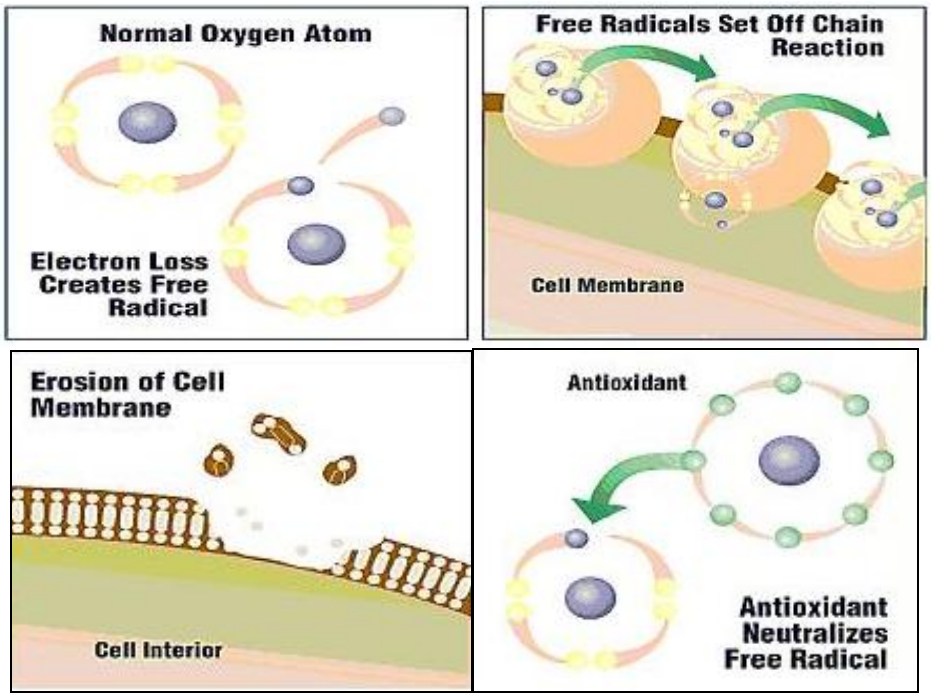

Figure 1.4: Illustration of oxidation reaction and antioxidant neutralizing free radical in human cell.

In this thesis the determination of antioxidant activity are evaluated using Ferric Reducing Power Assay (FRAP) technique.

2.0 LITERATURE REVIEW

2.1 *Schiff bases*

In 1864, German chemist Hugo Schiff established a new class of organic compounds containing imine (azomethine) group. This group of compounds are often referred to as Schiff bases in his honour. Modern chemists still synthesizing Schiff bases ligands due to the activity and well-designed, as stated by Cozzi (2004) considered the ligand as ‘‘privileged ligands’’. These ligands can be considered an important class of organic compounds which are good chelating agent (Mishra *et. al.*, 2005). Furthermore, Schiff bases are an important class of ligands in coordination chemistry and have been extensively studied (Eichhom *et. al.*, 1994; Hughes, 1984; Tarafder *et. al.*, 2001).

Schiff bases are generally bidentate (**1**), tridentate (**2**), tetradentate (**3**) or polydentate (**4**) ligands capable of forming very stable complexes with transition metals. They can only act as chelating ligands if they bear a functional group, generally hydroxyl group. Sufficiently near the condensation site in such a way that a five or six membered ring can be formed when reacting with a metal ion. Additionally, Schiff bases with donors (N, O, S, etc.) have structural similarities with natural biological systems. The presence of imine group which are utilized in elucidating the mechanism of transformation and rasemination reaction in biological systems (Balasubramanian *et. al.*, 2006).

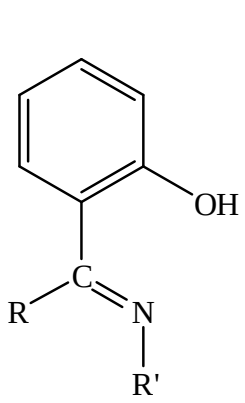

Bidentate (**1**)

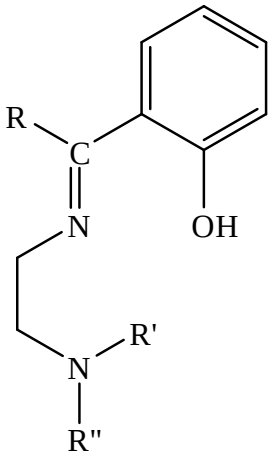

Tridentate (**2**)

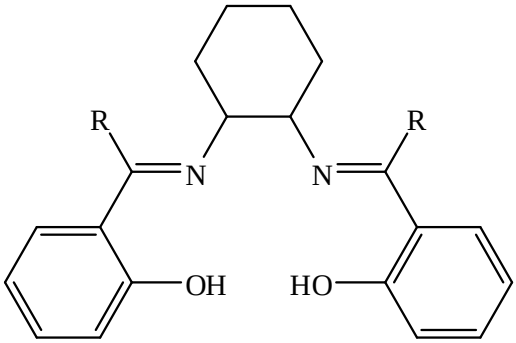

Tetradentate (**3**)

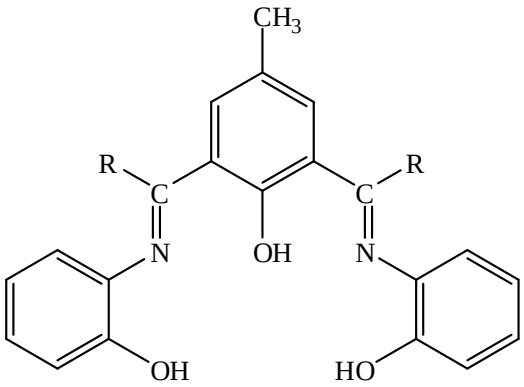

Polydentate (**4**)

Figure 2.1: Some examples of Schiff base ligands.

Schiff bases appear to be essential intermediates in a number of enzymatic reactions involving interaction of the amino group of an enzyme, usually that of a lysine residue, with a carbonyl group of the substrate. Otto *et. al.*, 1978 had conducted stereochemical studies with the support of molecular models showed that Schiff bases formed between methylglyoxal and the amino group of the lysine side chains of proteins can bend back in such a way towards the N atom of peptide groups. Hence, charge transfer can occur between the N atom of peptide groups and the oxygen atoms of the Schiff bases.

Schiff bases possess remarkable biological activities that have been reported in the literature as such antibacterial (Ali *et. al.*, 2006), antifungal, anti-inflammatory (Turan-Zitouni *et. al.*, 2007), antitumor (Panneerselvam *et. al.*, 2005) and anti HIV activities (Pandeya *et. al.*, 2000). In 2003 Shamspur mentioned that Schiff bases are reagents which are becoming increasingly important in the pharmaceutical, dye and plastic industries as well as for liquid–crystal technology and mechanistic investigations of the drugs used in pharmacology, biochemistry and physiology.

2.2 *Schiff base complexes*

For a long period of time considerable attention has been paid to the chemistry of the Schiff base metal complexes containing nitrogen and other donors and it has become an emerging area of research. Several reviews have been discussed about the structure and mechanism of the formation of the Schiff base complexes. The review paper by Calligaris *et. al.* (1972) also deliberated on the stereochemistry of four coordinate chelate complexes formed from Schiff bases and their analogues. The configuration of the chelate group in the four coordinate complexes may be square-planar, tetrahedral, distorted tetrahedral or distorted trigonal pyramidal with the metal atom at the apex. The configuration depends predominantly on the nature of the metal ions and also on the magnitude, as well as the symmetry of the ligand field. All the Schiff base complexes, those derived from salicylaldimine have been thoroughly studied so far. A variety of physiochemical investigations on these complexes provide a clear understanding of their stereochemical and electronic properties.

Various coordination modes of these compounds are useful models. Metal coordination modes in these complexes involve phenolate oxygen and imine nitrogen to form six-membered chelate rings. If the amine fragment contains other donors located for coordination to metal, the Schiff base can act as a polydentate ligand or, depending on

flexibility of the amine fragment, may show ambidentate behavior. As an example, the Schiff base derived from salicylaldehyde and N-(2-aminoethyl)piperazine (**5**) can be tetradentate or tridentate with nickel(II), depending on the piperazine ring conformation (chair or boat) (Mukhopadhyay *et. al.*, 2003). The study also showed the profound influence of substitution in the aromatic ring on coordination behavior. Indeed, this research showed the ability of the ligand to act as both tridentate and tetradentate modes, the 5-nitroderivative (**6**), coordinated only in a tridentate, while the 5-bromo analog (**7**), only in a tetradentate fashion.

Similar to piperazine, a morpholine ring in a ligand can adopt both chair and boat conformations, thus coordinating in different manners. An example is ligand **8** which has both chair and boat morpholine rings in its calcium complex (Poirier *et. al.*, 2009).

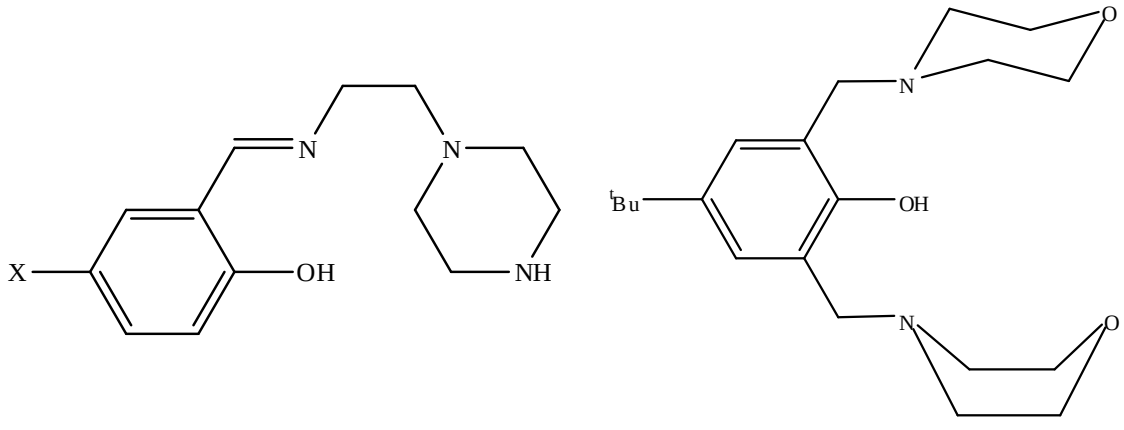

5 : X = H
6 : X = NO_2
7 : X = Br

8

Figure 2.2: Chemical diagram of ligands **5**, **6**, **7**, and **8**.

Liu *et. al.* (2012) had conducted structural evidences and theoretical calculations on *in situ* ligand and Schiff base complex transformation. In this study, *in situ* organic reactions are an effective method since they could provide a remarkable opportunity not only to generate organic ligands to be synthesized under conventional conditions. Generally, the mechanism of *in situ* ligand transformation was ascribed to the coordination

effect, in which the metal ion will cause a decrease in electron density on the aromatic ring, hence activating the ligand. The coordination effect can also be caused by the metal ions which play a role of template to tune the arrangement of molecular components in the crystals, making them satisfy the condition of ligand transformation. This paper showed the mechanism of the *in situ* ligand transformation based on the C–C coupling reaction that has been achieved at room temperature. The complex **9** were obtained by dissolving 2-(4-hydroxyphenyl)aminoacetic acid, NaOH and salicylaldehyde (the molar ratio 1:1:1.5) in methanol and heated with constant stirring for two hours. The complex **10** were obtained from the reaction solution of complex **9** after a week of disappearance of the crystals of complex **9** when some more salicylaldehyde and NaOH were added to the solution of complex **9.**

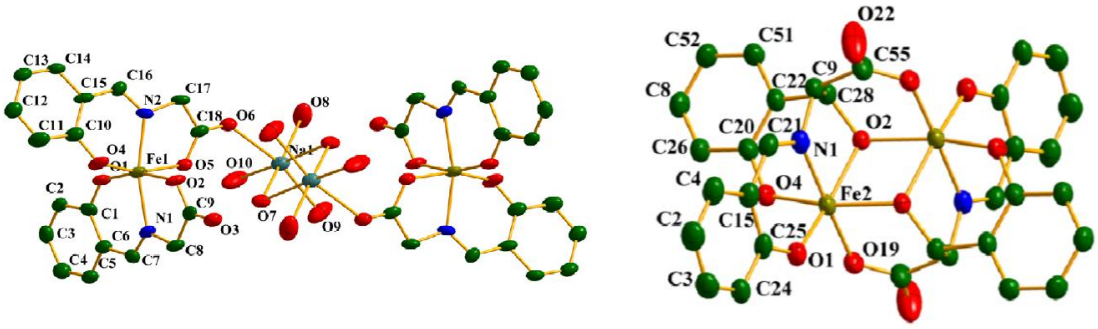

Figure 2.3: Crystal Structure of complex **9** and complex **10**.

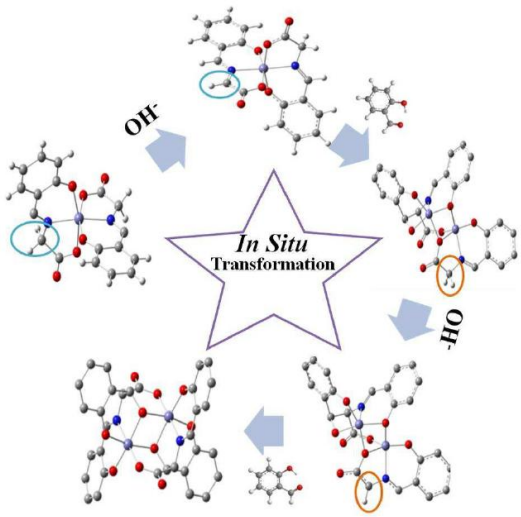

Scheme 2.1: The proposed mechanism of the *in situ* ligand transformation, C–C coupling.

2.3 *Biological Importance of Schiff Bases and the complexes*

The Schiff base metal complexes have been of great interest for many years due the chemistry and the biocidal activities of transition metal complexes containing O, N and S, N donor atoms. The transition metal complexes having oxygen and nitrogen donor Schiff bases possess unusual configuration, structural lability and are sensitive to molecular environment. The environment around the metal centre is the key role in the coordination of metals at the active sites of numerous metallobiomolecules (Golcu *et. al.*, 2005). It has been shown that Schiff base complexes derived from 4-hydroxysalicylaldehyde and amines have strong anticancer activity, e.g., against *Ehrlich ascites carcinoma* (EAC) (Zishen *et. al.*, 1993). Table 2.1 shows the summary of biological properties of several compounds related to these studies and Figure 2.4 illustrates chemical structures of the compounds.

Table 2.1: Biological application summary of several compounds.

Compound Name	Biological Application	References
Phendimentrazine (**11**)	Appetite suppressants	Sladojevich *et. al.*, 2008
(2S,3S,5R)-2-(3,5-Difluorophenyl)-3,5-dimethyl-2-morpholinol (**12**)	Antidepressant agent and selective inhibitor of norepinephrine uptake	Kelley *et. al*., 1996
2-(4-methyl-2-phenylmorpholin-2-yloxy)ethyl nitrate (**13**)	Antioxidants activity	Guillonneau *et. al.*, 2003
Heterocyclic piperazines (**14**)	Numerous physiological effects, including accelerated pulse and breathing and hypersensitivity to external stimuli	Prelog & Driza, 1933
Ipsapirone (**15**)	Antidepressant	Broekkamp *et. al.*, 1995
Buspirone (**16**)	Anxiolytic drug	Mahmood & Sahajwalla, 1999
Indinavir (**17**)	The HIV protease inhibitor indinavir, compound that blocks farnesyltransferase activity (anti-cancer)	Rossen *et. al.*, 1995 Rawls, 1998
N-benzylidine-2-morpholoinobenzenamine (**18**)	Analgesic and antiinflammatory activities	Panneerselvam *et. al.*, 2009

Compound Name	Biological Application	References
N-(3-nitrobenzylidine)-2-morpholino benzenamine (**19**)	Anti-microbial activity against *S. aureus*, *E. coli* and *C. albicans*	Panneerselvam *et. al.*, 2009
Salicylaldehyde thiosemicarbazone (**20**)	Antiproliferative activity potential antitumor agents	Lovejoy & Richardson, 2002
Salicylaldehyde 4-phenylthiosemicarbazone (**21**)	Display stronger antiproliferative activity than the parent compound **20**	Dilovic´ *et. al.*, 2008
Schiff base copper complexes of quinoline-2 carboxaldehyde (**22**)	Inhibited chymotrypsin-like proteasome activity in intact prostate LNCaP cancer cells	Adsule *et. al.*, 2006
2-[(2,3-dihydro-1*H*-inden-4-ylimino)methyl]-5-nitrophenol (**23**) and its Schiff base complexes $[ML_2]$ (**24**) Where, M= Pd or Zn	Pd(II) complex has the best anticancer activity against MCF-7 cells which is close to the activity of cis platin Zn(II) complex and the ligand have broad spectrum activity like gentamycin	Osowole *et. al.*, 2012
1-[(2-piperidin-1ylethylimino)methyl]naphthalen-2-ol) (**25**)	Antibacterial activities against *E. coli* and *S. aureus*	Sang & Lin, 2010

Compound Name	Biological Application	References
Schiff base Cu(II) complex (**26**)	Antibacterial activities against *E. coli*, *P. fluorescens*, and *S. aureus* of the complex are superior to the Penicillin	Sang & Lin, 2010
Copper(II) complexes derived from 1-[(2-morpholin-4-ylethylimino)methyl]-naphthalen-2-ol (**28**)	Stronger activities against the bacteria then its ligand (**27**)	Sang *et. al.*, 2009
Schiff base Ni(II) complexes derived for piperazine and salicylaldehyde analogue (**29**)	Highly active in catechol oxidase activity positive charged ligand system supposed to be instrumental for their catecholase-like activity	Guha *et. al.*, 2013
4-chloro-2-[(2-morpholin-4-ylethylimino)methyl]phenol (**30**)	Activity against Gram-negative bacterial strains (*E. coli* and *P. fluorescence*)	Sang *et. al.*, 2010 Wang *et. al.*, 2010
Schiff-base Zn(II) complex (**31**)	Bactericidal activities against the Gram-positive (*B. subtilis* and *S. aureus*) and Gram-negative bacteria (*E. coli* and *P. fluorescence*) similar or more patent with commercial antibiotics (kanamycin and penicillin)	Wang, 2010

Figure 2.4: Chemical structures of the biologically active compounds.

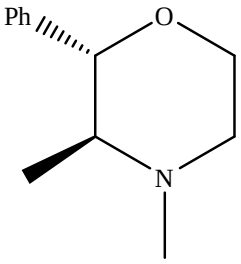

11

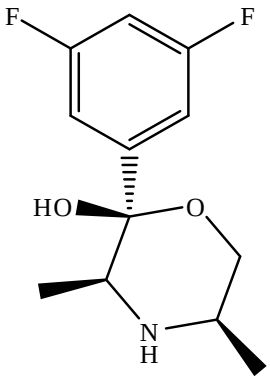

12

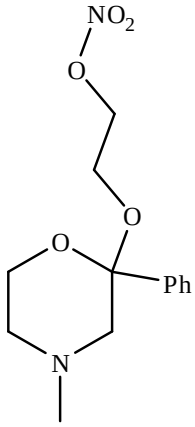

13

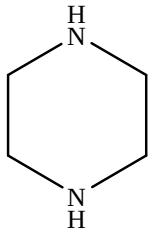

14

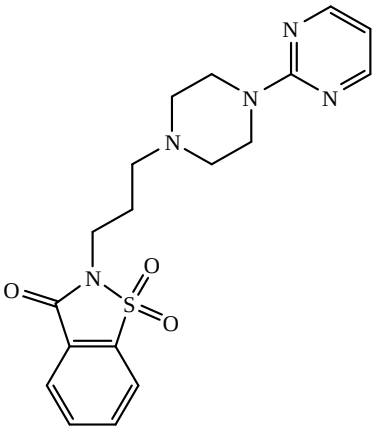

15

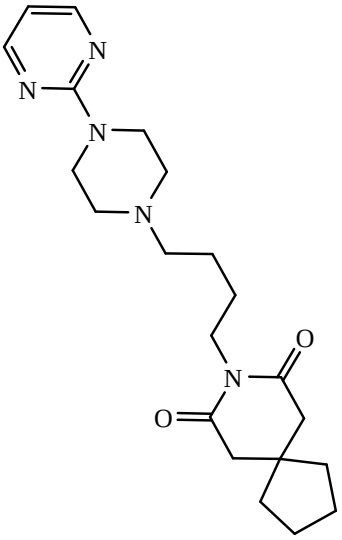

16

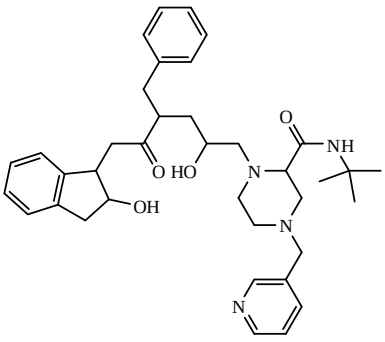

17

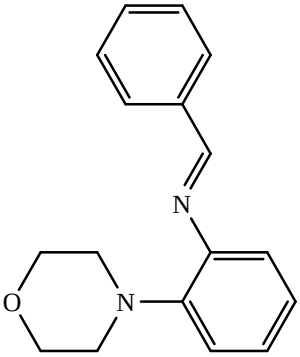

18

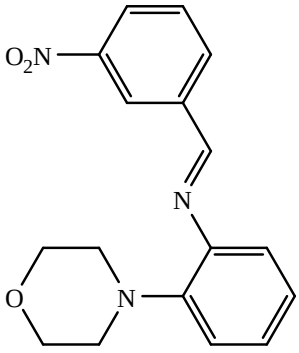

19

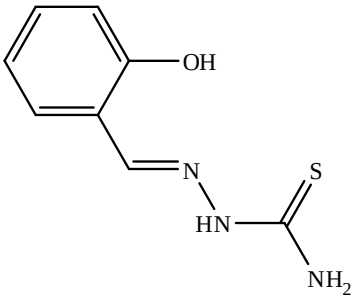

20

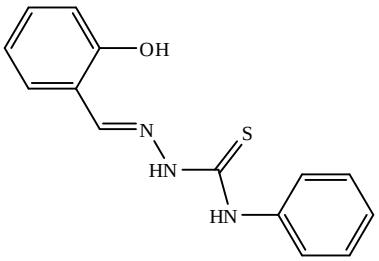

21

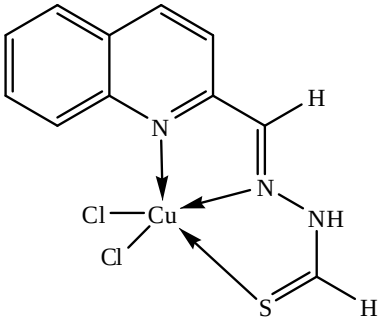

22

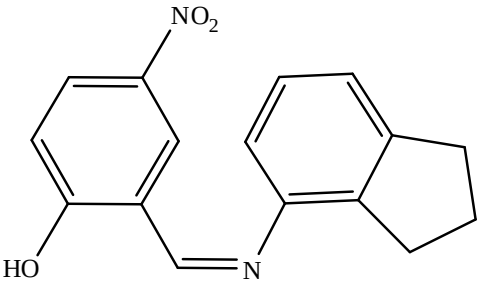

23

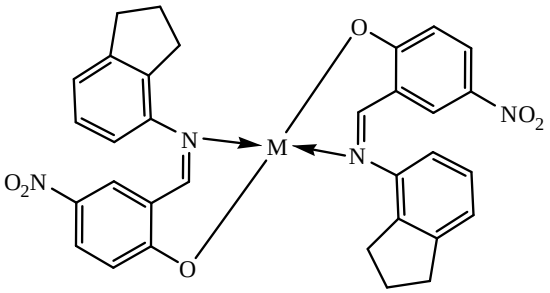

M = Pd or Zn

24

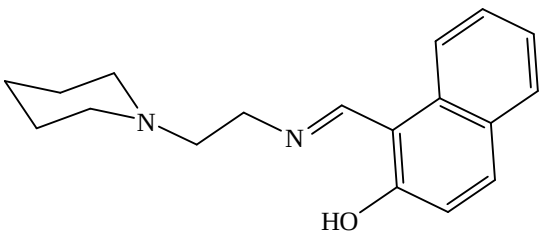

25

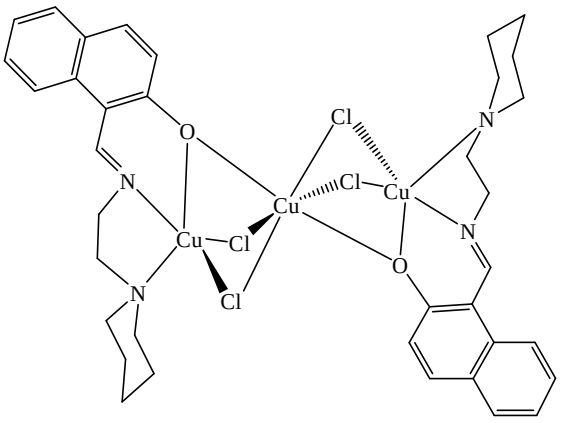

26

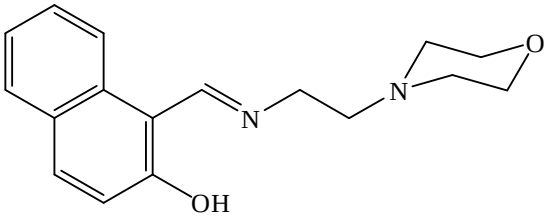
N
O
N
OH

27

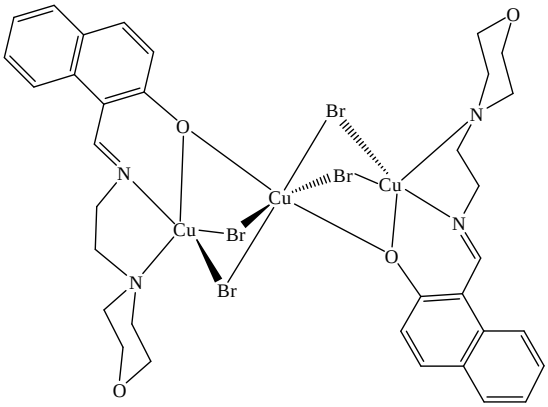
O
Br
N
O
Br
Cu
Cu
N
Cu
Br
N
Br
O
N
O

28

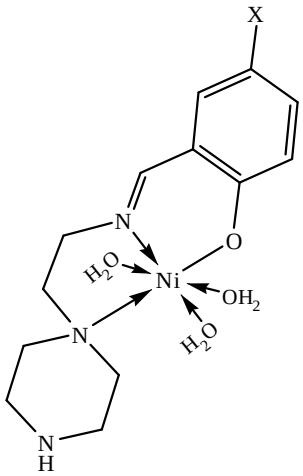
X
N
O
H_2O
Ni
OH_2
H_2O
N
N
H

29

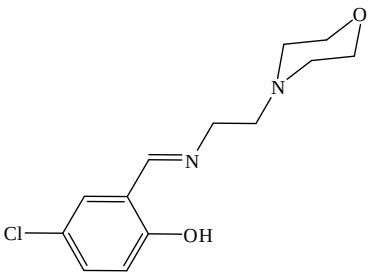
O
N
N
Cl
OH

30

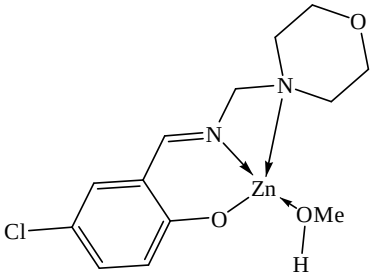
O
N
N
Zn
Cl
O
OMe
H

31

These complexes play an important role in the development of coordination chemistry and have received much attention in recent years (Paschke *et. al.*, 2003). Some of the complexes have been found to have pharmacological properties (You *et. al.*, 2006). These unusual structural features have led to increased interest in the synthesis of copper, nickel and zinc complexes with various ligands (Sun *et. al.*, 2006). Previous studies showed a morpholine ring in a bis(morpholinomethyl)phenoxy ligand upon complexation can adopt both tridentate and tetradentate modes, depends on the conformation of the mopholine ring either chair or boat conformation (Poirier *et. al.*, 2009).

The present studies were focused on the Schiff bases derived from salicylaldehyde derivatives and aliphatic amine, N-(3-aminopropyl)morpholine. Upon reacting the Schiff base with metal salts in a 2 : 1 ratio (ligand : metal), the ligands showed *N*,*O*-bidentate fashion. Whereas, the ligands with metal salts in a 1 : 1 ratio showed coordination *N*,*N*,*O*-tridentate behaviour of the morpholine. Herein, we describe the behaviour of the two flexidentate ligands: salicylaldehyde, L^1H and its 5-chlorosalicylaldimine analogue, L^2H (Figure 2.5), towards zinc(II), copper(II) and nickel(II) ions. The solid-state structures of the metal complexes were examined by X-ray diffraction analysis. The complexes and ligands were also tested for their *in vitro* cytotoxicity and antioxidant properties.

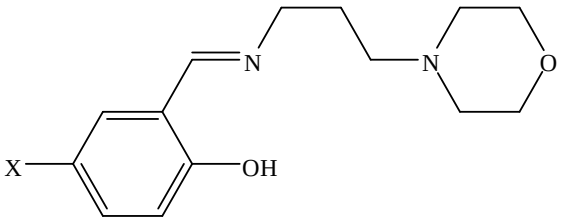

L^1H: X = H
L^2H: X = Cl

Figure 2.5: Chemical diagram of L^1H and L^2H.

2.4 *Aims and objectives of the present study*

Generally, the aims of this research include synthesis, characterization and determine biological properties of the new Schiff bases of morpholine analogue with salicylaldehyde derivatives and their metal complexes.

Specific, objectives of the research are:

1. To synthesize Schiff bases of salicylaldehyde derivatives and aliphatic amine, N-(3-aminopropyl)morpholine compounds.
2. To prepare metal complexes from the synthesize Schiff base with zinc(II),copper(II), and nickel(II) ions.
3. To elucidate the compounds structure using spectroscopic data such as elemental analysis (CHN), fourier transform-infrared (FT-IR), nuclear magnetic resonance (^{1}H & ^{13}C NMR), and UV-visible (UV-vis).
4. To determine the solid-sate structures of the complexes, studied by X-ray diffraction analysis. The X-ray crystallographic data and structural determination help to examine the flexibility of the Schiff base compounds.
5. To determine the biological properties such as cytotoxicity and anti-oxidant activities of the Schiff base ligands and their metal complexes.

3.0 EXPERIMENTAL

3.1 *Materials*

All the reagents used were commercially available (Merck, Acros or Sigma-Aldrich) and were used as supplied. Ethanol was distilled prior to use. All chemicals were of analytical grades and used without any further purification. Chemicals and solvents used for the preparation of Schiff base ligands and metal complexes are: *N*-(3-aminopropyl) morpholine, salicylaldehyde, 5-chlorosalicylaldehyde, zinc(II) acetate dehydrate [$Zn(CH_3COO)_2{\cdot}2H_2O$], copper(II) acetate monohydrate [$Cu(CH_3COO)_2{\cdot}H_2O$], nickel(II) acetate tetrahydrate [$Ni(CH_3COO)_2{\cdot}4H_2O$], zinc(II) chloride [$ZnCl_2$], copper(II) chloride dehydrate [$CuCl_2.2H_2O$], nickel(II) chloride [$NiCl_2$], triethylamine, ethanol, methanol, tetrahydrofuran (THF), and dimethyl sulphoxide (DMSO).

The materials of biological studies are potassium ferricyanide $K_3[Fe(CN)_6]$, trichloroacetic acid, ferric chloride solution and sodium phosphate from Sigma Chemical Co. (St. Louis, MO, USA). The solvents used are methanol and water (HPLC) were purchased from Chemolab Supplies (Kuala Lumpur, Malaysia). The instruments used for biological determination are an ELISA reader (Sunrise, Switzerland) and UV-vis spectrophotometer-1700 (Shimadzu, Japan) were used for absorbance determinations.

3.2 *Experimental Instruments*

A variety of physico-chemical methods have been employed to characterize the structure of the Schiff base ligands and their metal chelates. A brief account of these methods is given below.

3.2.1 **Elemental analyses**

Microanalysis of carbon, hydrogen and nitrogen composition in the all the synthesized compounds were analyzed on a Perkin- Elmer 2400 Series II CHNS Analyzer.

3.2.2 **Fourier Transform-infrared (FT-IR) spectroscopy**

Infrared spectra for the synthesized ligands were recorded using NaCl cells and the synthesized complexes were recorded using KBr pellets on Pelkin-Elmer RX1 FTIR (Fourier Transform Infra-Red) spectrometer for frequencies 4000-400cm^{-1} at ambient temperature.

3.2.3 **Nuclear Magnetic Resonance (NMR) spectra**

All the ligands and zinc complexes ^{1}H and ^{13}C NMR spectra were recorded in DMSO-d_6 on Bruker AVN 400 MHz FT-NMR or Lambda JEOL 400 MHz FT-NMR spectrometer with tetramethylsilane (TMS) as an internal standard.

3.2.4 **UV-Visible spectra**

The electronic spectra were measured by means of a Shimadzu 1601 spectrophotometer in the region 200–1100 nm using THF or DMSO as a solvent. The measurement using 1 cm quartz cuvettes with these following parameters: measuring mode, absorbance; scan speed, medium and the concentration of the samples is 1×10^{-6} M.

3.2.5 **X-ray crystallography data and structural determination**

Diffraction data were measured with a Bruker SMART Apex II CCD area-detector diffractometer (graphite-monochromated Mo-Kα radiation, λ = 0.71073 Å). The orientation matrix, unit-cell refinement, and data reduction were all handled by the Apex2 software (SAINT integration, SADABS absorption correction (Bruker, 2007)). The structures were solved using direct or Patterson methods in the program SHELXS-97 and were refined by the fullmatrix least-squares method on F^2 with SHELXL-97 (Sheildrick, 2008). All the non-hydrogen atoms were refined anisotropically and all the C-bound hydrogen atoms were placed at calculated positions and refined isotropically. O-bound hydrogen atoms were located in difference Fourier maps and refined with distance restraints of $O\text{-}H_{Methanol}$ 0.84(2) and $O\text{-}H_{water}$ 0.88(2) Å. Drawings of the molecules were produced with XSEED (Barbour, 2001).

3.3 *General Preparation of ligands and their complexes*

3.3.1 **Schematic diagram of the Schiff bases**

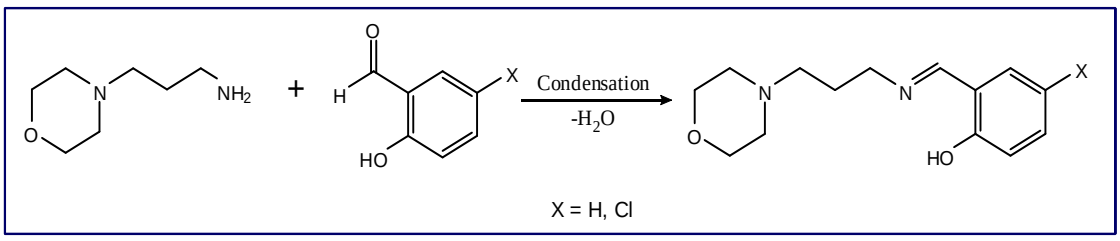

3.3.2 **Schematic diagram of the Schiff base complexes**

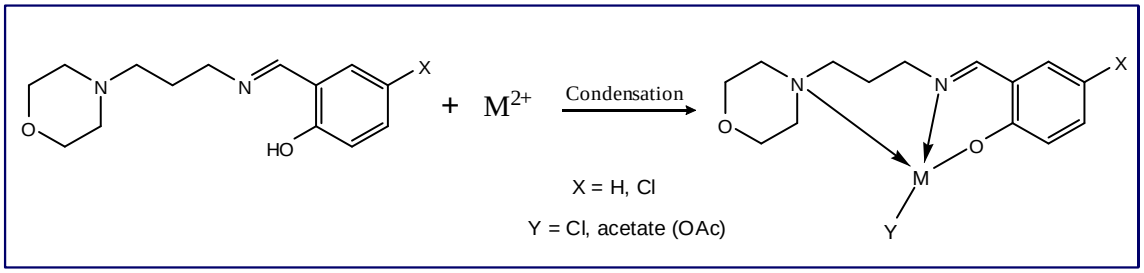

3.4 *Synthesis of Schiff bases*

Two ligands (L^1H, and L^2H) were prepared by the reaction of *N*-(3-aminopropyl) morpholine with two different aldehydes (salicylaldehyde and 5-chlorosalicycladehyde).

3.4.1 L^1H: (E)-2-((3-morpholinopropylimino)methyl)phenol

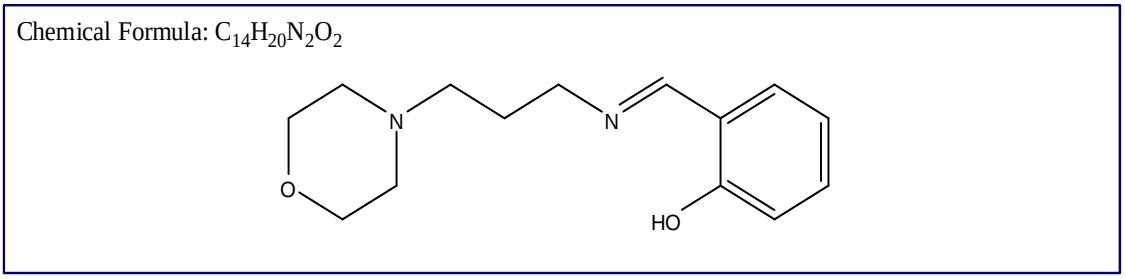

F

igure 3.1: Proposed chemical structure of L^1H.

The compound was synthesized by refluxing a mixture of *N*-(3-aminopropyl) morpholine (0.35 g, 2.46 mmol) and salicylaldehyde (0.3 g, 2.46 mmol) in ethanol (15 mL) for 2 hours. The solvent was then removed under reduced pressure to give a yellow oil of the Schiff base.

Anal. Calcd. for $C_{14}H_{20}N_2O_2$: C, 67.71%; H, 8.12%; N, 11.28%. Found: C, 66.79%; H, 7.79%; N, 10.77%. IR [ν max (cm^{-1}), NaCl cell]: 3525 br; 2948 m; 2853 m; 2810 m; 1630 s ($\nu_{C=N}$); 1460 s; 1279 s; 759 m. ^{1}H NMR (DMSO-d_6, δ ppm): 1.78 (quin, 2H, CH_2); 2.32 (m, 6H, CH_2); 3.56 (t, 4H, CH_2); 3.61 (t, 2H, CH_2); 6.90 (m, 2H, Ar-*H*); 7.32 (t, 1H, Ar-*H*); 7.42 (d, 1H, Ar-*H*); 8.55 (s, 1H, *H*C=N); 13.65 (s, 1H, O*H*). ^{13}C NMR (DMSO-d_6, δ ppm): 27.11, 53.29, 55.74, 56.20, 66.13 (*C*H_2); 116.49, 118.29, 118.51, 131.51, 132.18 (*Ar*); 160.91 (H*C*=N); 165.84 (*C*-OH).

3.4.2 L^2H: (E)-4-chloro-2-((3-morpholinopropylimino)methyl)phenol

Chemical Formula: $C_{14}H_{19}ClN_2O_2$

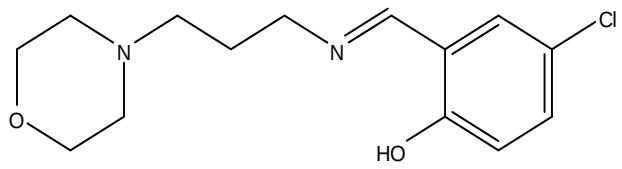

Figure 3.2: Proposed chemical structure of L^2H.

An equimolar mixture of *N*-(3-aminopropyl)morpholine(0.35 g, 2.46 mmol) and 5-chlorosalicycladehyde (0.39 g, 2.46 mmol) in ethanol (15 mL) was refluxed for 2 hours. The solvent was then removed under reduced pressure to give a yellow oil of L^2H ligand.

Anal. Calcd. for $C_{14}H_{19}ClN_2O_2$: C, 59.47%; H, 6.77%; N, 9.91%. Found: C, 60.63%; H, 7.07%; N, 10.12%. IR [ν max (cm^{-1}), NaCl cell]: 2950 m; 2853 m; 2810 m; 1636 s ($\nu_{C=N}$); 1483 s; 1279 s; 822 m; 697 m. ^{1}H NMR (DMSO-d_6, δ ppm): 1.78 (quin, 2H, CH_2); 2.32 (m, 6H, CH_2); 3.56 (t, 4H, CH_2); 3.62 (t, 2H, CH_2); 6.88 (d, 1H, Ar-*H*); 7.33 (dd, 1H, Ar-*H*); 7.53 (d, 1H, Ar-*H*); 8.53 (s, 1H, *H*C=N), 13.75 (s, 1H, O*H*). ^{13}C NMR (DMSO-d_6, δ ppm): 26.90, 53.27, 55.65, 55.92, 66.12 (*C*H_2); 118.76, 119.39, 121.37, 130.43, 131.94 (*Ar*); 160.28 (H*C*=N); 164.77 (*C*-OH).

3.5 *Synthesis of the metal complexes*

For the preparation of the metal complexes, the Schiff base ligands, L^1H and L^2H, were synthesized *in situ* by refluxing the solutions of N-(3-aminopropyl) morpholine (0.35 g, 2.46 mmol) with either salicylaldehyde (0.3 g, 2.46 mmol) or 5-chlorosalicycladehyde (0.39 g, 2.46 mmol) in ethanol or methanol (15 mL) for 2 hours. The resulting solutions were then used for the metal complexation reactions.

3.5.1 **[Zn(L^1)$_2$]**

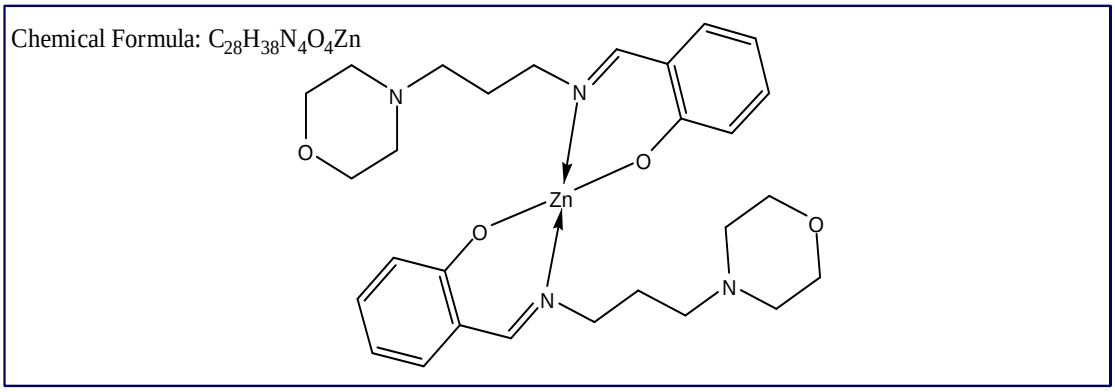

Figure 3.3: Proposed structure for [Zn(L^1)$_2$].

To a solution of the *in situ* prepared L^1H in ethanol, a few drops of triethylamine were added followed by addition of a solution of $Zn(OAc)_2 \cdot 2H_2O$ (0.27 g, 1.23 mmol) (OAc stands for acetate) in ethanol. The mixture was refluxed for 1 hour. The solvent was then removed under reduced pressure to give yellow oil product which crystallized from methanol at room temperature.

Yield: 0.58 g, 84.1%. Anal. Calcd. for $C_{28}H_{38}N_4O_4Zn$: C, 60.05%; H, 6.84%; N, 10.00%. Found: C, 60.25%; H, 7.05%; N, 10.03%. IR [ν max (cm^{-1}), KBr disc]: 2938 w; 2851 w; 1626 s ($\nu_{C=N}$); 1463 m; 1317 m; 759 m; 601 w; 462 w. ^{1}H NMR (DMSO-d_6, δ ppm): 1.24 (s, 1H, CH_2); 1.67 (m, 2H, CH_2); 2.12 (m, 6H, CH_2); 2.20 (t, 2H, CH_2); 2.33 (m, 1H, CH_2); 3.60 (t, 2H, CH_2); 6.50 (s, 1H, Ar-*H*); 6.64 (d, 1H, Ar-*H*); 7.27 (m, 2H, Ar-*H*); 8.47 (s, 1H, *H*C=N). ^{13}C NMR (DMSO-d_6, δ ppm): 26.65, 52.90, 54.89, 57.87, 66.02 (CH_2); 113.96, 118.07, 122.27, 134.43, 135.97 (*Ar*); 169.77 (H*C*=N); 171.90.

3.5.2 **[Zn(L^1)Cl_2]**

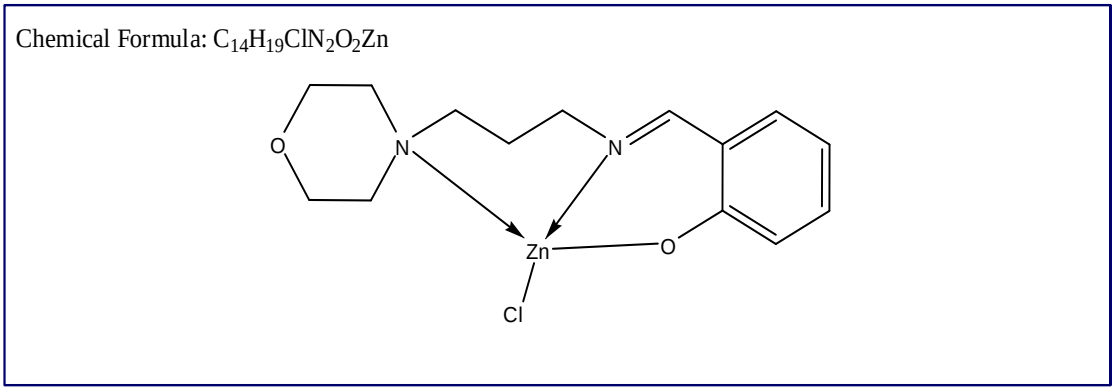

Figure 3.4: Proposed structure for [Zn(L^1)$_2Cl_2$].

An ethonolic solution of zinc(II) chloride (0.34 g, 2.46 mmol) were added to a solution of the *in situ* prepared L^1H in ethanol (15 mL). The resulting solution was refluxed for 30 minutes, then the solvent was removed under reduced pressure. The impure product was recrystallized from methanol to give the yellow crystals.

Yield: 0.51 g, 81.3%. Anal. Calcd. for $C_{28}H_{38}N_4O_4Zn$: C, 43.72%; H, 5.24%; N, 7.28%. Found: C, 43.73%; H, 4.89%; N, 7.24%. IR [ν max (cm^{-1}), KBr disc]: 3397 br; 2963 w; 2857 w; 1636 s ($\nu_{C=N}$); 1445 s; 1303 s; 755 s; 564 m; 465 w. ^{1}H NMR (DMSO-d_6, δ ppm): 2.09 (m, 2H, CH_2); 2.53 (m, 4H, CH_2); 2.84 (m, 4H, CH_2); 3.60 (m, 4H, CH_2); 6.98 (m, 2H, Ar-*H*); 7.29 (br, 1H, N-*H*); 7.53 (m, 1H, Ar-*H*); 7.66 (dd, 1H, Ar-*H*); 10.26 (s, 1H, *H*C=N). ^{13}C NMR (DMSO-d_6, δ ppm): 23.37, 30.64, 53.05, 65.57, 65.99 (*C*H_2); 117.19, 118.45, 119.47, 122.24, 129.27 (*Ar*); 136.39 (H*C*=N); 191.81.

3.5.3 **[Cu(L^1)$_2$]**

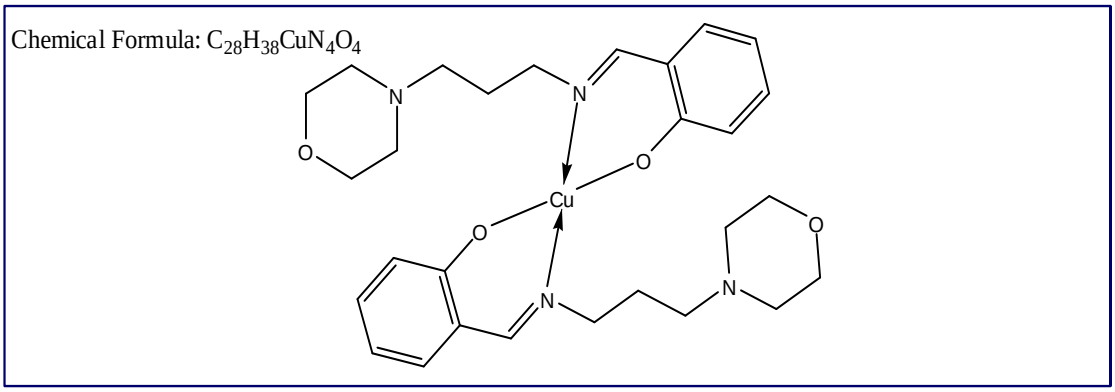

Figure 3.5: Proposed structure for [Cu(L^1)$_2$].

A few drops of triethylamine were added to a solution of the *in situ* prepared L^1H in methanol at room temperature. A methanolic solution of $Cu(OAc)_2 \cdot H_2O$ (0.25 g, 1.23 mmol) was added and the mixture was stirred at room temperature for two hours. It was then set aside for two weeks whereupon the x-ray quality crystals of the copper complex were obtained.

Yield: 0.60 g, 87.4%. Anal. Calcd. for $C_{28}H_{38}N_4O_4Cu$: C, 60.25%; H, 6.86%; N, 10.04%. Found: C, 60.25%; H, 7.05%; N, 10.03%. IR [ν max (cm^{-1}), KBr disc]: 2954 w; 2851 w; 2801 w; 1613 s ($\nu_{C=N}$); 1445 s; 1330 s; 760 s; 609 w; 456 w. UV-Vis [λ_{max} (nm), THF (ε, $mol^{-1}dm^3cm^{-1}$)] 245 (37185); 295 (7363); 307 (10158); 363 (11836); 619 (112).

3.5.4 **[Ni(L^1)$_2$]**

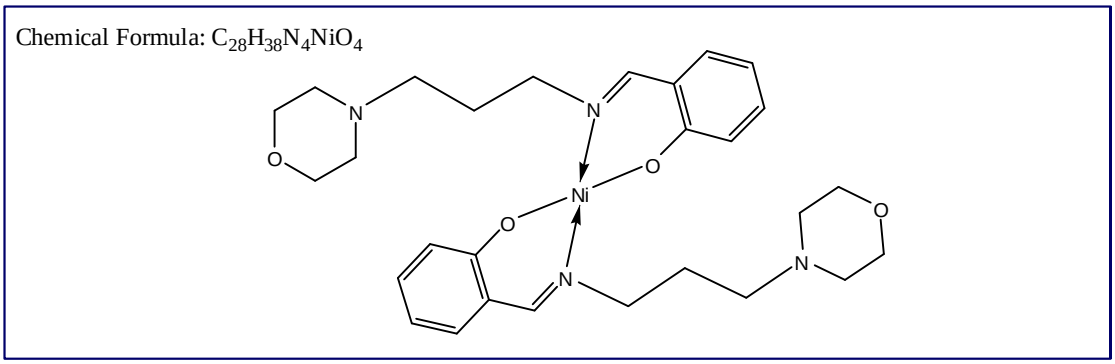

Figure 3.6: Proposed structure for [Ni(L^1)$_2$].

The complex was prepared by mixing equimolar of the Schiff base ligand with a solution of nickel chloride and was left stirring overnight. Successive 24 hours of stirring followed by solvent evaporation under reduced pressure to give viscous oil, then gradual addition of distilled water yielded the nickel complexes as green solids. Diffraction quality crystals of [Ni(L^1)$_2$] was obtained by slow evaporation of methanol solution of the complex at ambient temperature.

Yield: 0.72 g, 82.3%. Anal. Calc. for $C_{28}H_{38}N_4O_4Ni$: C, 60.78; H, 6.92; N, 10.13. Found: C, 60.63; H, 7.07; N, 10.12%. IR [ν max (cm^{-1}), KBr disc]: 2957 w; 2851 w; 1607 s ($\nu_{C=N}$); 1447 s; 1332 s; 757 s ; 599 m; 470 m. UV-Vis [λ_{max} (nm), THF (ε, $mol^{-1}dm^3cm^{-1}$)] 245 (19703); 266 (13028); 326 (3312); 413 (1751); 614 (75).

3.5.5 **[Zn(L^2)$_2$]·3H$_2$O**

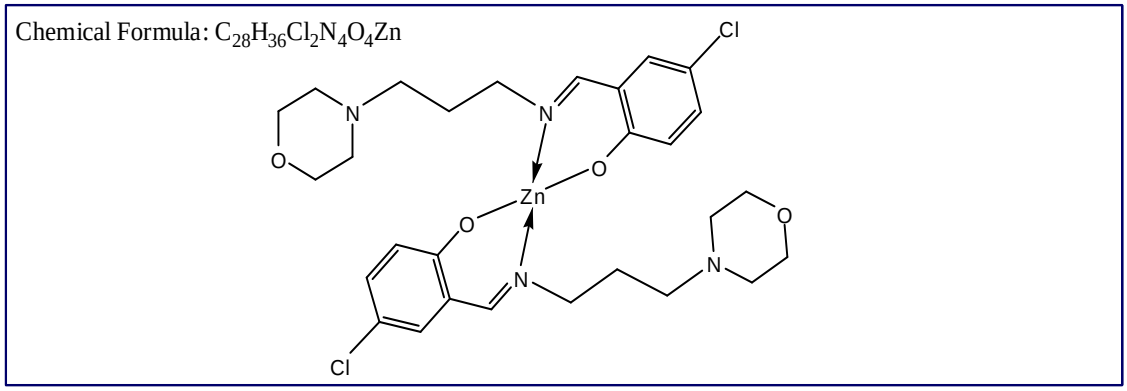

Figure 3.7: Proposed structure for [Zn(L^2)$_2$]·3H$_2$O.

The complex was prepared following the same procedure as for the preparation of [Zn(L^1)$_2$] except for using L^{2}H (0.39 g, 2.46 mmol) as the ligand. Yellow crystals, suitable for single crystal X-ray diffraction analysis were obtained by slow evaporation of an ethanol solution of the complex at room temperature.

Yield: 0.57 g, 67.6%. Anal. Calcd. for $C_{28}H_{42}Cl_2N_4O_7Zn$: C, 49.24%; H, 6.20%; N, 8.20%. Found: C, 49.24%; H, 6.19%; N, 8.20%. IR [ν max (cm^{-1}), KBr disc]: 3340 br (ν_{H2O}); 2959 w; 2852 w; 2822 w; 1618 s ($\nu_{C=N}$); 1461 s; 1296 s; 832 m; 716 s; 552 w; 476 w. ^{1}H NMR (DMSO-d_6, δ ppm): 1.24 (s, 1H, CH_2); 1.63 (m, 2H, CH_2); 2.12 (m, 6H, CH_2); 2.20 (t, 2H, CH_2); 2.33 (m, 1H, CH_2); 3.55 (m, 2H, CH_2); 6.66 (d, 1H, Ar-*H*); 7.25 (dd, 1H, Ar-*H*); 7.36 (d, 1H, Ar-*H*); 8.47 (s, 1H, *H*C=N). ^{13}C NMR (DMSO-d_6, δ ppm): 26.65, 52.65, 54.95, 58.10, 66.00 (*C*H$_2$); 116.60, 118.84, 124.20, 133.93, 134.04 (*Ar*); 168.44 (H*C*=N); 170.96.

3.5.6 **[Zn(L^2)(OAc)]**

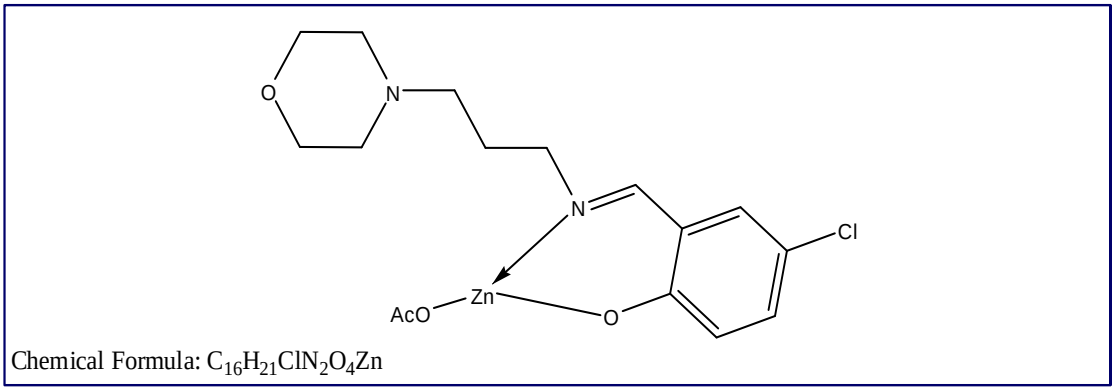

Chemical Formula: $C_{16}H_{21}ClN_2O_4Zn$

Figure 3.8: Proposed structure for [Zn(L^2)(OAc)].

An ethanolic solution of $Zn(OAc)_2 \cdot 2H_2O$ (0.54 g, 2.46 mmol) was added to an *in situ* prepared ligand (L^{2}H) solution in ethanol (15 mL). The mixture was refluxed for two hours and then was left undisturbed at room temperature for two days whereupon X-ray quality crystals of the complex were obtained.

Yield: 0.54 g, 58.7%. Anal. Calcd. for $C_{16}H_{23}N_2O_4ClZn$: C, 47.31%; H, 5.21%; N, 6.90%. Found: C, 47.43%; H, 5.05%; N, 6.85%. IR [ν max (cm^{-1}), KBr disc]: 2928 w; 2847 w; 1646 s ($\nu_{C=N}$); 1577 s; 1461 s; 1314 s; 850 s; 703 s; 559 m; 470 m. ^{1}H NMR (DMSO-d_6, δ ppm): 1.22 (s, 1H); 1.84 (m, 6H); 2.13 (m, 2H); 2.71 (br, 2H); 3.66 (m, 6H); 6.63 (d, 1H, Ar-*H*); 7.16 (d, 1H, Ar-*H*); 7.25 (s, 1H, Ar-*H*); 8.29 (s, 1H, *H*C=N). ^{13}C NMR (DMSO-d_6, δ ppm): 21.69 (CH_3)$_{acetate}$; 25.51, 53.76, 53.76, 58.52, 58.91, 65.12 (CH_2); 116.19, 118.99, 124.22, 133.42, 133.73 (*Ar*); 168.38 (H*C*=N); 168.85 (*C*=O)$_{acetate}$.

3.5.7 **[Cu(L^2)$_2$]**

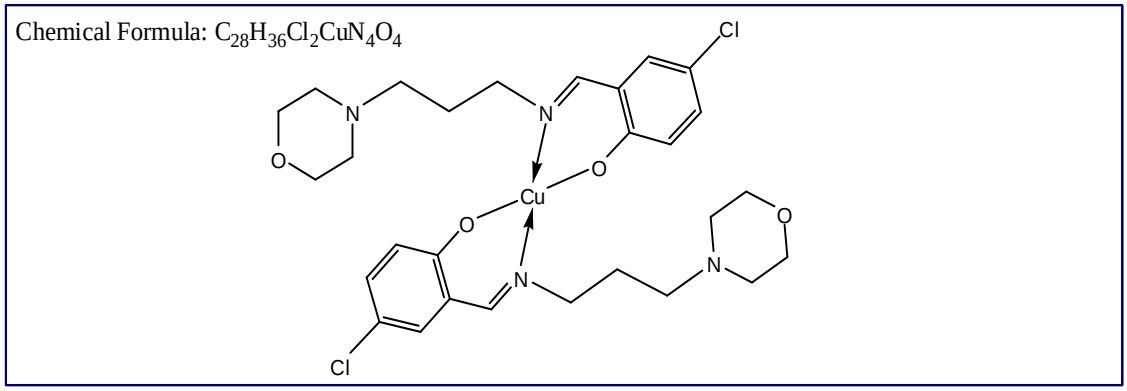

Figure 3.9: Proposed structure for [Cu(L^2)$_2$].

To a methanolic solution (15 mL) of an *in situ* prepared L^2H, a few drops of triethylamine were added followed by addition of a methanolic solution of $Cu(OAc)_2 \cdot H_2O$ (0.25 g, 1.23 mmol) at ambient temperature. During the addition, a dark green precipitate was formed. The precipitate was filtered off and the filtrate was left undisturbed at room temperature. After one week, the X-ray quality crystals were collected by filtration, washed with cold methanol and air dried.

Yield: 0.52 g, 68.1%. Anal. Calcd. for $C_{28}H_{36}Cl_2N_4O_4Cu$: C, 53.63%; H, 5.79%; N, 8.93%. Found: C, 53.56%; H, 5.82%; N, 8.91%. IR [ν max (cm^{-1}), KBr disc]: 2951w; 2858 w; 2808 w; 1624 s ($\nu_{C=N}$); 1455 s; 1312 m; 834 s; 720 s; 560 m; 478 w. UV-Vis [λ_{max} (nm), THF (ε, $mol^{-1}dm^3cm^{-1}$)] 246 (38735); 295 (8313); 307 (9157); 374 (9819); 597 (115).

3.5.8 **[Cu(L^2)Cl]·CH_3OH**

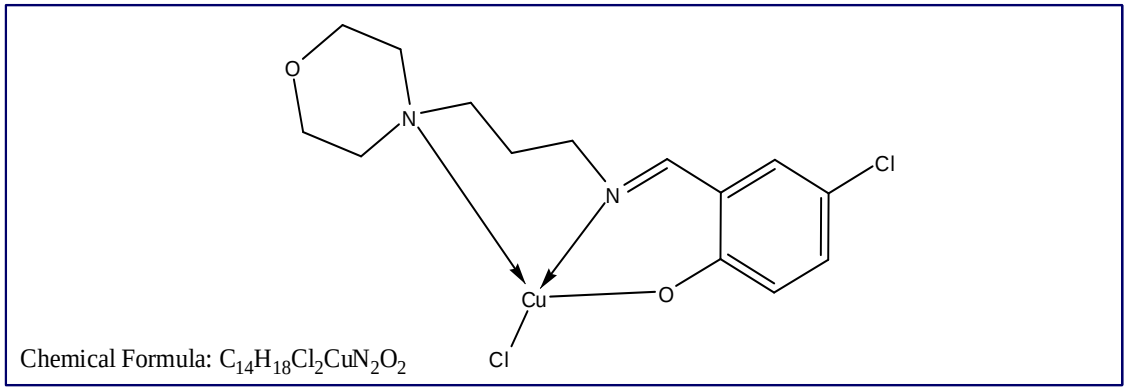

Figure 3.10: Proposed structure for [Cu(L^2)Cl]·CH_3OH.

A methanolic solution of $CuCl_2$ $2H_2O$ (0.42 g, 2.46 mmol) was added to an *in situ* prepared L^2H in methanol (15 mL) at room temperature. The mixture was stirred for 1 hour, and then left undisturbed at room temperature. The crystals suitable for crystallographic analysis were obtained after one week.

Yield: 0.71 g, 70.1%. Anal. Calcd. for $C_{15}H_{22}N_2O_3Cl_2Cu$: C, 43.64%; H, 5.37%; N, 6.79%. Found: C, 43.30%; H, 4.69%; N, 7.23%. IR [ν max (cm^{-1}), KBr disc]: 3440 m. (ν_{OH}); 2942 w; 2872 w; 1625 s ($\nu_{C=N}$); 1460 m; 1316 m; 1024 s; 850 m; 703 s; 562 w; 470 w. UV-Vis [λ_{max} (nm), THF (ε, $mol^{-1}dm^3cm^{-1}$)] 247 (22413); 295 (4932); 353 (6165); 377 sh; 559 (265); 772 (116).

3.5.9 **[Ni(L^2)$_2$]**

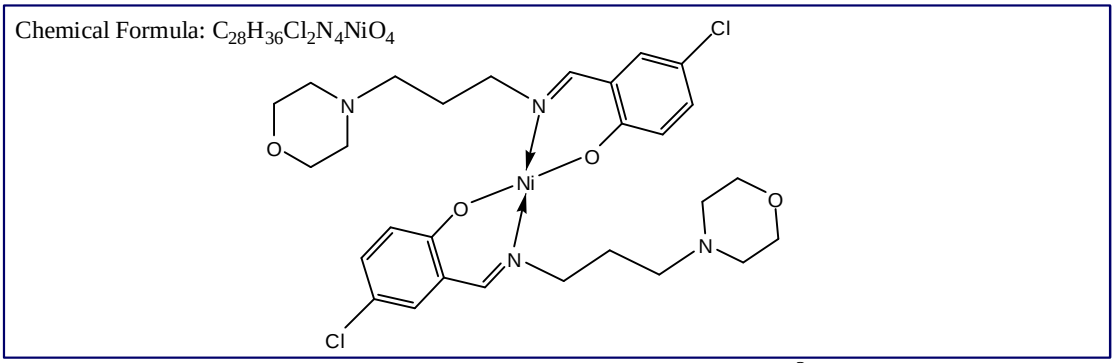

Figure 3.11: Proposed structure for [Ni(L^2)$_2$].

A few drops of triethylamine were added to a solution of the *in situ* prepared L^2H in ethanol (15mL) at ambient temperature. An equimolar ethanolic solution of $Ni(CH_3COO)_2 \cdot 4H_2O$ (0.31 g, 1.23 mmol) was added and the mixture was continued refluxing for one hour. The resulting mixture was left undisturbed at room temperature. The impure product was recrystallized from methanol to give green single crystal suitable for X-ray diffraction analysis.

0.49 g, 64.1 %. Anal. Calc. for $C_{28}H_{36}N_4O_4Cl_2Ni$: C, 54.05; H, 5.83; N, 9.00. Found: C, 53.96; H, 5.83; N, 8.91%. IR [ν max (cm^{-1}),KBr disc]: 2952 w; 2925 w; 2850 w; 1614 s ($\nu_{C=N}$); 1461 s; 1323 m; 822 s; 731 s; 549 w; 461 w. UV-Vis [λ_{max} (nm), THF (ε, $mol^{-1}dm^3cm^{-1}$)] 257 (18190); 290 (10191); 337 (9164); 415 (4897); 619 (79).

3.6 *Biological Screening Assay*

3.6.1 **Cytotoxicity assay**

The 3-(4,5-dimethylthiazol-2-yl)-2,5-diphenyl tetrazolium bromide (MTT) assay is an indirect colorimetric assay to assess the number of viable cells which has been adapted to measure the growth modulation of cells *in vitro*. The assay measures the amount of purple MTT formazan salt produced from metabolically cleaved yellow MTT tetrazolium salt. It has been established previously that the amount of MTT formazan salt produced is proportional to the amount of viable cells (Mosmann, 1983). The MTT formazan salt is dissolved in appropriate solvents and quantified spectrophotometrically.

The assay was adapted to 96-well plates. The cancer cells and normal cells per well was seeded one day before the introduction of test samples to allow for cell attachment. Cells were either seeded in 90 or 180 µl of growth media and treated with 10 or 20 µl of test compound, respectively. Vehicle dimethyl sulfoxide (DMSO) was used as a control. The test samples were prepared 10X more concentrated to account for the dilution. The cells were treated with the samples for 48 hours. At the end of treatment, 10 % (v/v) of MTT (5 mg/ml) was added into each well and incubated for 4 hours at 37 °C. The medium was then gently aspirated, and 150µl dimethyl sulfoxide (DMSO) was added to dissolve the formazan crystals. The amount of formazan product was measured spectrophotometrically at 570 nm (OD readings were referenced to 650 nm to eliminate background signals.). Cytotoxicity of compounds was tested against four different types of human cancer cell lines and one normal cell line. The cancer cell line are breast carcinoma (MCF-7 and MDA-MB-213) and colon carcinoma (HT-26), and leukimia (JURKAT). Whereas, the normal liver cells (WRL-68) and normal colon cells (CCD-841) are used to test the toxicity of the compound on healthy cell.

Growth inhibition of cells was calculated according to the following formula. A negative value indicates proliferation of cells compared to the blank or carrier. Otherwise, the value could be expressed as proliferation (%) if the OD_{sample} is higher than the OD_{blank}.

$$\text{Inhibition (\%)} = \frac{(OD_{blank} - OD_{sample})}{(OD_{blank})} \times 100\ \%$$

$$\text{Proliferation (\%)} = \frac{(OD_{sample} - OD_{blank})}{(OD_{blank})} \times 100\ \%$$

3.6.2 **Antioxidant - Ferric reducing antioxidant power (FRAP)**

The FRAP assay utilizes the antioxidant present in the sample as a reductant to reduce oxidant present in the reagent through a redox-linked colorimetric assay. The assay has been reported to be well suited for biological fluids, such as plasma and plant extracts, to assess their "antioxidant" activity (Benzie & Strain, 1996). This redox reaction occurs at a low pH. The ferric tripyridyltriazine (TPTZ- Fe^{3+}) complex is reduced to the ferrous form (TPTZ- Fe^{2+}) by electron donating antioxidants; the reduced complex is detected spectrophotometrically at 593 nm. Therefore, the reducing power of the sample may be referred as the total antioxidant power. The reaction is summarized as follows:-

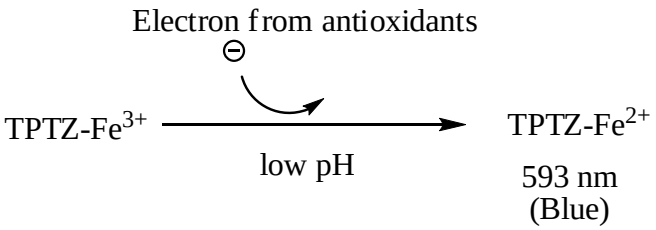

The FRAP reagent was prepared by combining 300 mM acetate buffer, 10 mM TPTZ solution in 40 mM HCl and 20 mM $FeCl_3.6H_2O$, at a ratio of 10:1:1. FRAP reagent was incubated at 37 ºC prior to use. Ten µl of sample reconstituted in carrier (solvent or ultrapure water) was mixed with 300 µl of FRAP reagent and the mixture was incubated at 37 ºC for 4

minutes in the microplate reader. Absorbance of the complex was read at 593 nm. Sample readings were referenced to the standard curve of ferrous sulphate heptahydrate, $FeSO_4 \cdot 7H_2O$. The FRAP value was expressed as mmol Fe^{2+}/100g sample

$$\text{FRAP value (mmol } Fe^{2+} \text{ / 100g sample)} = \frac{\mu M\ Fe^{2+}}{\mu g/ml \text{ sample}} = \frac{\mu mol/1000 \text{ ml } Fe^{2+}}{\mu g/ml \text{ sample}} = \frac{mmol\ Fe^{2+}}{100g \text{ sample}} \times 100$$

4.0 RESULTS AND DISCUSSION

The present study is based upon, two Schiff base ligands which can be prepared *via* the condensation reactions of *N*-(3-aminopropyl)morpholin with salicyclaldehyde (for L^1H) or 5-chlorosalicylaldehyde (for L^2H). Both ligands were obtained as yellow oil and characterized by elemental analyses, IR, ^{1}H-NMR, ^{13}C-NMR, and electronic spectra (UV-Vis). Although the ligands can be isolated and then used for the metal complexation, it was found more convenient to prepare them *in situ*. Treatment of the *in situ* prepared ligands with the appropriate divalent zinc, copper or nickel salts, in 1:1 or 2:1 ratio, led to the formation of the corresponding Schiff base metal complexes. The metal complexes have been characterized, both in the solid state and in solution, by a variety of techniques, including single-crystal X-ray diffraction analyses, IR, ^{1}H NMR, ^{13}C-NMR, and electronic spectra.

The Schiff ligands and their complexes are soluble in most polar solvents such as ethanol, methanol, tetrahydrofuran (THF), and dimethyl sulfoxide (DMSO) but they are insoluble in non-polar solvent such as chloroform.

4.1 *Characterizations of ligand, L^1H and its metal complexes*

4.1.1 Elemental analyses

The analytical data of L^1H, zinc, copper and nickel complexes are consistent with the proposed structures. Table 4.1 shows molecular formulae and microanalysis data of ligand, L^1H and its complexes.

Table 4.1: Analytical data of ligand, L^1H and its complexes.

Compound	Molecular Formulae	Elemental Compositions Percentage(%), Found (Calculated)		
		C	H	N
L^1H	$C_{14}H_{20}N_2O_2$	66.79 (67.71)	7.79 (8.12)	10.77 (11.28)
$[Zn(L^1)_2]$	$C_{28}H_{38}N_4O_4Zn$	60.25 (60.05)	7.05 (6.84)	10.03 (10.00)
$[Zn(L^1)_2Cl]$	$C_{14}H_{20}N_2O_2Cl_2Zn$	43.73 (43.72)	4.89 (5.24)	7.24 (7.28)
$[Cu(L^1)_2]$	$C_{28}H_{38}N_4O_4Cu$	60.25 (60.25)	7.05 (6.86)	10.03 (10.04)
$[Ni(L^1)_2]$	$C_{28}H_{38}N_4O_4Ni$	60.63 (60.78)	7.07 (6.92)	10.12 (10.13)

4.1.2 **IR Spectral Data**

The IR spectra of the free ligand and the complexes exhibit various bands in the 450-4000 cm^{-1} region. Table 4.2 shows some important vibrational bands for the IR spectra of ligand L^1H and its complexes.

The infrared spectrum provides information of the elucidation of functional groups attached to the investigated compounds. The characteristic vibration frequencies of the complexes on comparison with the free ligands reveal remarkable changes. The mode of coordination of the ligands are observed by the absence of the free hydroxyl group ν(O-H) band, shifting of imine ν(C=N) and ν(C-O) phenolic signals and also the formation of new metal-oxygen ν(M-O) and metal-nitrogen ν(M-N) bands. As pointed out by Percy and Thornton (1973), the ν(M-O) and ν(M-N) at lower frequency assignments are at times very difficult due to the interference with the vibration bands of the ligand.

IR spectrum of the free ligand shows a weak intensity broad band at frequency 3505 cm^{-1} assigned to ν(O-H) stretching (Mikhaylova *et. al.*, 2006). The broadness of the signal indicates the involvement of hydroxyl group in the intramolecular or intermolecular hydrogen bonding interaction (Denisov *et. al.*, 1997). The spectra exhibits very strong and sharp absorption band at 1630cm^{-1} attributed to the C=N stretching vibration (Gaballa *et. al.*, 2007). It was confirmed that the amino and carbonyl groups of the starting reagents have been converted into their corresponding Schiff base (Nakamoto, 1986; Leovoc *et. al.*, 2005).

Treatment of the *in situ* prepared ligands with the appropriate zinc, copper or nickel divalent salts, led to the formation of the corresponding Schiff base metal complexes. The complexation of the ligands is accompanied by shifts of IR ν(C=N) bands to lower or higher frequencies, implying the involvement of the azomethine N atoms in the coordination (Sang & Lin, 2010; El-Sonbati, 1991). This can be explained by donation of electrons from

nitrogen to empty *d*-orbitals of the metal ion (Aranha *et, al.*, 2007). In addition, the withdrawal of electron density from the nitrogen atom owing to co-ordination (Mustafa *et. al.*, 2009), indicate complexation with the metal center (Sarkar *et. al.*, 2008; Cukurovali *et. al.*, 2006; Yin *et. al.*, 2005).

Furthermore, the disappearance of a broad band, ν(O-H) vibration at around 3500 cm^{-1} indicate the deprotonation of the phenolic oxygen and cleavage of the hydrogen bond with involvement of the oxygen atom in bonding. Hence, the stretching vibration of the phenolic C-O group bands in IR spectra of the complexes was shifted about 20-30 cm^{-1} to higher frequencies compared to ν(C-O) in ligand L^1H (Martin *et. al.*, 1986). This confirms the participation phenolic oxygens in coordination, subsequent to deprotonation. The appearance of new bands in the region 564-609 cm^{-1} and 456-470 cm^{-1} which are assigned to ν(M-O) and ν(M-N) respectively (Deshmukh *et. al.*, 2010; Chandra *et. al.*, 2006). These bands show evidence regarding the bonding of the metal ion with the nitrogen and oxygen atom of the Schiff base ligands.

For the $[Zn(L^1)Cl_2]$ complex, broad bands appeared at 3397 cm^{-1} attributable to N-H at the morpholine ring (Appendix A.2).

In summary, the IR study shows that the ligand L^1H coordinates to metal ion via phenolic oxygen and imine nitrogen.

Table 4.2: Important IR data for L^1H and metal complexes.

Compound	Wavenumber (cm^{-1})						
	ν(O-H) / ν(N-H)	ν(C=N)	ν_{ar}(C=C)	ν(C-O)$_{ph}$	ν_{ar}(C-H)$_{bend}$	ν (M-O)	ν(M-N)
L^1H	3525 broad	1630 strong	1460 strong	1279 strong	759 medium	–	–
$[Zn(L^1)_2]$	–	1626 strong	1463 medium	1317 medium	759 medium	601 weak	462 weak
$[Zn(L^1)Cl_2]$	3397 broad	1636 strong	1445 strong	1303 strong	755 strong	564 medium	465 weak
$[Cu(L^1)_2]$	–	1613 strong	1445 strong	1330 strong	760 strong	609 weak	456 weak
$[Ni(L^1)_2]$	–	1607 strong	1447 strong	1332 strong	757 strong	599 medium	470 medium

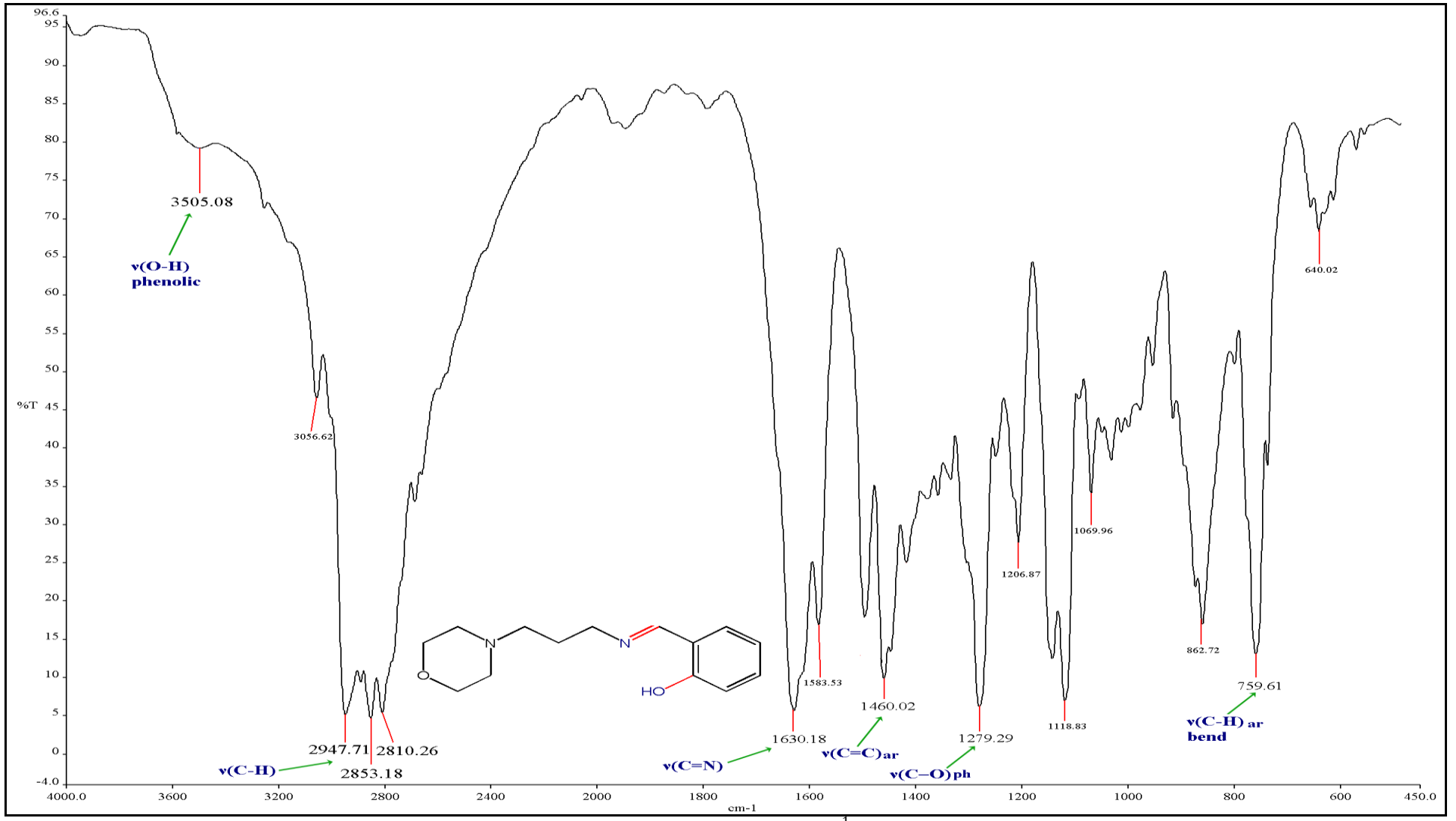

Figure 4.1: IR spectra for L^1H.

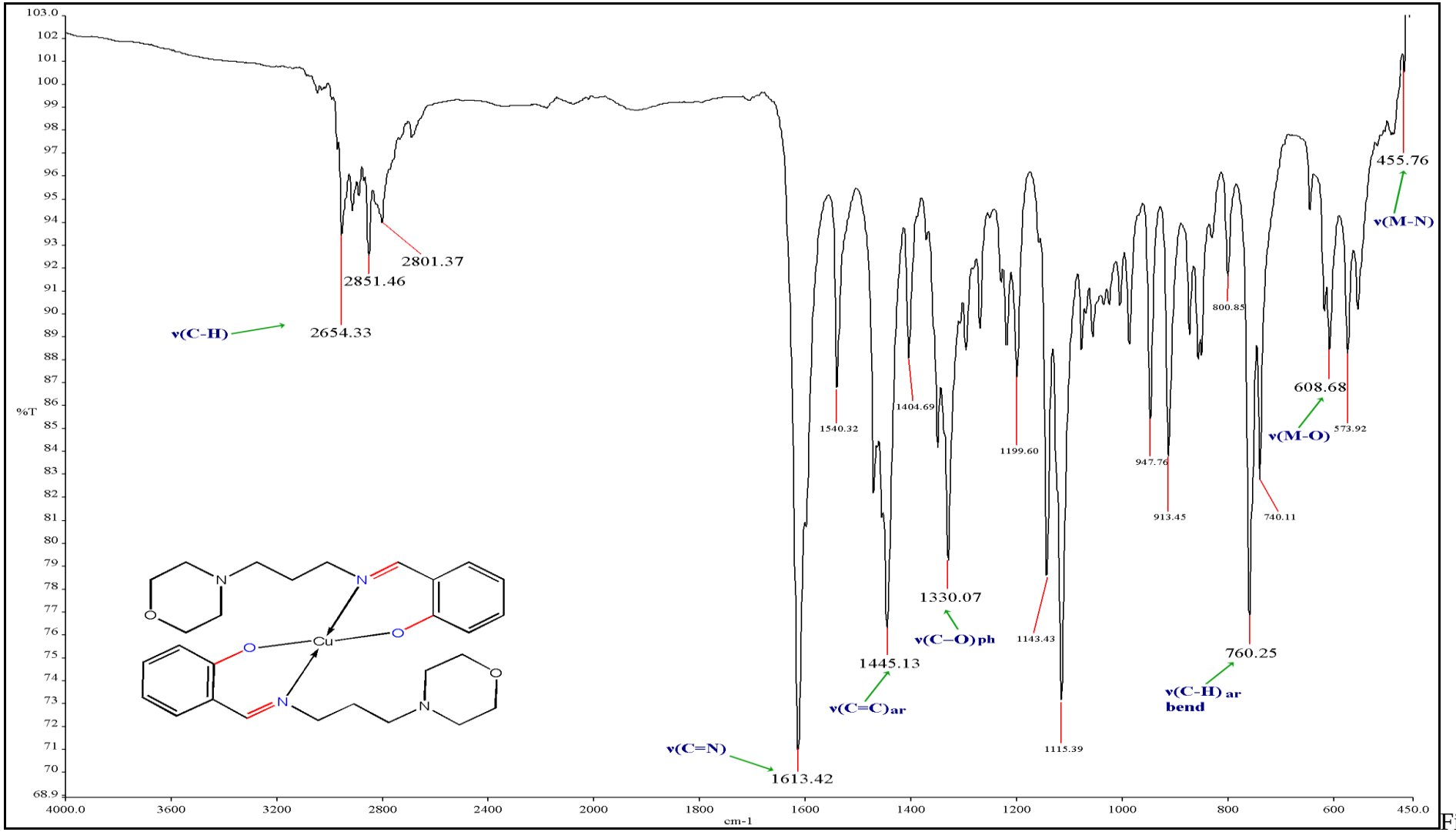

Figure 4.2: IR spectra for $[Cu(L^1)_2]$

4.1.3 ^{1}H NMR Spectral Data

The ^{1}H NMR spectral data of L^{1}H and its zinc(II) complexes were recorded in d_6-dimethylsulphoxide (DMSO-d_6) solution using tetramethylsilane (TMS) as internal reference. The spectral data were summarized in Table 4.3 and the spectrum given in Figures 4.3 and 4.4 respectively.

The ^{1}H NMR spectrum of the L^{1}H ligand with four different proton environments were observed, phenol hydrogens, azomethine hydrogens, aromatic hydrogens and also the aliphatic hydrogens. ^{1}H NMR data displays singlet signal at 13.65 ppm attributed to O-H proton of the phenolic group. Generally, the phenol proton was shifted downfield due to intramolecular hydrogen bonding (Bu *et. al.*, 1997). The singlet characteristic peak at 8.55 ppm was assigned to the imine *H*C=N hydrogen (Nelson *et. al.*, 1981). The aromatic protons of the Schiff base ligand appear in the region 7.42-6.90 ppm with integration value corresponding to four protons. The aliphatic peaks resonate at the most shielded range from 3.61-1.78 ppm. Based on the ^{1}H NMR data and the proposed structure, the ligand L^{1}H are successfully synthesized.

The complexation of the ligand with 1:1 or 2:1 ligand/metal ratios shows significant changes in the ^{1}H NMR spectra. The phenol hydrogens signals in the L^{1}H spectrum disappear in the spectrum of zinc(II) complexes, indicating the chelation of metal ion through phenolic oxygen upon deprotonation (Agarwala *et. al.*, 1994). This is supported by upfield shifts of the imine HC=N signals in spectra of the zinc complexes when compared to those of the free ligands (Szlyk *et. al.*, 2002). Whereas, for the [Zn(L^{1})$_2$Cl] complex the imine HC=N peak shifted to lowfield at 10.26 ppm due to the coordination of the imine nitrogen lone pair to the metal ion(Syamal & Maurya, 1989; Selvakumar & Vancheesan, 1995). This downfield shift is explained on the basis of the close proximity of the imine proton to the zinc(II) ion (Ustynyuk *et. al.*, 1971).The data also shows that aromatic

hydrogens, underwent slight shifting to higher field, whereas the aliphatic protons remain unchanged.

Briefly, loss of phenolic hydrogens and shifting of imine peaks demonstrated the divalent zinc ion chelate *via* nitrogen from azomethine and phenolic oxygen. Therefore, the L^1H has probably functioned as a *N*,*O*-bidentate ligand.

Table 4.3: ^{1}H-NMR spectral data of $L^{1}H$ and its zinc complexes.

Compound	Chemical Shift, δ(ppm)				Proton Numbering Scheme
	OH^{1}	$H^{2}C$=N	H Aromatic	H Aliphatic	
$L^{1}H$	13.65	8.55	7.42–6.90	3.61–1.78	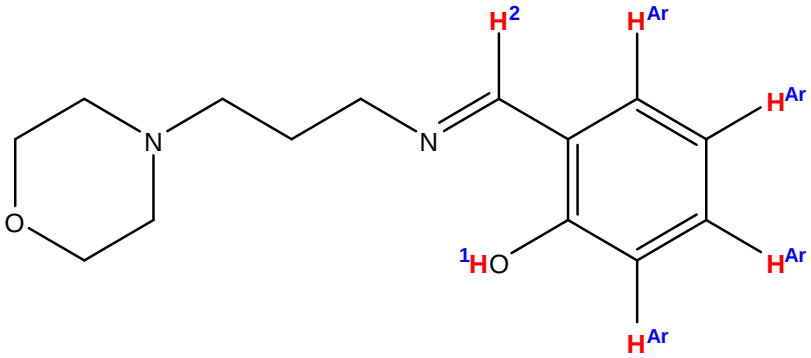
$[Zn(L^{1})_2]$		8.47	7.27–6.50	3.60–1.24	
$[Zn(L^{1})_2Cl_2]$		10.26	7.66-6.98	3.60-2.09	

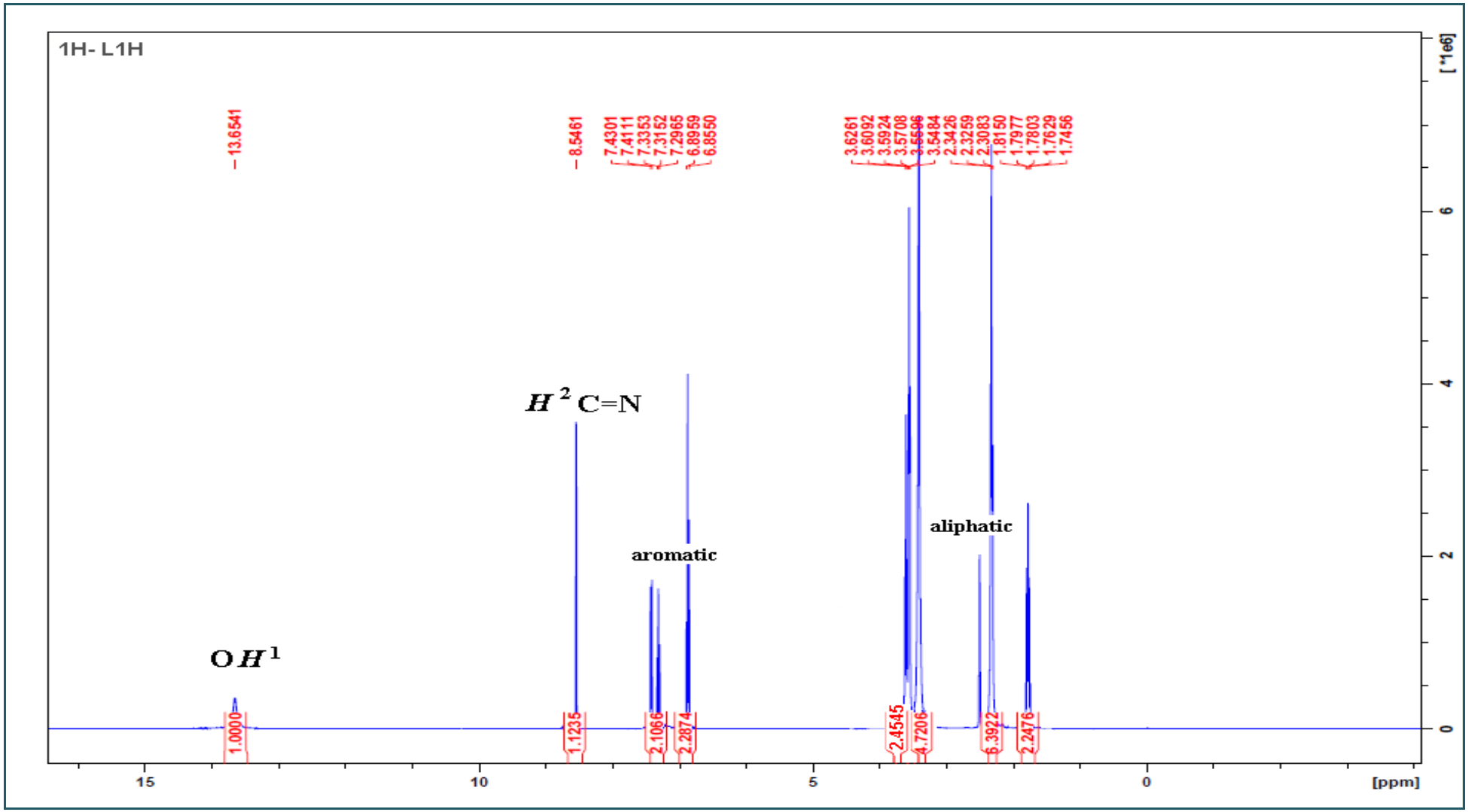

Figure 4.3: ^{1}H-NMR spectra for L^{1}H.

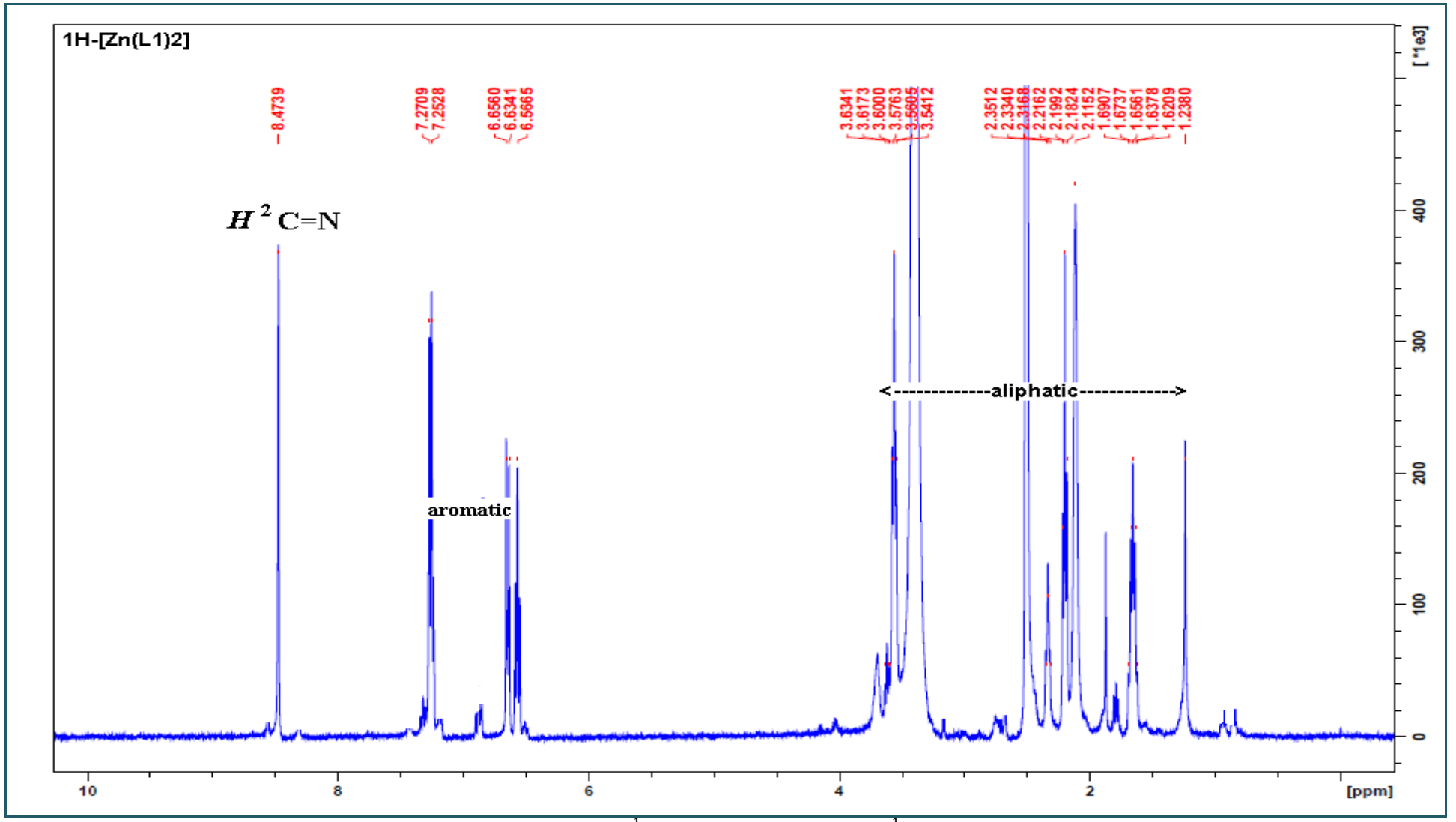

Figure 4.4: ^{1}H-NMR spectra for [Zn(L^{1})$_2$].

4.1.4 ^{13}C-NMR Spectral Data

The ^{13}C-NMR spectral data of the Schiff base ligand (L^1H) and its zinc(II) complexes were recorded in d_6-dimethylsulphoxide (DMSO-d_6) solution. The spectrums are given in Figure 4.5, 4.6 respectively and the spectral data are tabulated in Table 4.4.

The spectrum exhibits 12 signals attributed to 12 different types of carbon environment. The azomethine carbon H*C*=N resonates at 160.9 ppm and the aromatic carbons attached to the hydroxyl groups appear in the most downfield peak at 164.8 ppm. The analogous Schiff base carbon atoms bonded to the nitrogen is of the sp^2 type which is expected to resonate at about 160 ppm (Bocâ *et. al.*, 2000). The spectrum display downfield shifts of the ligand HC=N resonances upon complexation with Zn(II). Loss of phenolic hydrogen atoms in ^{1}H NMR spectra and downfield shifts of C-O resonances in ^{13}C NMR spectra of the zinc complexes, further suggest participation of the phenolate in metal coordination. The chemical shift in region 136-110 ppm clearly assigned to carbon at the aromatic rings. Besides, the aliphatic carbon indicated by the peaks at the range 66-25 ppm in spectra of the ligand and the zinc(II) complexes.

Nevertheless, the $[Zn(L^1)Cl_2]$ complex shows upfield shifting of the imine HC=N due to the zinc(II) ions attached to two chlorides atoms. The chlorides atom have high electron density, thus it increases the shielding effect of the carbon atom (Ning, 2011).

In summary, these results implied that ligand L^1H coordinated to zinc ions through the phenol oxygen and azomethine nitrogen, which has also been concluded from IR and ^{1}H NMR spectral studies.

Table 4.4: ^{13}C-NMR spectral data of L^1H and its zinc complexes.

Compound	Chemical Shift, δ(ppm)				Carbon Numbering Scheme
	C–OH	H*C*^{1}=N	H $_{Aromatic}$	H $_{Aliphatic}$	
L^1H	165.84	160.91	132.2–116.5	66.1–27.1	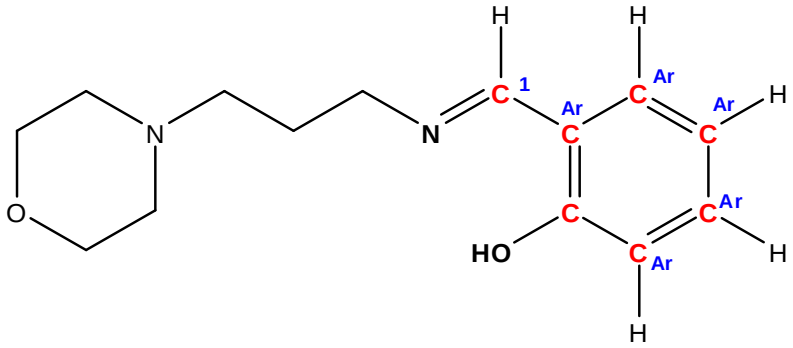
$[Zn(L^1)_2]$		167.77	135.9–113.9	66.0–26.7	
$[Zn(L^1)_2Cl]$		136.39	129.27-117.19	65.99-23.37	

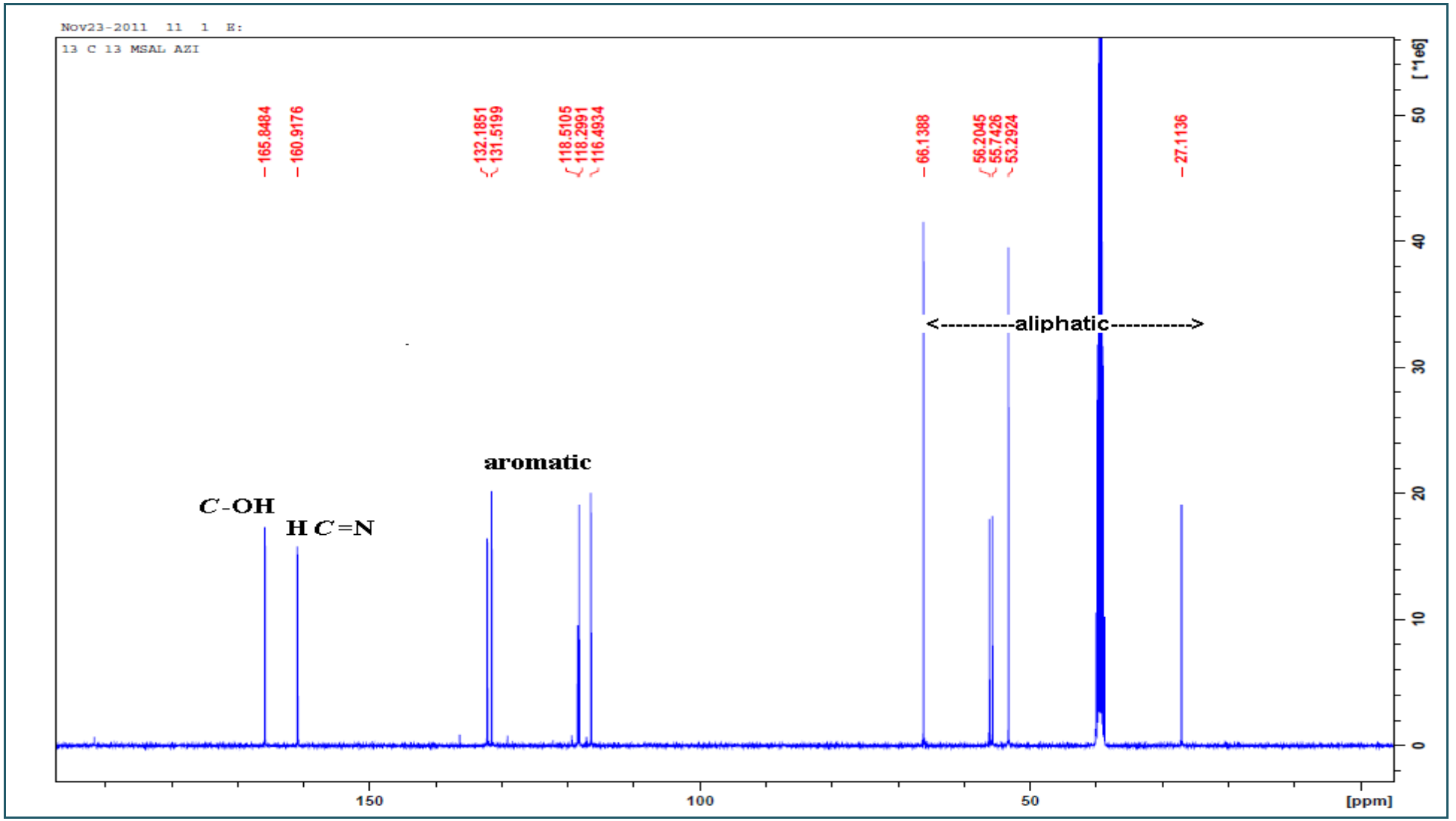

Figure 4.5: ^{13}C-NMR spectra for L^{1}H.

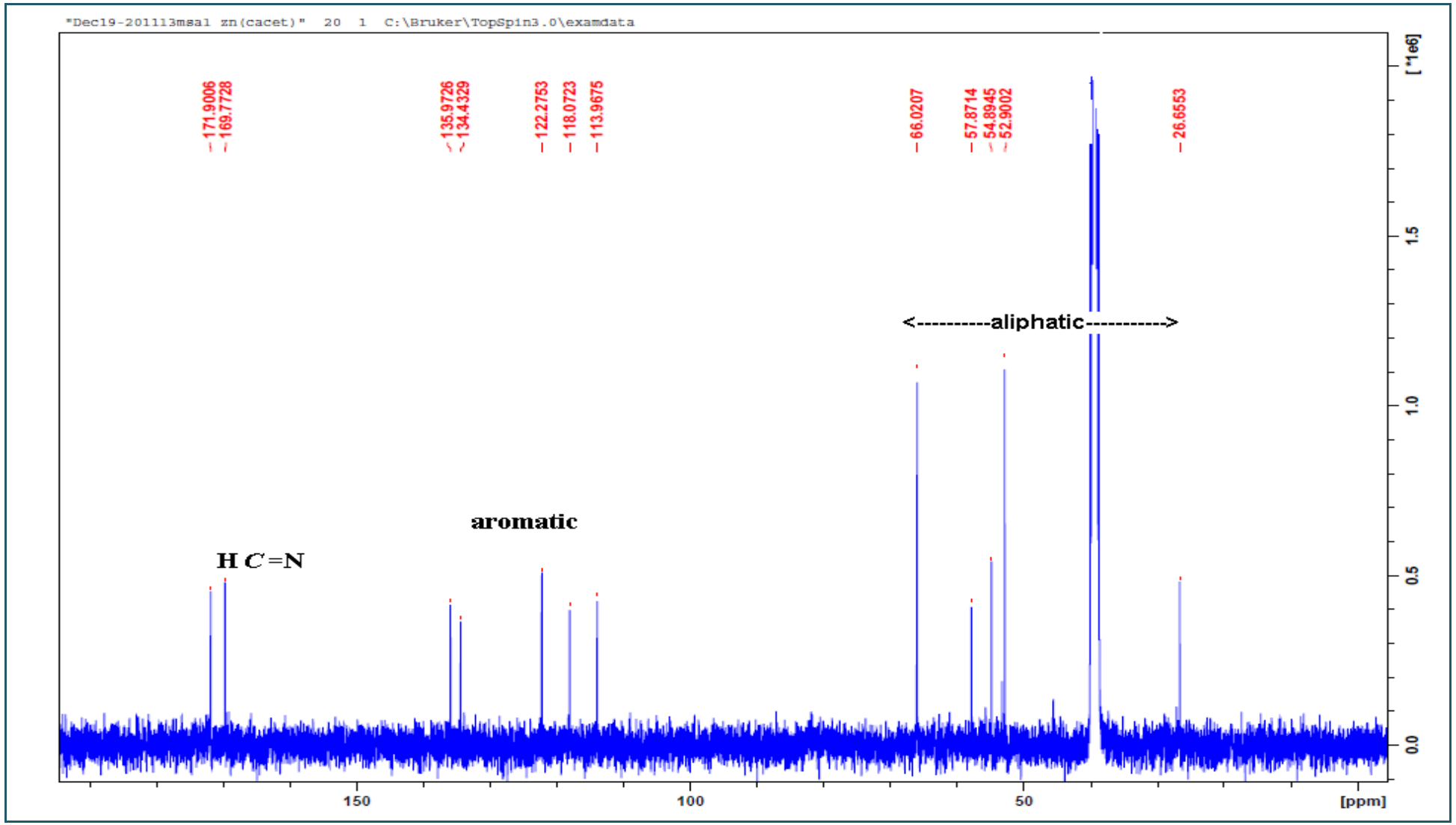

Figure 4.6: ^{13}C-NMR spectra for [Zn(L^1)$_2$].

4.1.5 **UV-Vis spectra**

The electronic absorption of the L1H and its divalent Cu(II) and Ni(II) chelates have been recorded in THF and their corresponding data are listed in Table 4.5.

The Schiff base ligand electronic spectra shows an intense bands at 255 ppm attributed to intraligand π→π* transition of the aromatic ring. The absorption at 316 ppm assigned to n→π* transition involving molecular orbitals of C=N chromophore (Tas *et. al.*, 2010). These absorptions also appear in the spectra of the complexes with different energy and intensity which most likely originates from the metalation. Hence, these increases the conjugation and delocalization of the whole electronic system resulting in the energy change of π→π* and n→π* transitions (Kalanithia *et. al.*, 2012).

The spectrum of Cu(II) complex exhibit π→π* and n→π* transitions bands at the higher energy due to hypsochromic shift, confirming the complexation (Lu *et. al.*, 2000). The presence of new absorption band at 307 nm assignable to the charge transfer transition of the ligand to metal (LMCT) between the lone pair of phenolate oxygen donor and the Cu(II) ions. This further confirms the coordination of ligand toward the metal ions (Vanco *et. al.*, 2008). Moreover, the complex spectrum displays bands at 364 nm and 619 nm. This band corresponds to *d-d* transitions which are attributed to $^2B_{1g}\rightarrow{}^2E_g$ and $^2B_{1g}\rightarrow{}^2B_{2g}$ transitions respectively. Therefore, these indicate the possibility of the square planar geometry for this complex (Chandra *et. al.*, 2009).

In the Ni(II) complex spectra, the intense absorptions assigned to π→π* and n→π* transitions bands shifted to the higher energy (red shift) upon complexation (Lu et. al., 2000).The LMCT transition appears at 326 ppm indicates the chelation within the lone pair of phenolate oxygen donor and the metal ions (Vanco *et. al.*, 2008).

Spectrum of the nickel complex shows an absorption band at 614 nm, assignable to a $^1A_{1g} \rightarrow {}^1A_{2g}$ transition and a shoulder band at 413 nm attributed to the $^1A_{1g} \rightarrow {}^1B_{1g}$ transition in the Molecular Orbital. Thus, these suggest the nickel complex exhibit a square planar stereochemistry (Singh *et. al.*, 2007).

In summary from the electronic spectra, the charge transfer and the *d-d* transition in complexes have provides evidence suggesting that the complexes form four-coordinate. The Cu(II) and Ni(II) complexes are most likely a square planar geometry (Chandra et. al., 2009; Singh *et. al.*, 2007).

Table 4.5: UV-Visible spectral data for L^1H and its complexes.

Compound	λ_{max} (nm)	λ_{max} (cm^{-1})	ε_{max} ($mol^{-1}dm^3cm^{-1}$)	Assignment
L^1H	255	39216	11794	$\pi \rightarrow \pi^*$
	316	31646	4568	$n \rightarrow \pi^*$
$[Cu(L^1)_2]$	245	40816	37185	$\pi \rightarrow \pi^*$
	296	33784	7363	$n \rightarrow \pi^*$
	307	32573	10158	LMCT
	364	27473	11836	*d-d* transition $^2B_{1g} \rightarrow {}^2E_g$
	619	16155	112	*d-d* transition $^2B_{1g} \rightarrow {}^2B_{2g}$
$[Ni(L^1)_2]$	245	40816	19703	$\pi \rightarrow \pi^*$
	266	37594	13028	$n \rightarrow \pi^*$
	326	30675	3312	LMCT
	413	24213	1751	*d-d* transition $^1A_{1g} \rightarrow {}^1B_{1g}$
	614	16287	75	*d-d* transition $^1A_{1g} \rightarrow {}^1A_{2g}$

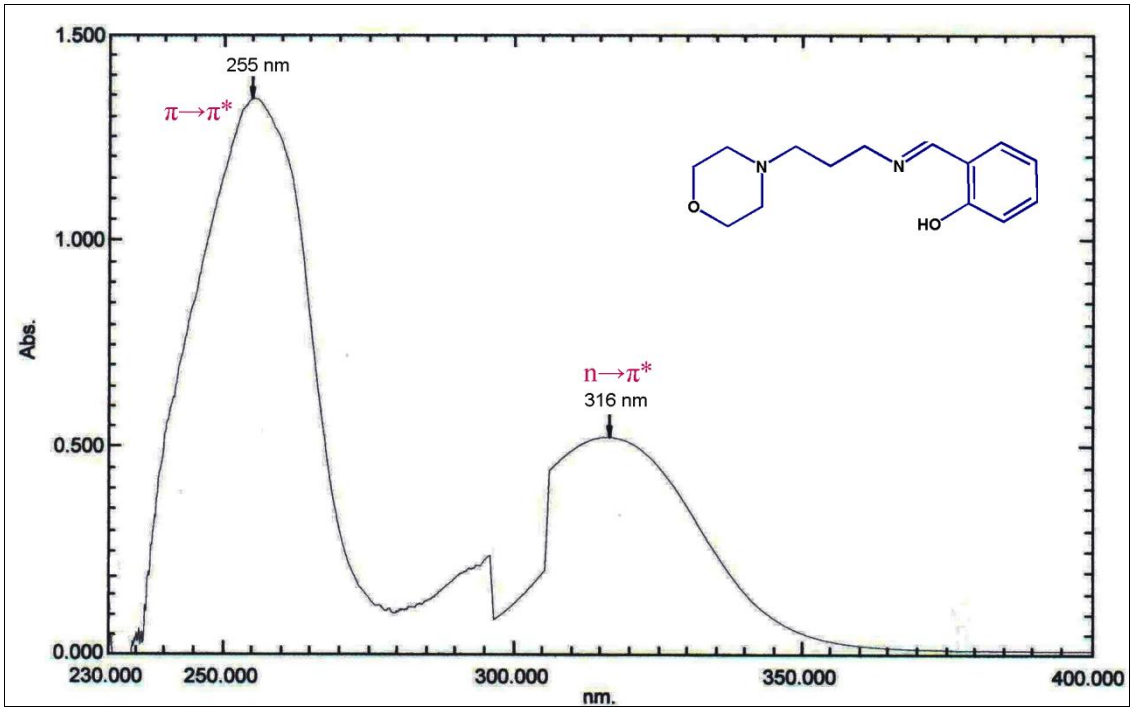

Figure 4.7: UV-Vis spectra for L^1H.

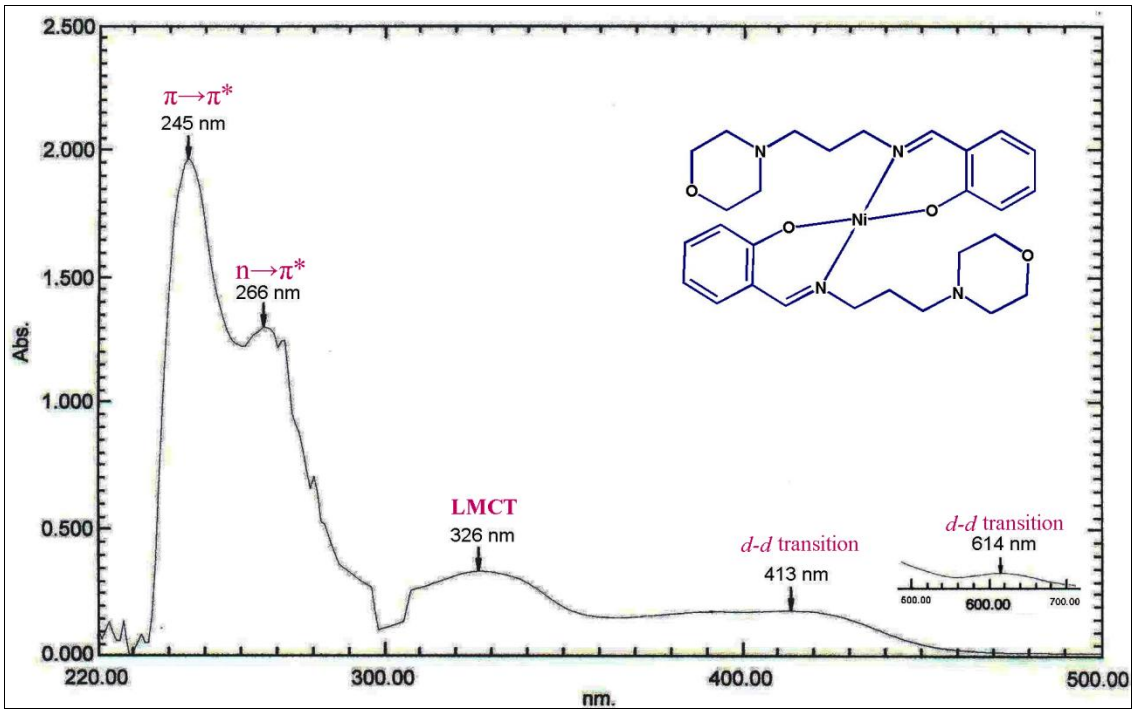

Figure 4.8: UV-Vis spectra for $[Ni(L^1)_2]$.

4.1.6 **X-ray Crystallographic Data Collection**

The complexes of L^1 crystal data and refinement are summarized in Table 4.6.

4.1.6.1 *Crystal structure of [Zn(L^1)$_2$]*

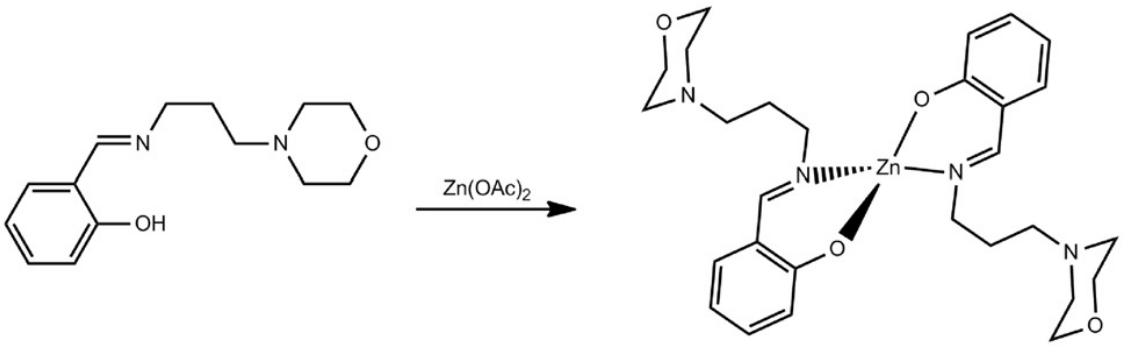

Scheme 4.1: Synthesis of [Zn(L^1)$_2$].

Crystals of [Zn(L^1)$_2$] were obtained through the reaction of L^1H with zinc(II) acetate in a 2 : 1 ratio (scheme 4.1). As depicted in figure 4.9, the deprotonated Schiff base, L^1, chelates Zn(II) via phenolate oxygen and imine nitrogen. The metal is on a crystallographic two-fold rotational axis of symmetry and is four-coordinate by two mono-anionic ligands to form two six-membered chelating rings. The dihedral angle between the two rings is 79.61(7)˚ and the coordination geometry can be best described as a distorted tetrahedron. Table 4.7 lists selected bond lengths and angles for the structure. The Zn–O and Zn–N distances of 1.9221(14) and 1.9916(16) Å are comparable with values reported for similar structures (Torzilli *et. al.*, 2002; Schon *et. al.*, 2004; Pastor *et. al.*, 2011).

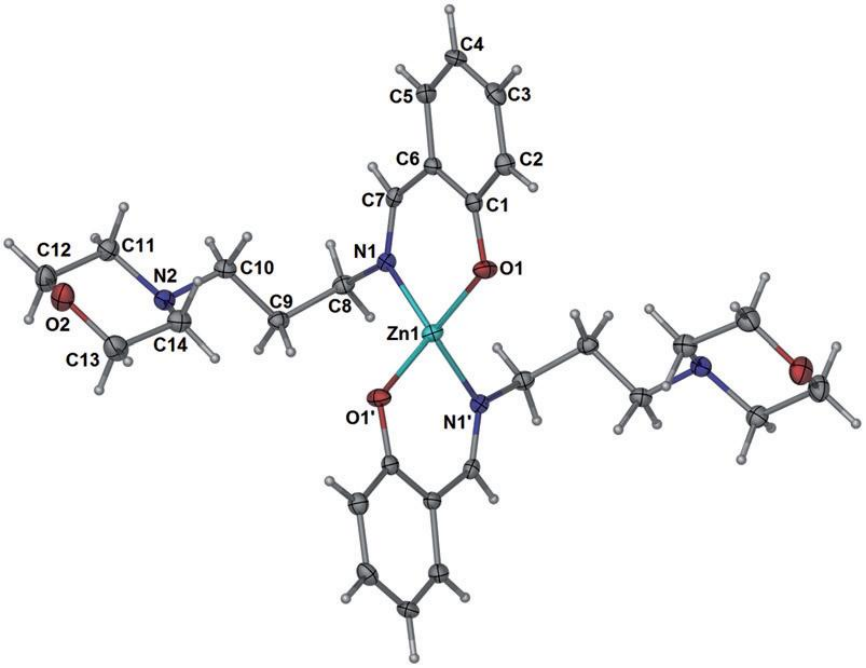

Figure 4.9: The crystal structure and atom-labeling scheme of $[Zn(L^1)_2]$ (50% probability ellipsoids). The two-fold rotation axis is perpendicular to the plane of the paper.

4.1.6.2 *Crystal structure of* $[Zn(L^1)Cl_2]$

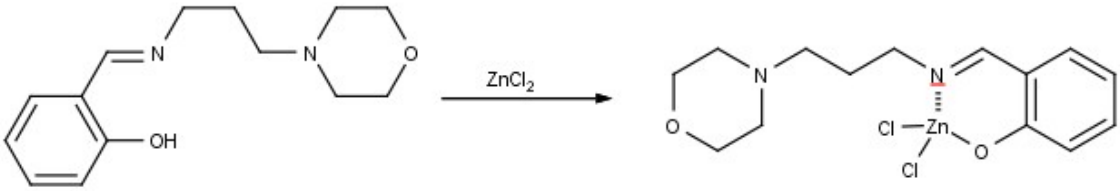

Scheme 4.2: Synthesis of $[Zn(L^1)Cl_2]$.

The $[Zn(L^1)Cl_2]$ complex was obtained via the complexation of $ZnCl_2$ with the *in situ* prepared Schiff base. The Schiff base ligand coordinates the metal ion via its phenolate oxygen and imine nitrogen atoms. The morpholine ring N atom stays away from the coordination and is protonated, implying the zwitterionic nature of the molecule. The tetrahedral geometry around the zinc(II) ion is completed by two Cl atoms. The coordination bond lengths in the complex are comparable to the corresponding values in similar structures (Qui, 2006; Ye & You, 2008; Zhu, 2008). In the crystal, N—H···O hydrogen bonding connects pairs of the molecules into centrosymmetric dimers. The

dimers are linked through C—H···O, C—H···Cl and C—H···π interactions into a three-dimensional network.

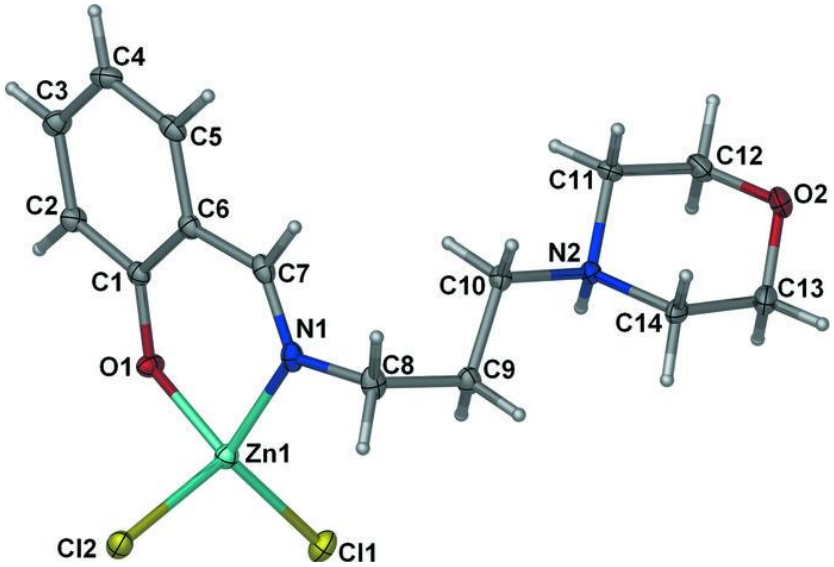

Figure 4.10: The crystal structure and atom-labeling scheme of $[Zn(L^1)Cl_2]$ (50% probability ellipsoids). Hydrogen atoms are drawn as spheres of arbitrary radius.

4.1.6.3 *Crystal structure of* $[Cu(L^1)_2]$

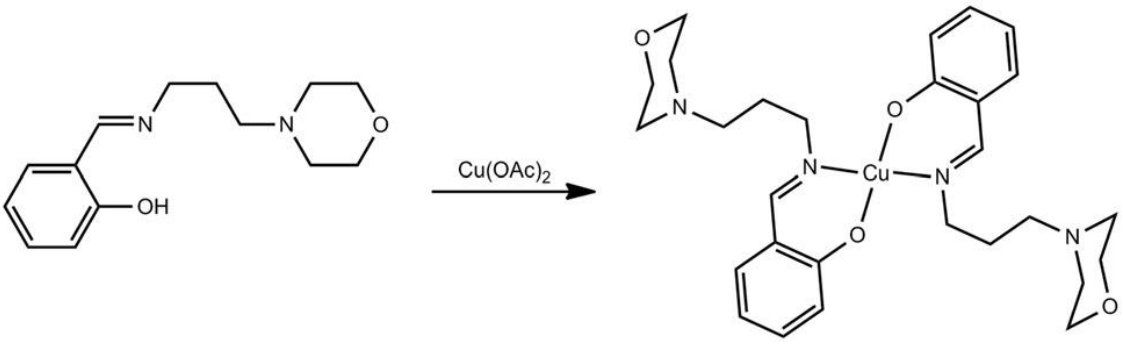

Scheme 4.3: Synthesis of $[Cu(L^1)_2]$.

The reaction of L^1H with copper(II) acetate in a 2 : 1 ratio led to the formation of $[Cu(L^1)_2]$ (scheme 4.3). As shown in Figure 4.11, the copperis placed on a centre of inversion and is four-coordinate by two deprotonated Schiff bases, L^1, in a square- planar environment. The ligand uses phenolate oxygen and imine nitrogen to chelate. The morpholine ring adopts a chair conformation and its nitrogen and oxygen atoms stay away

from coordination. Deviations from ideal square-planar geometry are reflected in the O1–Cu1–N1 bite angle of 91.50(5)°. For four-coordinate Cu(II) complexes, bis-chelated by salicylaldimine ligands, both tetrahedral (Dhar *et. al.*, 2003; Fernandez *et. al.*, 2010) and square-planar (Chen *et. al.*, 2005; You & Chi, 2006) geometries have been observed. There is an example wherein the unit cell of the structure of a salicylaldimine Cu(II) complex contains both square-planar and flattened tetrahedral structures (Polishchuk *et. al.*, 1986).

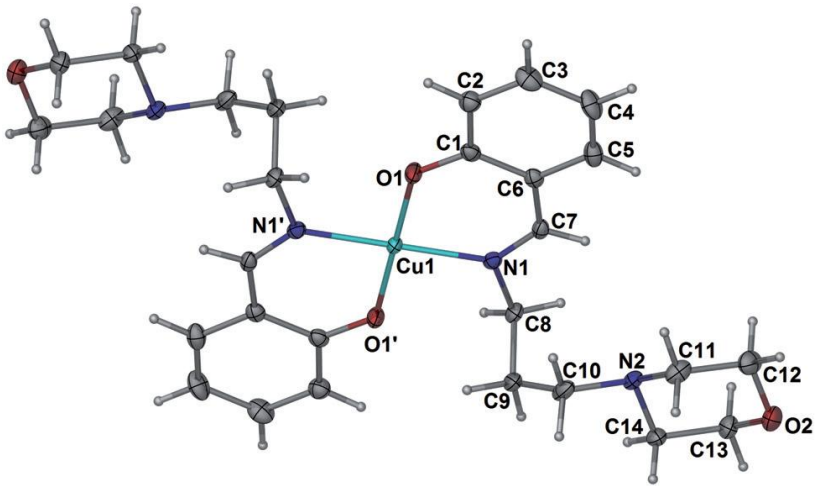

Figure 4.11: The crystal structure and atom-labeling scheme of $[Cu(L^1)_2]$ (50% probability ellipsoids).

4.1.6.4 *Crystal structure of* $[Ni(L^1)_2]$

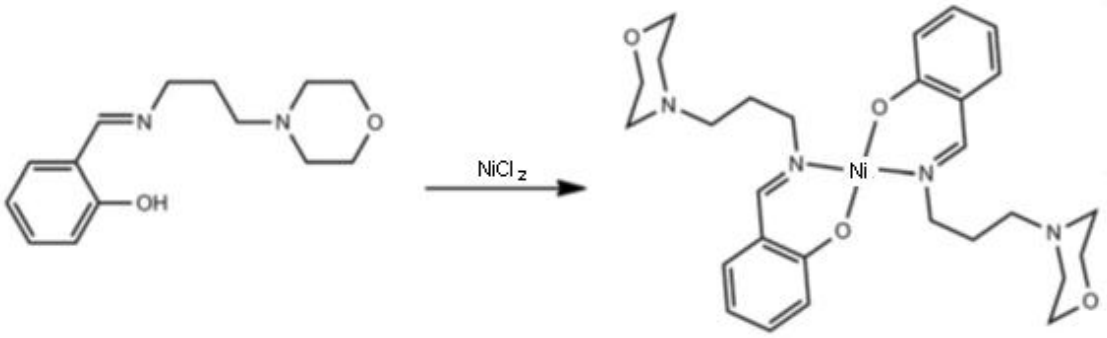

Scheme 4.4: Synthesis of $[Ni(L^1)_2]$.

The crystal structure is represented in Figure 4.12 and selected bond lengths and angles are given in Table 4.7. The nickel, located on a centre of is four-coordinate in a distorted square plane geometry defined by two N,O-bidentate mono-anionic L^1.

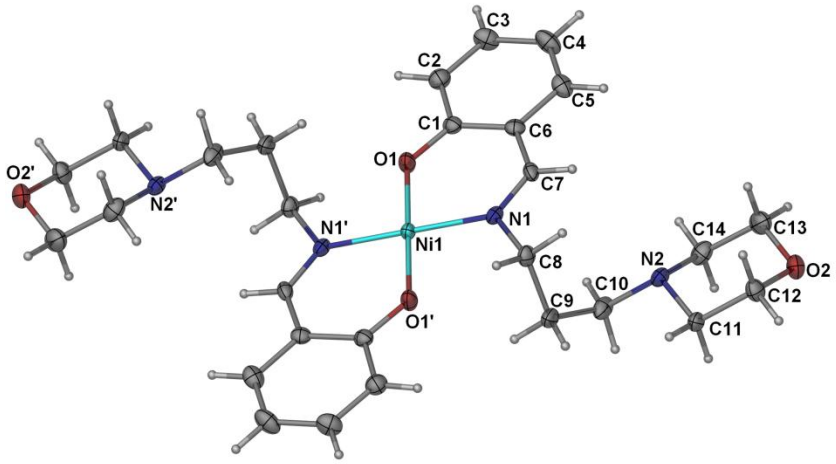

Figure 4.12: The crystal structure and atom-labelling scheme of $[Ni(L^1)_2]$ (50% probability ellipsoids).

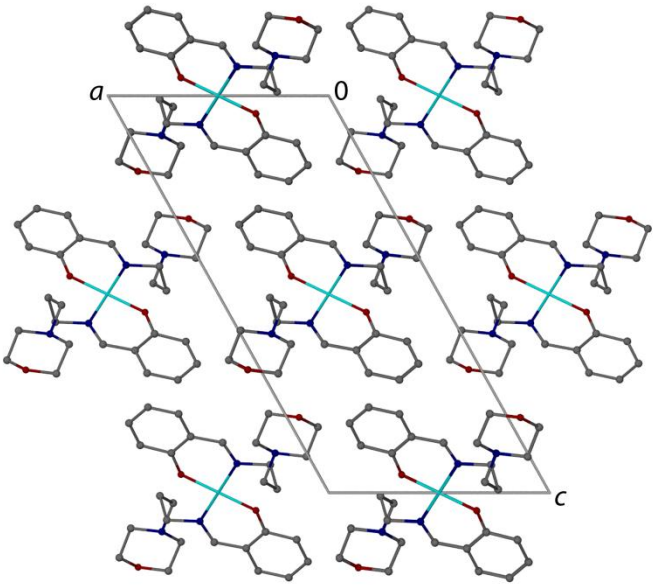

Figure 4.13: The crystal packing structure $[Ni(L^1)_2]$ along b-axis.

Table 4.6: Crystal data and refinement parameters for $\mathbf{L^1}$ complexes.

	$\mathbf{[Zn(L^1)_2]}$	$\mathbf{[Zn(L^1)Cl_2]}$	$\mathbf{[Cu(L^1)_2]}$	$\mathbf{[Ni(L^1)_2]}$
Empirical formula	$C_{28}\ H_{38}\ N_4\ O_4\ Zn$	$C_{14}\ H_{20}\ Cl_2\ N_2\ O_2\ Zn$	$C_{28}\ H_{38}\ Cu\ N_4\ O_4$	$C_{28}\ H_{38}\ N_4\ Ni\ O_4$
Crystal system	Orthorhombic	Monoclinic	Monoclinic	Monoclinic
Space group	*F d d 2*	*P 21/c*	*P 21/n*	*P 21/n*
Unit cell dimensions				
a (Å)	19.7143(12)	8.11276 (10)	9.6854(3)	9.7050(2)
b (Å)	48.358(3)	11.21021 (13)	7.9100(3)	7.9293(2)
c (Å)	5.5790(4)	18.4097 (2)	17.6325(2)	19.9434(4)
β (°)		92.0168 (6)	90.067(3)	119.1190(10)
Volume ($Å^3$)	5318.7(6)	1673.24 (4)	1350.85(3)	1340.75(5)
Z	8	4	2	2
Density (calculated) (g cm^{-3})	1.399	1.527	1.372	1.371
Crystal size (mm^3)	0.26 x 0.11 x 0.05	0.37 × 0.32 × 0.25	0.26 x 0.19 x 0.11	0.21 x 0.13 x 0.09
θ range for data collection (°)	2.23 to 26.76	2.2 to 30.4	2.31 to 27.00	2.34 to 24.99
Reflections collected	11709	9373	9091	2358
Independent reflections	2816 [R_{int} = 0.0407]	3557 [R_{int} = 0.017]	2932 [R_{int} = 0.0262]	2358 [R_{int} = 0.0000]
Completeness	To *θ* = 26.77° : 99.9 %	To *θ* = 26.77° : 99.9 %	To *θ* = 27.50° : 99.4 %	To *θ* = 24.99° : 99.9 %
Data / restraints / parameters	2816 / 1 / 168	2824 / 1 / 193	2932 / 0 / 169	2358 / 0 / 170
Goodness-of-fit on F^2	1.040	1.070	1.035	1.040
Final *R* indices [$I > 2\sigma$ (I)]	R_1 = 0.0268, wR_2 = 0.0579	R_1 = 0.0200, wR_2 = 0.0510	R_1 = 0.0304, wR_2= 0.0757	R_1 = 0.0280, wR_2= 0.0673
R indices (all data)	R_1 = 0.0303, wR_2 = 0.0592		R_1 = 0.0367, wR_2= 0.0787	R_1 = 0.0301, wR_2= 0.0690

Table 4.7: Selected bond lengths (Å) and bond angles (°) for $\mathbf{L^1}$ complexes.

$[Zn(L^1)_2]$		**$[Zn(L^1)Cl_2]$**		**$[Cu(L^1)_2]$**		**$[Ni(L^1)_2]$**	
Bond lengths							
Zn(1)-O(1)	1.9221(14)	Zn(1)-O(1)	1.9644 (9)	Cu(1)-O(1)	1.8908(12)	Ni(1)-O(1)	1.8355(17)
Zn(1)-N(1)	1.9916(16)	Zn(1)-N(1)	2.0049 (11)	Cu(1)-N(1)	2.0029(14)	Ni(1)-N(1)	1.9214(19)
O(1)-C(1)	1.319(2)	Zn(1)-Cl(1)	2.2206 (3)	O(1)-C(1)	1.308(2)	O(1)-C(1)	1.299(3)
N(1)-C(7)	1.285(2)	Zn(1)-Cl(2)	2.2570 (3)	N(1)-C(7)	1.294(2)	N(1)-C(7)	1.292(3)
		O(1)-C(1)	1.3254(15)				
		N(1)-C(7)	1.2825(17)				
Bond angles							
O(1)-Zn(1)-O(1)#1	113.70(9)	O(1)-Zn(1)-N(1)	95.72(4)	O(1)#2-Cu(1)-O(1)	180.0	O(1)-Ni(1)-O(1)#1	180.00(5)
O(1)-Zn(1)-N(1)	96.18(6)	O(1)-Zn(1)-Cl(1)	112.95(3)	O(1)-Cu(1)-N(1)#2	88.50(5)	O(1)-Ni(1)-N(1)	92.63(8)
O(1)-Zn(1)-N(1)#1	120.66(6)	O(1)-Zn(1)-Cl(2)	105.87(3)	O(1)-Cu(1)-N(1)	91.50(5)	O(1)-Ni(1)-N(1)#1	87.37(8)
N(1)-Zn(1)-N(1)#1	111.23(9)	N(1)-Zn(1)-Cl(1)	112.96(3)	N(1)#2-Cu(1)-N(1)	180.0	N(1)-Ni(1)-N(1)#1	180.0
		N(1)-Zn(1)-Cl(2)	112.88(3)				
		Cl(1)-Zn(1)-Cl(2)	112.363(13)				

Symmetry transformations used to generate equivalent atoms: #1 -*x*+1,-*y*+2, *z*; #2 -*x*+1,-*y*+2,-*z*

4.2 *Characterizations of ligand, L^2H and its metal complexes*

4.2.1 Elemental analyses

Table 4.8 shows molecular formulae and the analytical data of ligand L^2H, zinc, copper and nickel complexes. The microanalysis data are in a good agreement with the proposed formulations. Based on elemental compositions values, some of the complexes have molecule of water and methanol are found outside the coordination sphere.

Table 4.8: Analytical data of ligand, L^2H and its complexes.

Compound	Molecular Formulae	Elemental Compositions Percentage (%), Found (Calculated)		
		C	H	N
L^2H	$C_{14}H_{19}N_2O_2Cl$	60.63 (59.47)	7.07 (6.77)	10.12 (9.91)
$[Zn(L^2)_2]\cdot 3H_2O$	$C_{28}H_{42}N_4O_7Cl_2Zn$	49.24 (49.24)	6.19 (6.20)	8.20 (8.20)
$[Zn(L^2)(OAc)]$	$C_{16}H_{21}N_2O_4ClZn$	47.43 (47.31)	5.05 (5.21)	6.85 (6.90)
$[Cu(L^2)_2]$	$C_{28}H_{36}N_4O_4Cl_2Cu$	53.56 (53.63)	5.82 (5.79)	8.91 (8.93)
$[Cu(L^2)Cl]\cdot CH_3OH$	$C_{15}H_{22}Cl_2CuN_2O_3$	43.30 (43.64)	4.69 (5.37)	7.23 (6.79)
$[Ni(L^2)_2]$	$C_{28}H_{36}N_4O_4Cl_2Ni$	53.96 (54.05)	5.82 (5.83)	8.91 (9.00)

4.2.2 **IR Spectral Data**

The important feature of solid IR spectra of ligand, L^2H and its Zn(II), Cu(II) and Ni(II) complexes are summarized in Table 4.9.

The coordination of the ligand to the metal centre is based by comparing the IR spectra of the Schiff base complexes with the free ligand. The vibrational bands of the complexes are similar to the ligand and additional of two new bands correspond to the formation of the metal-ligand bond. The interference of signals of the free ligand, complicates the assignment of the ν(M-O) and ν(M-N) bands (Percy & Thornton, 1973).

The synthesized Schiff base ligand which gave oily products exhibits a strong intensity absorption band of the azomethine ν(C=N) groups at 1636 cm^{-1} that formed *via* condensation of morpholine and chlorosalicyclaldehyde (Gaballa *et. al.*, 2007). In addition, a frequency band at 3384 cm^{-1} which is attributed to ν(O-H) stretching from chlorosalicyclaldehyde (Mikhaylova *et. al.*, 2006), further indicates the absence of the amino group from the morpholine.

Treatment of the ligands with the corresponding metal salts, accompanied by deprotonation upon complexation, led to the coordination of the metal ion through the oxygen atom of the chlorosalicylaldehyde hydroxyl group. The deprotonation of the phenolic group is confirmed by the disappearance of the phenolic O-H stretching bands in the spectrum of the complexes. Furthermore, stretching vibration of the phenolic ν(C-O) groups occur at higher frequencies as compared to L^2H spectra. The shifting to the higher energy suggested the chelation of metal(II) ions to phenolic oxygen atom (Tamizh *et. al.*, 2009). Another evidence shows the participation of (C=N) group in the coordination site is attributable to the shifting of ν(C=N) bands to the lower or higher frequencies. The

changes in this vibrational frequencies shows that the imine nitrogen atom has coordinated to the metal(II) ions (Golcu *et. al.*, 2005).

Further conclusive idea of the complexation was shown by the presence of two new bands at the lower frequencies range of 549-562 and 461-478 which are assigned to ν(M-O) and ν(M-N) respectively. These newly bands, further indicated the chelation of the metal ion to the ligand *via* phenolic oxygen and azomethine nitrogen atom.

For the $[Zn(L^2)_2]\bullet 3H_2O$ and $[Cu(L^2)Cl]\bullet CH_3OH$ complexes, strong bands appeared at 3340 and 3440cm^{-1} respectively that can be assigned to the ν(OH) modes of coordinated and lattice water or methanol, present in the complexes (Nakamoto, 1986; Leovoc *et. al.*, 2005).

In conclusion, the IR study shows that the ligand L^2H coordinates to metal ion *via* phenolic oxygen and imine nitrogen.

Table 4.9: Important IR data for L^2H and metal complexes.

Compound	Wavenumber (cm^{-1})							
	ν(O-H)	ν(C=N)	ν_{ar}(C=C)	ν(C-O)	ν_{ar}(C-H)$_{bend}$	ν(C-Cl)	ν (M-O)	ν(M-N)
L^2H	3384 weak	1636 strong	1483 strong	1279 strong	822 medium	697 medium	–	–
$[Zn(L^2)_2]\cdot 3H_2O$	3340 broad	1618 strong	1461 strong	1296 strong	832 medium	716 strong	552 weak	476 weak
$[Zn(L^2)(OAc)]$	–	1646 strong	1461 strong	1314 strong	850 strong	703 strong	559 medium	470 medium
$[Cu(L^2)_2]$	–	1624 strong	1455 strong	1312 medium	834 strong	720 strong	560 medium	478 weak
$[Cu(L^2)Cl]\cdot CH_3OH$	3440 medium	1625 strong	1460 medium	1316 medium	850 medium	703 strong	562 weak	470 weak
$[Ni(L^2)_2]$	–	1614 strong	1461 strong	1323 medium	822 strong	731 strong	549 weak	461 weak

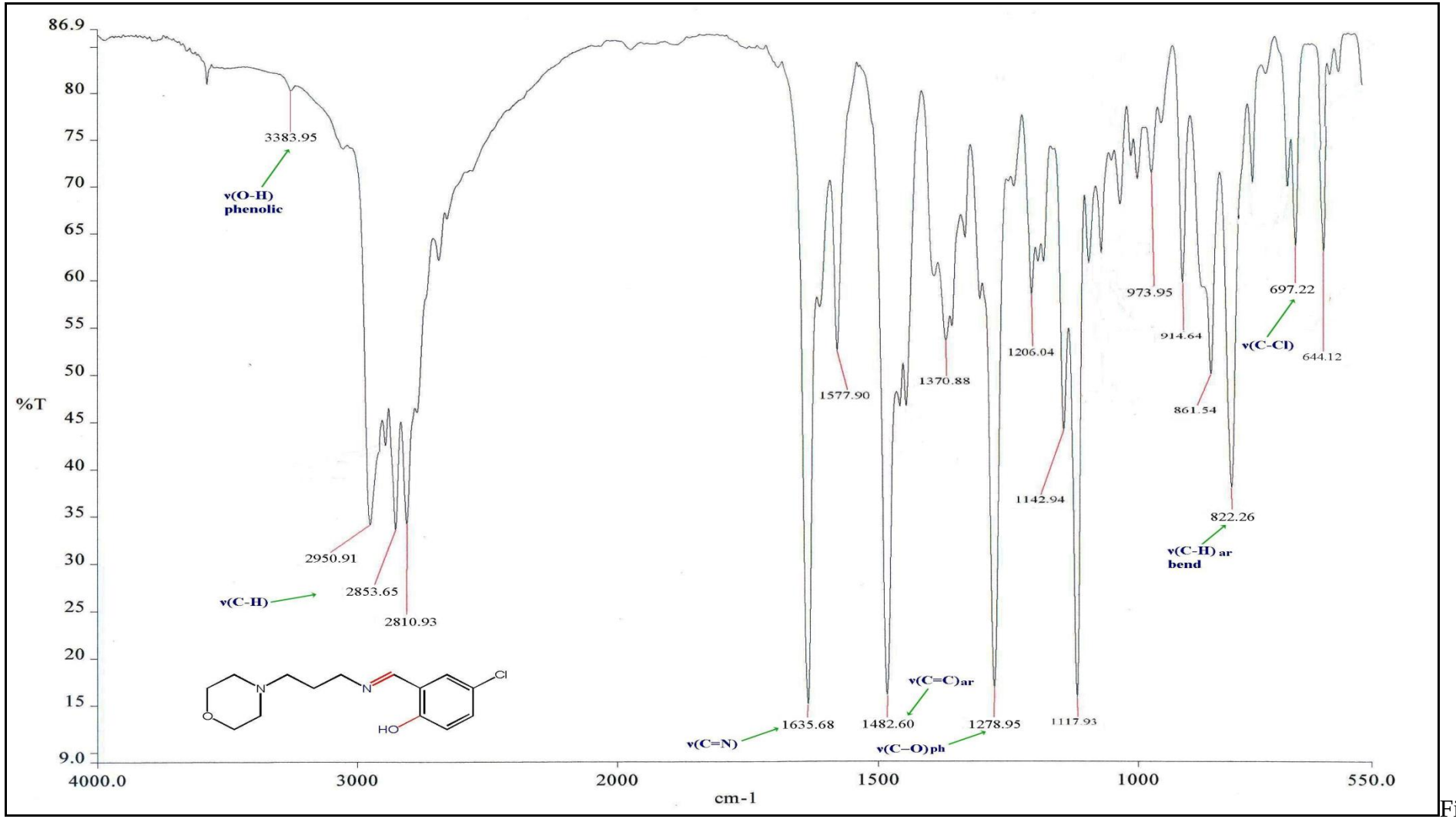

Figure 4.14: IR spectra for L^2H.

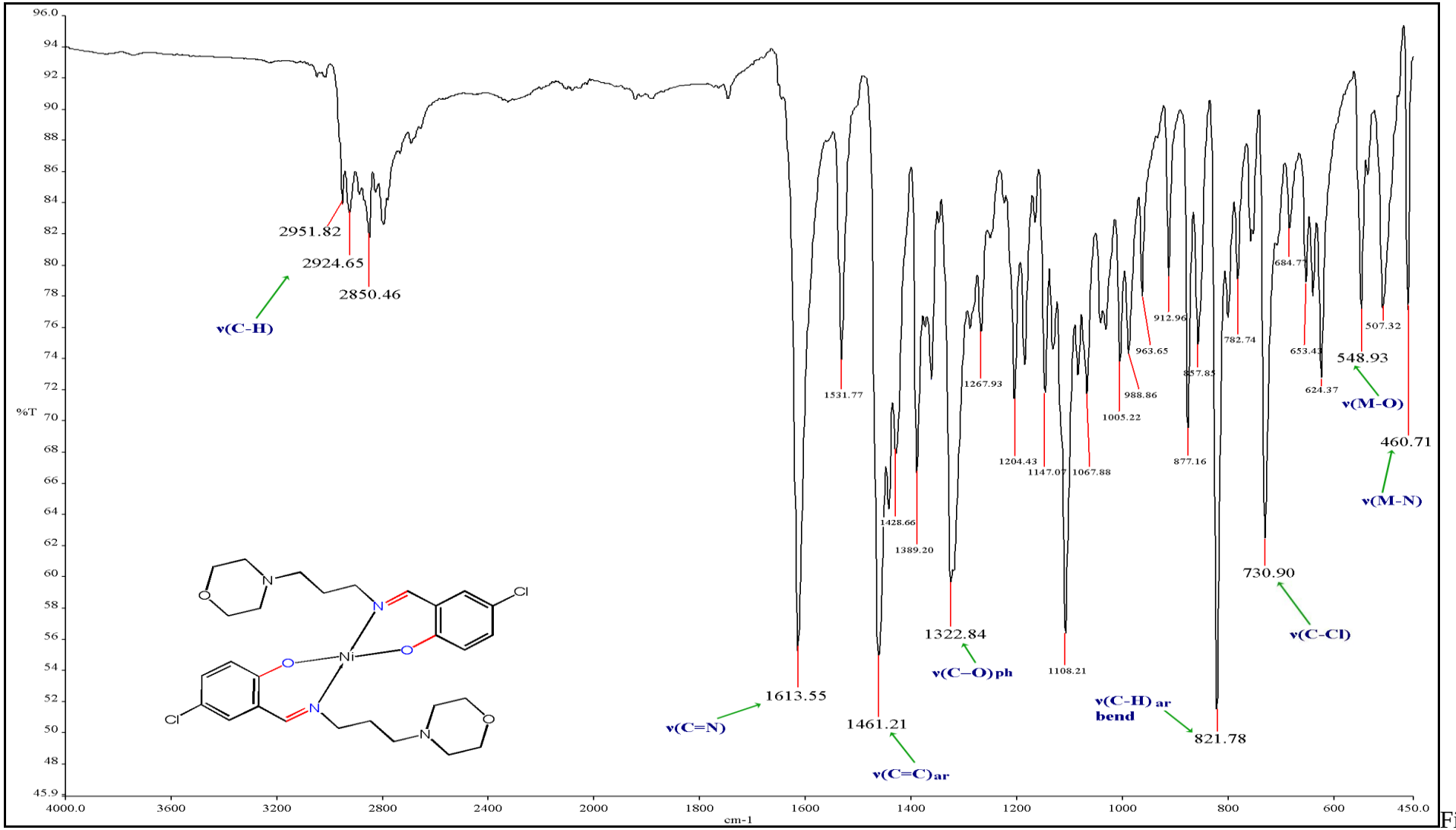
%T
cm-1
2951.82
2924.65
2850.46
ν(C-H)
1613.55
ν(C=N)
1531.77
1461.21
ν(C=C)ar
1428.66
1389.20
1322.84
ν(C–O)ph
1267.93
1204.43
1147.07
1067.88
1108.21
1005.22
988.86
963.65
912.96
877.16
857.85
821.78
ν(C-H) ar bend
782.74
730.90
ν(C-Cl)
684.77
653.43
624.37
548.93
ν(M-O)
507.32
460.71
ν(M-N)
Cl
Ni
O
N

Fig

ure 4.15: IR spectra for $[Ni(L^2)_2]$.

4.2.3 ^{1}H NMR Spectral Data

The ^{1}H NMR spectral data of $L^{2}H$ and its zinc(II) complexes were recorded in d_6-dimethylsulphoxide (DMSO-d_6) solution. The spectrum data were illustrated in Table 4.10 and in Figures 4.16 and 4.17 respectively.

The spectrum of ligand $L^{2}H$ exhibits two singlet signals at 13.75 and 8.53 ppm attributed to the hydrogen of the phenol groups and imine *H*C=N protons (Nelson *et. al.*, 1981) respectively. The intramolecular hydrogen bonding effect causes the phenol hydrogen peak to appear at the most downfield region (Bu *et. al.*, 1997). The aromatic protons of Schiff base ligand resonate at the range 7.53-6.88 ppm with integration corresponding to three protons. Nevertheless, the fourteen hydrogens from the aliphatic side were observed at the upfield region 3.62–1.78 ppm. The $L^{2}H$ ligands are successfully synthesized and correspond to the structural predicated.

The comparison between the ^{1}H NMR of the ligand and its zinc(II) complexes shows that zinc ion chelate through phenol oxygen and imine nitrogen. The spectrum disappearance of the most deshielded peak indicates deprotonation of the phenolic oxygen, upon complexation (Agarwala *et. al.*, 1994). Further supported by negative shifts of the imine *H*C=N protons illustrated in the spectrum of zinc(II) complexes as compared to the ligand (Szlyk *et. al.*, 2002). This shift provides evidence of the coordination of the imine nitrogen lone pair to the metal ions. Whereas, the chemical shift of the aromatic and aliphatic protons remain unaffected.

In summary, the zinc(II) complexes were successfully synthesized but the coordination modes have to be further investigated.

Table 4.10: ^{1}H-NMR spectral data of $L^{2}H$ and its zinc complexes.

Compound	Chemical Shift, δ(ppm)				Proton Numbering Scheme
	OH^{1}	$H^{2}C$=N	H Aromatic	H Aliphatic	
$L^{2}H$	13.75	8.53	7.53–6.88	3.62–1.78	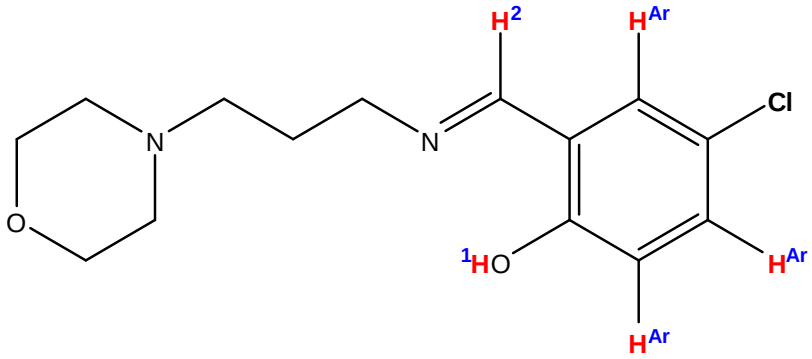
$[Zn(L^{2})_{2}]\cdot 3H_{2}O$		8.47	7.53–6.66	2.33–1.24	
$[Zn(L^{2})(OAc)]$		8.29	7.25–6.63	3.66–1.22	

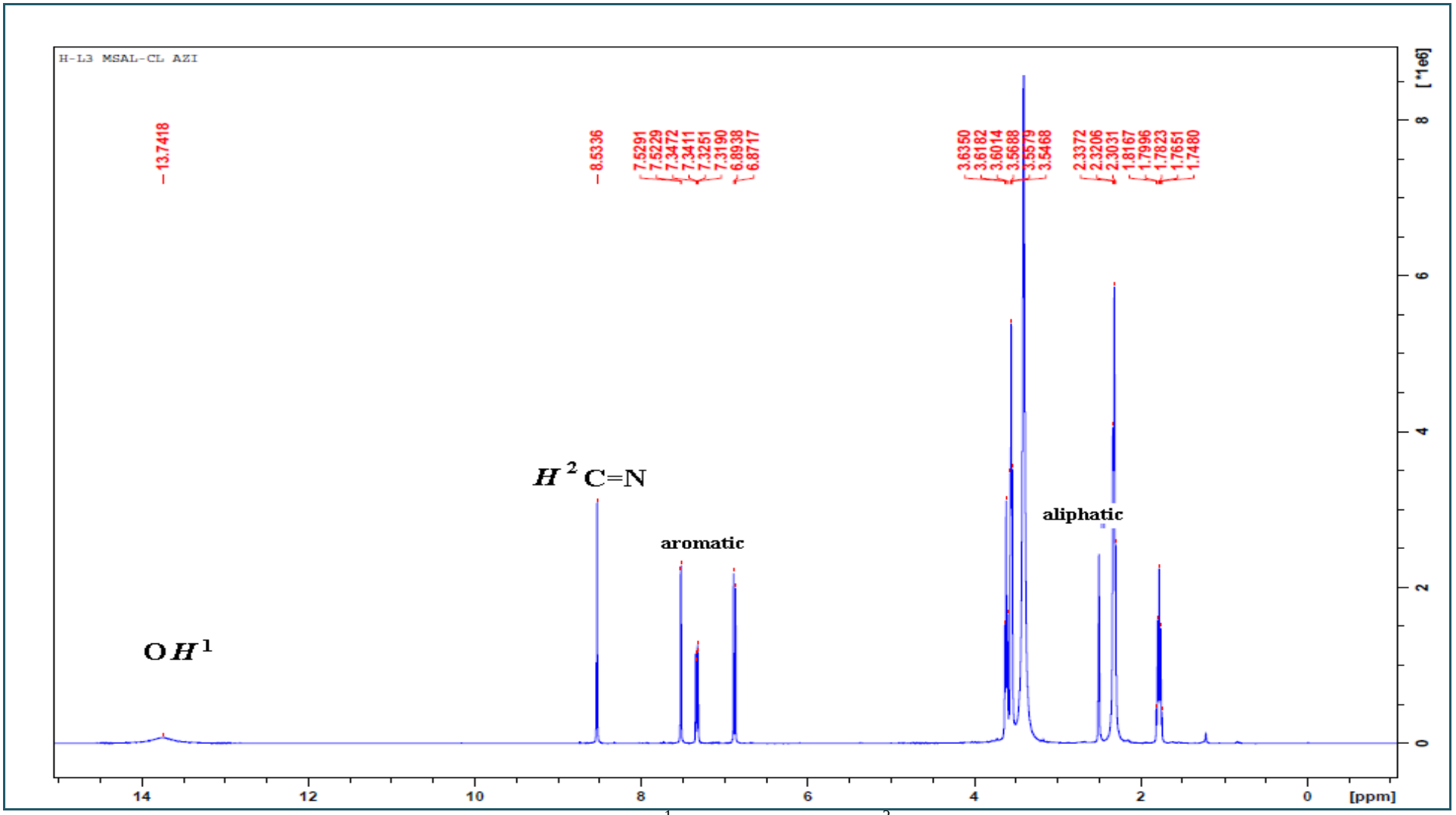

Figure 4.16: ^{1}H-NMR spectra for L^{2}H.

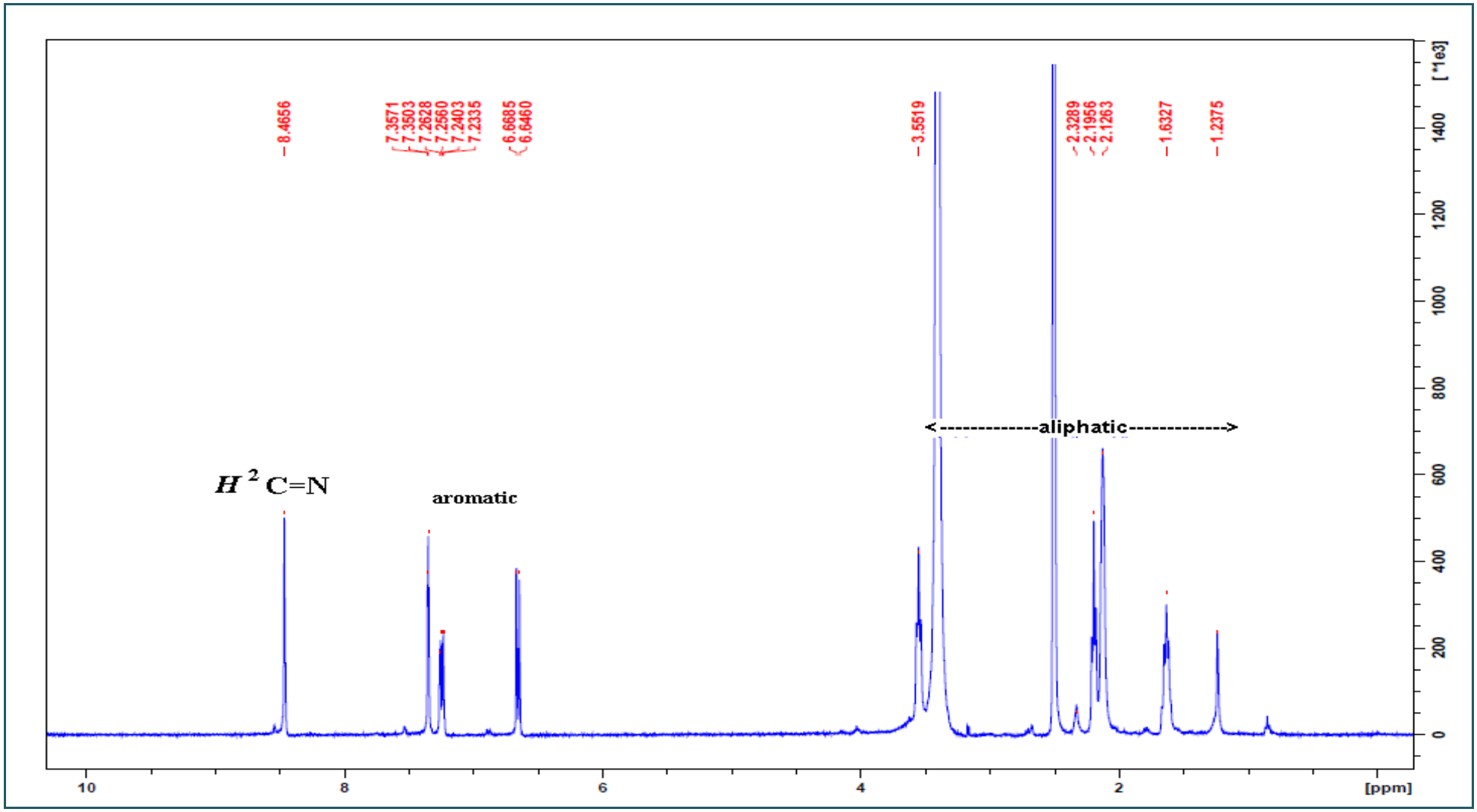

Figure 4.17: ^{1}H-NMR spectra for $[Zn(L^{2})_{2}]\bullet 3H_{2}O$.

4.2.4 ^{13}C NMR spectra

The spectral data of ligand L^2H and its zinc(II) complexes are summarized in Table 4.11 and the spectra are given in Figures 4.18, 4.19 respectively.

The ^{13}C NMR spectrum of the ligand displays 12 peaks which corresponding to 12 types of carbon. The most deshielded signal was assigned to phenolic hydroxyl carbon at 164.77 ppm due to the electronegative effect of the oxygen attached to the carbon. While, slightly lower chemical shift at 160.28 ppm are assigned to azomethine carbon (Bocâ *et. al.,* 2000). Furthermore, for the complexes, the azomethine carbon peaks was shifted downfield. This led to participation of the nitrogen atom in the chelation. The shifts of C-O resonances further confirmed involvement of the phenolate group *via* complexation as shown in Figure 4.19. The chemical shift in region 134-116 ppm attributed to five carbon at the aromatic rings and the peak exhibits at the range 65-22 ppm represents the aliphatic carbons in spectra of the L^2H ligand and the zinc(II) complexes.

Therefore, these results indicate that ligand L^2H coordinated to zinc ions through phenolate oxygen and azomethine nitrogen, which has been inferred from IR and ^{1}H NMR spectral studies.

Table 4.11: ^{13}C-NMR spectral data of L^2H and its zinc complexes.

Compound	Chemical Shift, δ(ppm)				Carbon Numbering Scheme
	C–OH	*H*C=N	H Aromatic	H Aliphatic	
L^2H	164.77	160.28	131.9–118.8	66.1–26.9	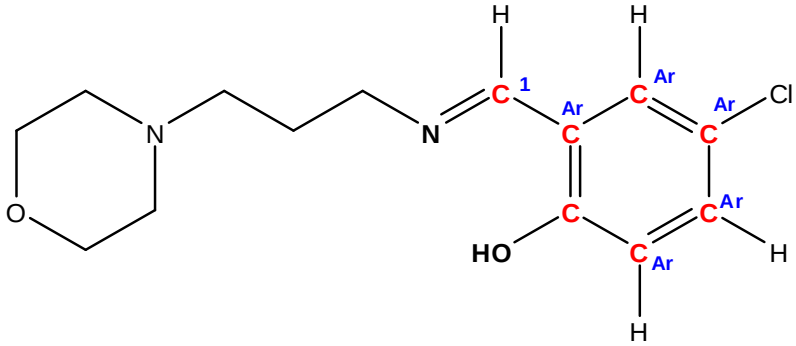
$[Zn(L^2)_2]\cdot 3H_2O$		168.44	134.0–116.6	66.0–26.7	
$[Zn(L^2)(OAc)]$		168.38	133.7–116.2	65.1–21.7	

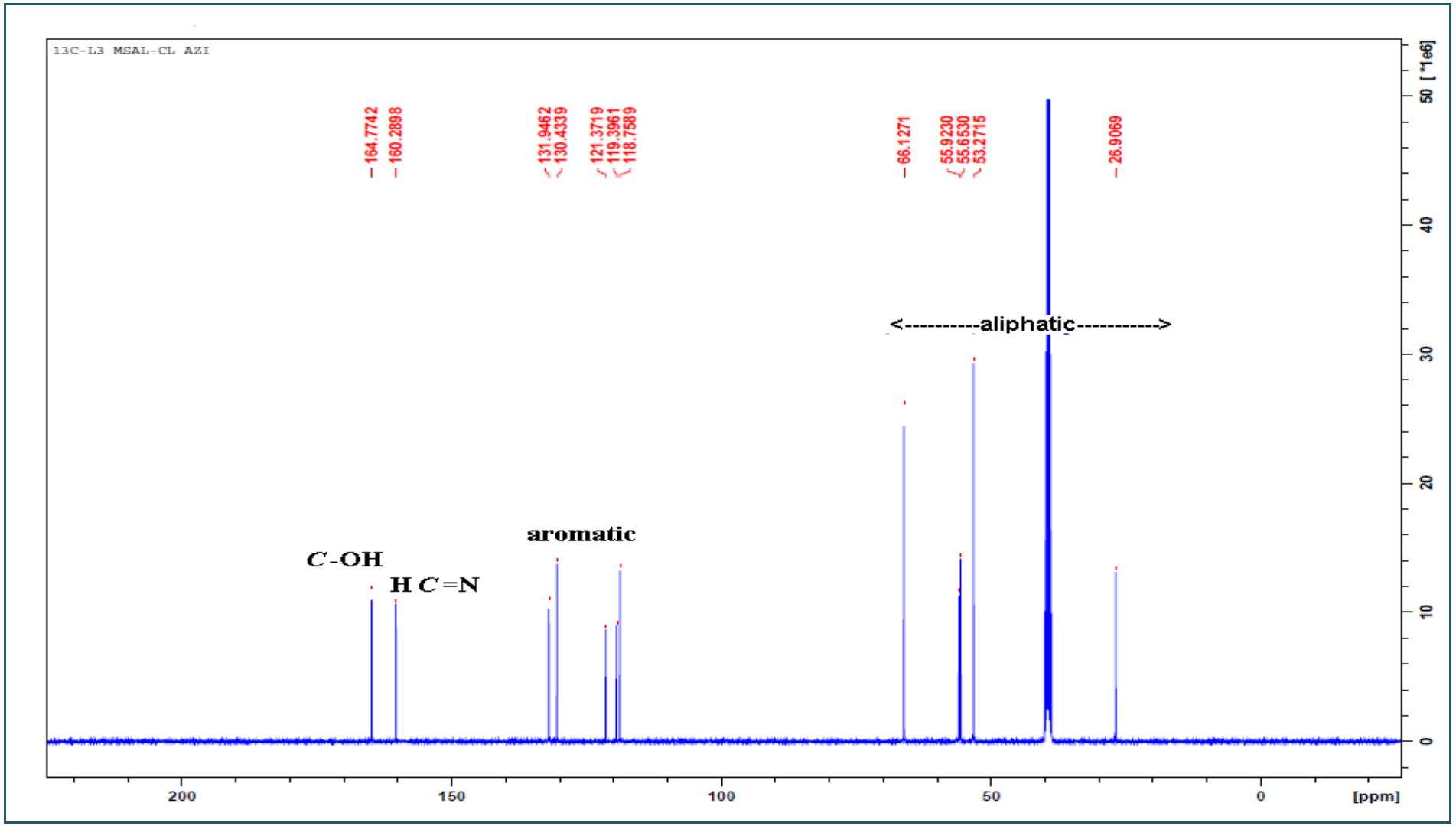

Figure 4.18: ^{13}C-NMR spectra for L^{2}H.

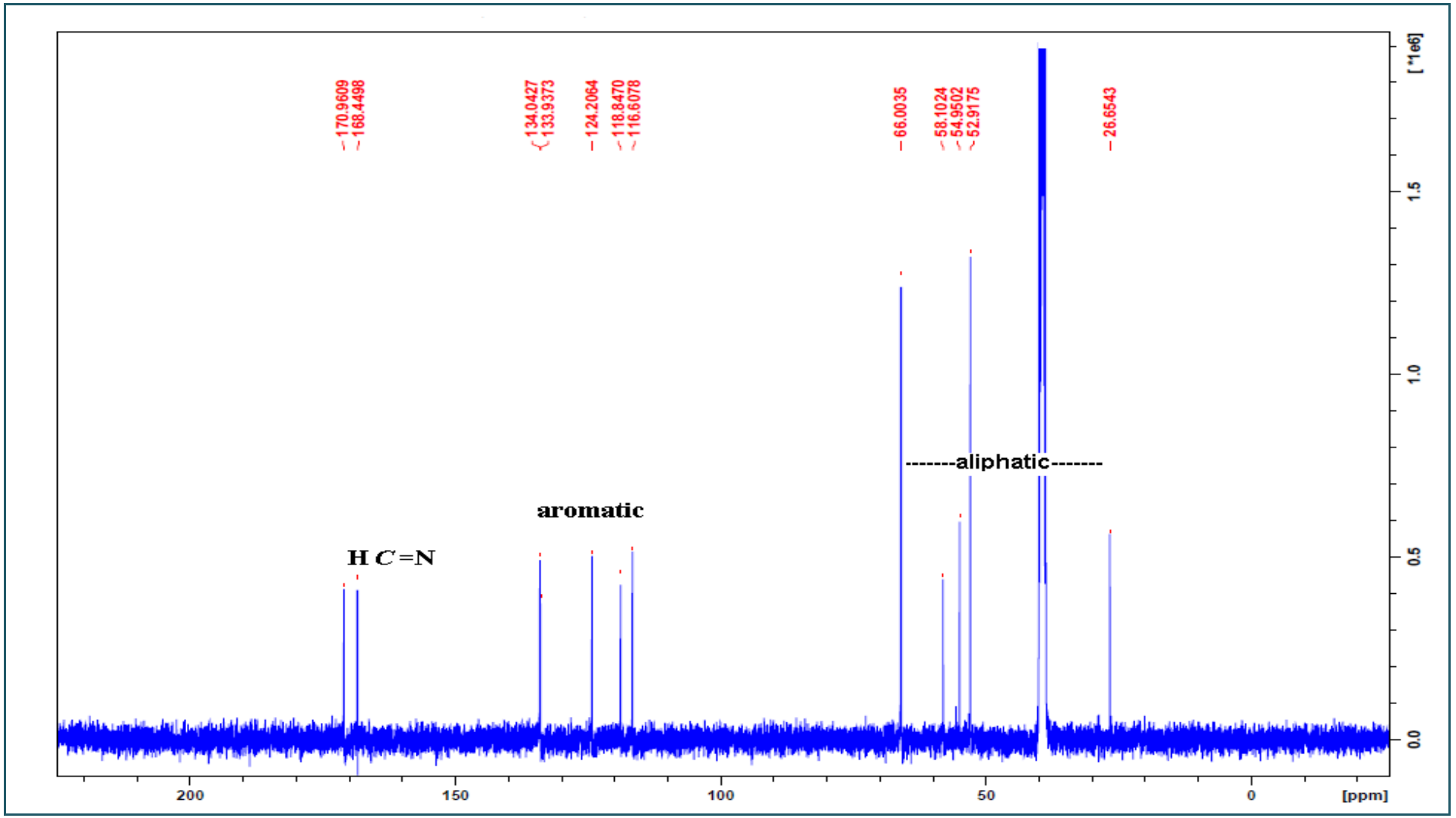

Figure 4.19: ^{13}C-NMR spectra for [Zn(L^2)$_2$].

4.2.5 **UV-Vis spectra**

The ligand electronic spectra displays two bands at 254 and 327 ppm assignable to intraligand π→π* transition of the aromatic ring n→π* transition of C=N chromophore repectively (Tas *et. al.*, 2010). Upon complexation, the π→π* and n→π* transitions bands shifted to higher energy due to hypsochromic shift (Lu *et. al.*, 2000). The increased in the conjugation and delocalization of the whole electronic system, led to the energy change of π→π* and n→π* transitions (Kalanithia *et. al.*, 2012). Additionally, the spectra of the complexes show absorptions peaks at the region 306-354 ppm attributed to ligand metal charge transfer (LMCT). The charge transfers are between the lone pair of phenolic oxygen donor and the divalent ions (Vanco *et. al.*, 2008).

The spectra of $[Cu(L^2)_2]$ exhibits two new bands corresponding to *d-d* transitions. The shoulder band at 567 nm assigned to $^2B_{1g}\rightarrow{}^2B_{2g}$ transition and the absorption at 374 nm was attributed to $^2B_{1g}\rightarrow{}^2E_g$ transition. Hence, these suggest the complex demonstrate a square planar stereochemistry (Chandra *et. al.*, 2009).

The UV spectrum of the $[Cu(L^2)Cl]\bullet CH_3OH$ complex show the absorption bands at 772 nm, 559 nm and 378 nm attributed to $^2B_{1g}\rightarrow{}^2A_{1g}$, $^2B_{1g}\rightarrow{}^2B_{2g}$ and $^2B_{1g}\rightarrow{}^2E_g$ transitions respectively (Geeta *et. al.*, 2010). It indicates the square planar geometry for this Cu(II) complex.

Furthermore, in the nickel complex spectrum appears a low intensity broad band at 619 nm which is attributed to $^1A_{1g}\rightarrow{}^1A_{2g}$ transition of d-d orbital. Another band appears at 415 nm corresponding to the $^1A_{1g}\rightarrow{}^1B_{1g}$ transition. These transitions suggest the square planar geometry (Singh *et. al.*, 2007).

In summary, the charge transfer and the *d-d* transition in complexes provides significant evidence proposing that the complexes form four-coordinate. The Cu(II) and Ni(II) complexes are expected to be a square planar geometry (Chandra *et. al.*, 2009; Singh *et. al.*, 2007; Geeta *et. al.*, 2010). The coordination modes of the complexes will be further deliberate in X-ray crystallographic analysis.

Table 4.12: UV-Visible spectral data for L^2H and its complexes.

Compound	λ_{max} (nm)	λ_{max} (cm^{-1})	ε_{max} ($mol^{-1}dm^3cm^{-1}$)	Assignment
L^2H	254	39370	8907	$\pi\rightarrow\pi^*$
	327	30581	4273	$n\rightarrow\pi^*$
$[Cu(L^2)_2]$	246	40650	38735	$\pi\rightarrow\pi^*$
	296	33784	8373	$n\rightarrow\pi^*$
	306	32680	9157	LMCT
	374	26738	9819	*d-d* transition $^2B_{1g}\rightarrow{}^2E_g$
	597	16750	116	*d-d* transition $^2B_{1g}\rightarrow{}^2B_{2g}$
$[Cu(L^2)Cl]\cdot CH_3OH$	247	40486	22413	$\pi\rightarrow\pi^*$
	296	33784	4932	$n\rightarrow\pi^*$
	354	28249	6165	LMCT
	378	26455	5768	*d-d* transition $^2B_{1g}\rightarrow{}^2E_g$
	559	17889	265	*d-d* transition $^2B_{1g}\rightarrow{}^2B_{2g}$
	772	12953	117	*d-d* transition $^2B_{1g}\rightarrow{}^2A_{1g}$
$[Ni(L^2)_2]$	257	38911	18190	$\pi\rightarrow\pi^*$
	290	34483	10191	$n\rightarrow\pi^*$
	327	30581	9164	LMCT
	415	24096	4897	*d-d* transition $^1A_{1g}\rightarrow{}^1B_{1g}$
	619	16155	79	*d-d* transition $^1A_{1g}\rightarrow{}^1A_{2g}$

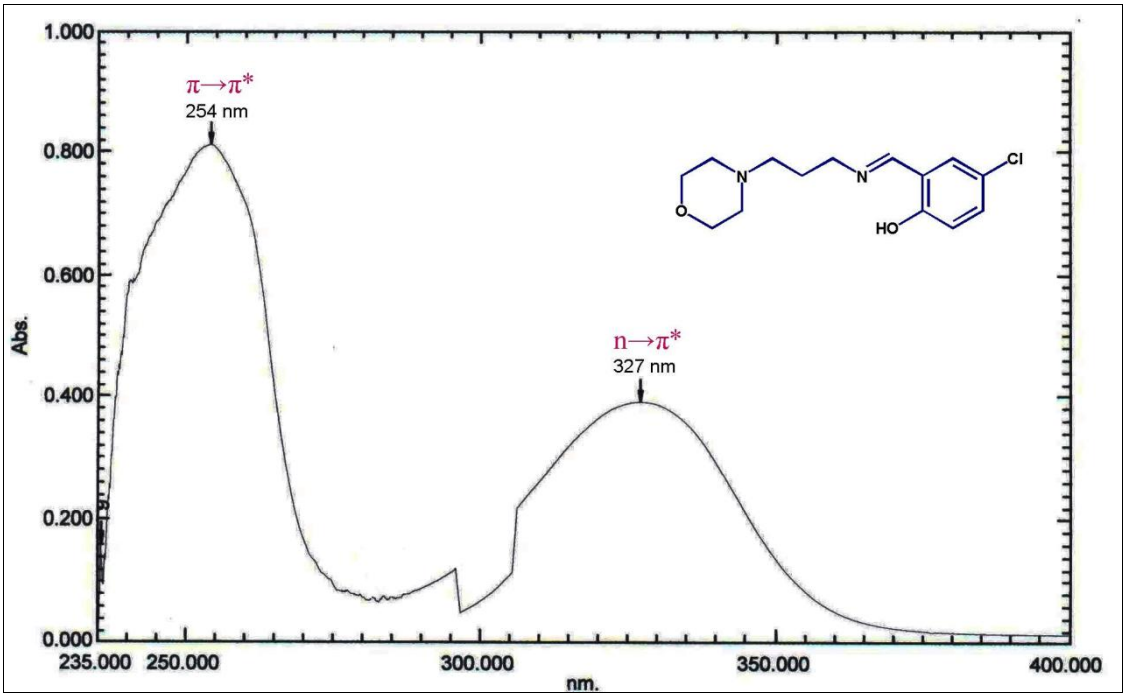

Figure 4.20: UV-Vis spectra for L^2H.

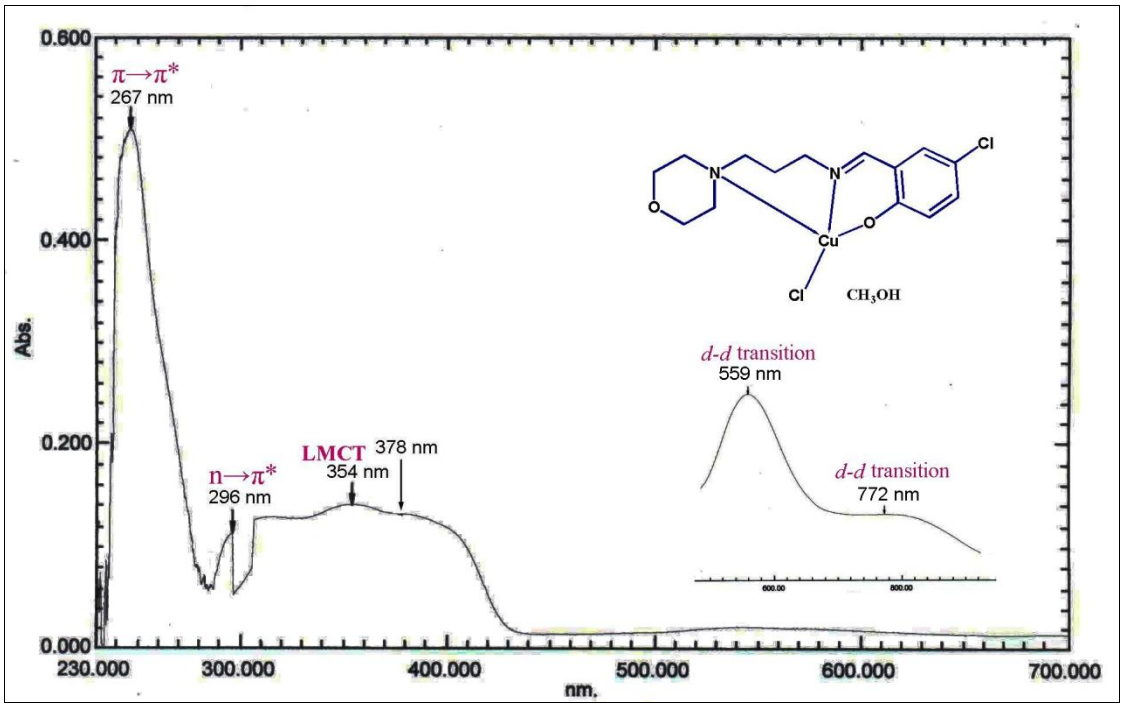

Figure 4.21: UV-Vis spectra for [Cu (L^2)Cl]·CH_3OH.

4.2.6 **X-ray Crystallographic Data Collection**

The complexes of L^2 crystal data and refinement are summarized in Table 4.13.

4.2.6.1 *Crystal structure of $[Zn(L^2)_2]$ •$3H_2O$*

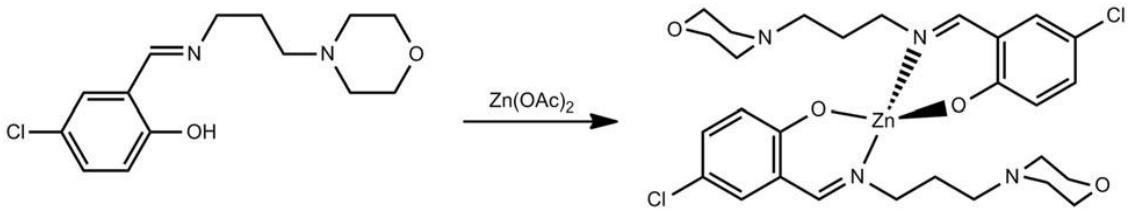

Scheme 4.5: Synthesis of $[Zn(L^2)_2]$•$3H_2O$.

The complex was obtained via reaction of L^2H with zinc(II) acetate in a 2 : 1 ratio (scheme 4.5). The asymmetric unit of the crystal structure contains one metal complex molecule, co-crystallized with three molecules of water. Figure 4.22 shows the molecular structure of the metal complex. Zn, located in a general position, is four-coordinated by two deprotonated L^2 ligands through their phenolate O and azomethine N. The geometry of the coordination sphere can be described as a distorted tetrahedron from the dihedral angle of 86.80(7)° formed between the two six-membered chelating rings. Dissimilar to the structure of $[Zn(L^1)_2]$, the three methylene groups of the spacer in each L^2 adopt an all-trans conformation. Selected bond lengths and angles for the structure are given in table 4.14. The geometrical parameters pertaining to the coordination spheres are within normal ranges (Torzilli et. al., 2002; Schon et. al., 2004; Pastor et. al., 2011).

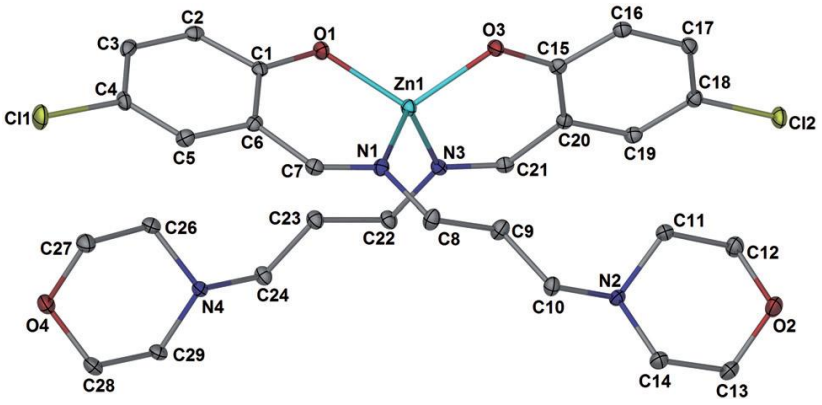

Figure 4.22: The crystal structure of $[Zn(L^2)_2]\bullet 3H_2O$ with 30% thermal ellipsoids. Water molecules and hydrogen atoms have been omitted for clarity.

4.2.6.2 *Crystal structure of [Zn(L^2)(OAc)]*

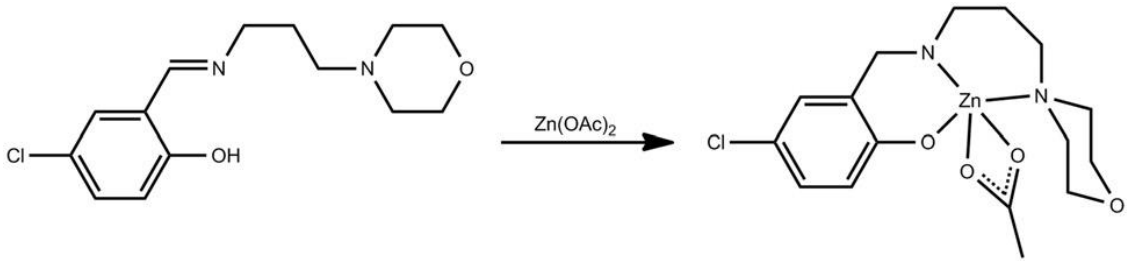

Scheme 4.6: Synthesis of $[Zn(L^2)(OAc)]$.

The reaction of L^2H with $Zn(OAc)_2$ in a 1 : 1 ratio gave $[Zn(L^2)(OAc)]$ (scheme 4.6). The asymmetric unit of the crystal structure consists of two crystallographically independent molecules with slightly different geometries. The weighted root mean square (rms) fit for the superposition of the non-H atoms in both molecules is 0.0412Å. Figure 4.23 displays the molecular structure of one molecule. In contrast with the former structures, in this complex, the deprotonated Schiff base, L^2, coordinates through not only the phenolate O and imine N, but also its morpholine nitrogen. Each ligand forms two six-membered chelate rings with zinc, one of which (Zn1/O1/C1/C6/C7/N1) is planar whereas the other (Zn1/N1/C8/C9/C10/N2) adopts a chair conformation. The zinc is five-coordinate by tridentate L^2 and a bidentate acetate. The coordination geometry is distorted square-pyramidal as determined by Addison index of 0.11 (Addison *et. al.*, 1984). Table 4.14

provides selected bond lengths and angles for [Zn(L^2)(OAc)]. The Zn–Ophenolate distance of 1.9392(18)Å is within the normal range as are the Zn–N distances of 2.005(2) and 2.140(2)Å (Tai *et. al.*, 2008; Li & Huaxue, 2007).

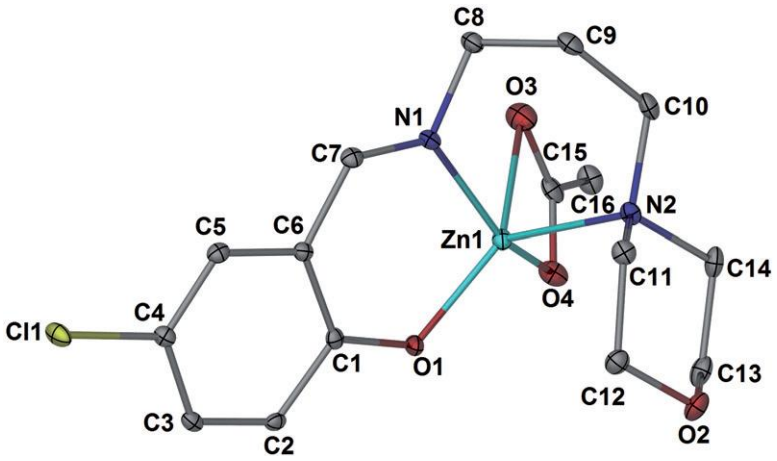

Figure 4.23: The molecular structure of [Zn(L^2)(OAc)] with 40% thermal ellipsoids. Hydrogen atoms have been omitted for clarity.

4.2.6.3 *Crystal structure of [Cu(L^2)$_2$]*

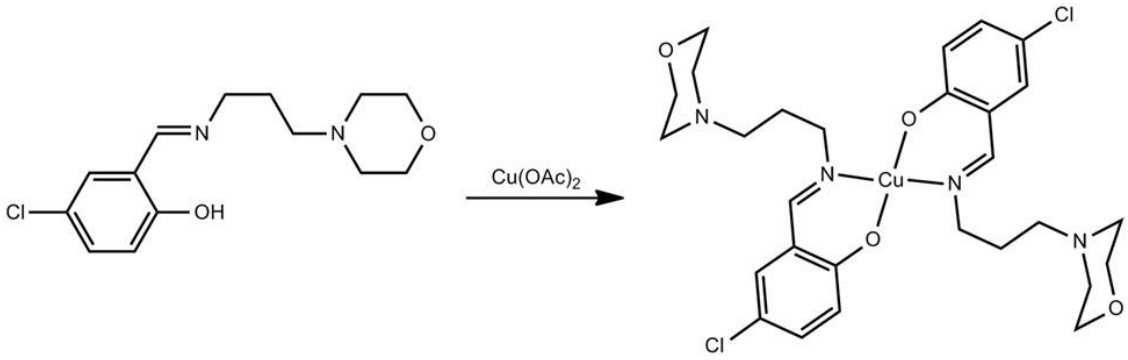

Scheme 4.7: Synthesis of [Cu(L^2)$_2$].

Reaction of Cu(II) with two equivalents of H^2L generated [Cu(L^2)$_2$] (scheme 4.7). The crystal structure is represented in figure 4.24 and selected bond lengths and angles are given in table 4.14. The copper, located on a centre of inversion, is four-coordinate in a distorted square plane defined by two N,O-bidentate mono-anionic L^2. Distortion from ideal geometry is evident from cisoid-angles of 87.44(10)° and 92.56(10)°. The morpholine nitrogen and oxygen are not involved in coordination. The coordination

geometrical parameters are comparable to values observed in similar structures (Dhar *et. al.*, 2003; Fernandez *et. al.*, 2010).

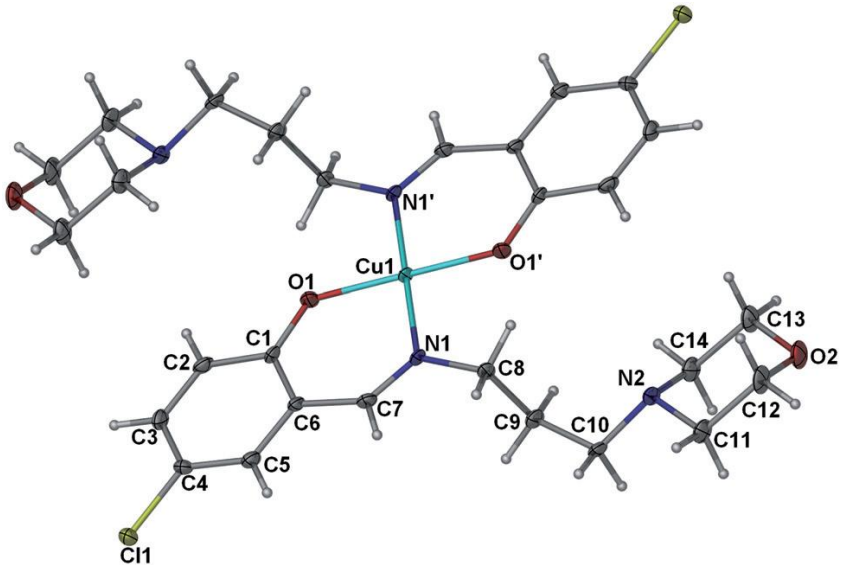

Figure 4.24: The crystal structure and atom-labeling scheme of $[Cu(L^2)_2]$ (50% probability ellipsoids).

4.2.6.4 *Crystal structure of $[Cu(L^2)Cl]\bullet CH_3OH$*

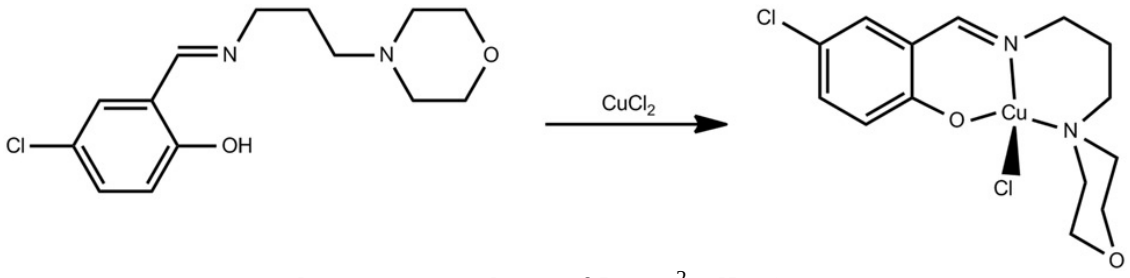

Scheme 4.8: Synthesis of $[Cu(L^2)Cl]\bullet CH_3OH$.

The complex was obtained through reaction of H^2L with an equimolar amount of copper(II) chloride (scheme 4.8). The crystal structure contains one methanol co-crystallized with each Cu(II) complex. Figure 2.25 demonstrates the molecular structure of the copper(II) complex. Similar to the structure of $[Zn(L^2)(OAc)]$, the morpholine nitrogen of the deprotonated Schiff base, L^2, is involved in metal coordination. Thus, the ligand is a mono-anionic N,N,Otridentate chelate to form one planar and one chair-like six-membered ring with copper.The four-coordinate copper is completed by Cl^-. The rms

deviation from the least squares plane involving Cu1/Cl2/O1/N1/N2 is 0.0182(4) Å and copper atom is 0.0228(5) Å out of the coordination plane, Cl2/O1/N1/N2. Table 4.14 gathers selected bond lengths and angles for [Cu(L^2)Cl]•CH_3OH. The coordination geometrical parameters are in agreement with the values observed in similar structures (Latour *et. al.*, 1989; Shnulin *et. al.*, 1977; Hisham *et. al.*, 2009).

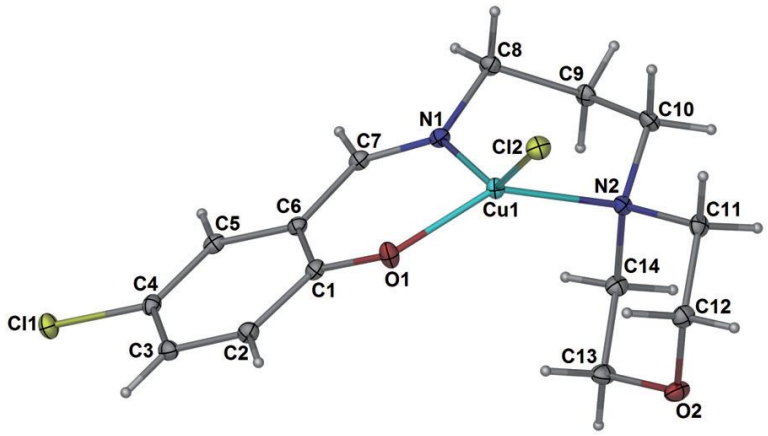

Figure 4.25: The crystal structure of [Cu(L^2)Cl]•CH_3OH with 40% thermal ellipsoids. The methanol and hydrogen atoms have been omitted for clarity.

Table 4.13: Crystal data and refinement parameters for L^2 complexes.

	$[Zn(L^2)_2].3H_2O$	**$[Zn(L^2)(OAc)]$**	**$[Cu(L^2)_2]$**	**$[Cu(L^2)Cl].CH_3OH$**
Empirical formula	$C_{28}\,H_{42}\,Cl_2\,N_4\,O_7\,Zn$	$C_{16}\,H_{21}\,Cl\,N_2\,O_4\,Zn$	$C_{28}\,H_{36}\,Cl_2\,Cu\,N_4\,O_4$	$C_{15}\,H_{22}\,Cl_2\,Cu\,N_2\,O_3$
Crystal system	Monoclinic	Orthorhombic	Triclinic	Monoclinic
Space group	*P 21/c*	*P c a 21*	*P -1*	*P 21/c*
Unit cell dimensions				
a (Å)	14.6066(14)	13.0216(2)	6.4917(14)	8.8556(3)
b (Å)	11.7494(11)	10.2210(2)	8.5461(18)	13.8205(2)
c (Å)	18.4867(18)	25.8385(4)	13.199(3)	14.0612(2)
α (°)			88.348(3)	
β (°)	101.488(3)		81.750(4)	99.964(3)
γ (°)			70.792(3)	
Volume ($Å^3$)	3109.1(5)	3438.94(10)	684.2(3)	1694.98(4)
Z	4	8	1	4
Density (calculated) ($g\ cm^{-3}$)	1.459	1.569	1.522	1.618
Crystal size (mm^3)	0.31 x 0.19 x 0.06	0.32 x 0.22 x 0.20	0.18 x 0.13 x 0.12	0.51 x 0.41 x 0.30
θ range for data collection (°)	2.07 to 27.00	1.99 to 27.00	2.52 to 25.48	2.08 to 27.50
Reflections collected	16987	29957	4784	12966
Independent reflections	6729 [R_{int} = 0.0357]	7401 [R_{int} = 0.0352]	2511 [R_{int} = 0.0758]	3894 [R_{int} = 0.0179]
Completeness	To *θ* = 27.00° : 99.4 %	To *θ* = 27.00° : 100.0 %	To *θ* = 25.48° : 98.7 %	To *θ* = 27.50° : 99.9 %
Data / restraints / parameters	6729 / 6 / 397	7401 / 1 / 435	2511 / 0 / 178	3894 / 1 / 212
Goodness-of-fit on F^2	1.033	1.048	1.055	1.041
Final *R* indices [$I>2\sigma$ (I)]	R_1 = 0.0344, wR_2 = 0.0728	R_1 = 0.0254, wR_2 = 0.0574	R_1 = 0.0574, wR_2 = 0.1497	R_1 = 0.0212, wR_2 = 0.0533
R indices (all data)	R_1 = 0.0493, wR_2 = 0.0781	R_1 = 0.0300, wR_2 = 0.0592	R_1 = 0.0649, wR_2 = 0.1591	R_1 = 0.0235, wR_2 = 0.0543

Table 4.14: Selected bond lengths (Å) and bond angles (°) for L^2 complexes.

$[Zn(L^2)_2].3H_2O$		**$[Zn(L^2)(OAc)]$**		**$[Cu(L^2)_2]$**		**$[Cu(L^2)Cl].CH_3OH$**	
Bond lengths							
Zn(1)-O(1)	1.9122(15)	Zn(1)-O(1)	1.9392(18)	Cu(1)-O(1)	1.892(2)	Cu(1)-O(1)	1.8883(10)
Zn(1)-O(3)	1.9277(14)	Zn(1)-N(1)	2.005(2)	Cu(1)-N(1)	2.013(3)	Cu(1)-N(1)	1.9507(12)
Zn(1)-N(3)	2.0116(17)	Zn(1)-N(2)	2.140(2)	O(1)-C(1)	1.306(4)	Cu(1)-N(2)	2.0473(12)
Zn(1)-N(1)	2.0164(17)	Zn(1)-O(3)	2.435(2)	N(1)-C(7)	1.284(4)	Cu(1)-Cl(2)	2.2496(4)
O(1)-C(1)	1.315(2)	Zn(1)-O(4)	2.0027(18)			O(1)-C(1)	1.3121(17)
O(3)-C(15)	1.323(2)	O(1)-C(1)	1.316(3)			N(1)-C(7)	1.2877(18)
N(1)-C(7)	1.287(3)	N(1)-C(7)	1.273(4)				
N(3)-C(21)	1.288(3)						
Bond angles							
O(1)-Zn(1)-O(3)	112.51(6)	O(1)-Zn(1)-O(4)	104.25(7)	O(1)-Cu(1)-O(1)#1	180.00	O(1)-Cu(1)-N(1)	94.72(5)
O(1)-Zn(1)-N(3)	119.48(7)	O(1)-Zn(1)-N(1)	95.03(9)	O(1)-Cu(1)-N(1)	92.56(10)	O(1)-Cu(1)-N(2)	141.79(5)
O(3)-Zn(1)-N(3)	95.83(6)	O(4)-Zn(1)-N(1)	145.12(9)	O(1)-Cu(1)-N(1)#1	87.44(10)	N(1)-Cu(1)-N(2)	94.36(5)
O(1)-Zn(1)-N(1)	97.02(6)	O(1)-Zn(1)-N(2)	121.30(9)	N(1)-Cu(1)-N(1)#1	180.00	O(1)-Cu(1)-Cl(2)	95.98(3)
O(3)-Zn(1)-N(1)	119.24(7)	O(4)-Zn(1)-N(2)	103.38(8)			N(1)-Cu(1)-Cl(2)	141.51(4)
N(3)-Zn(1)-N(1)	114.35(7)	N(1)-Zn(1)-N(2)	90.46(8)			N(2)-Cu(1)-Cl(2)	99.60(3)
		O(1)-Zn(1)-O(3)	138.32(8)				
		O(4)-Zn(1)-O(3)	58.45(7)				
		N(1)-Zn(1)-O(3)	87.89(8)				
		N(2)-Zn(1)-O(3)	100.20(8)				

Symmetry transformations used to generate equivalent atoms: #1 -*x*+1,-*y*+2,-*z*+1

4.3 *Biological studies*

4.3.1 **Cytotoxicity**

The measure of cytoxicity used in this study, IC_{50}, is the concentration required to reduce growth of cancer cells by 50%. Table 4.15 shows the cytotoxicity of the two ligands and L^1H zinc complex on several cancer cell lines and normal cell line (IC_{50} μg/ml).

Table 4.15: The cytotoxicity of selected compounds on several cancer cell lines and normal cell line (IC_{50} μg/ml).

Cancer cell line	Compound		
	L^1H	L^2H	$[Zn(L^1)Cl]$
WRL-68	–	5.06	–
MCF-7	0.43	0.59	2.96
MDA-MB-231	10.39	2.63	–
CCD-841	9.71	18.32	–
HT-29	0.55	2.57	14.42
JURKAT	–	4.71	–

- WRL-68– Normal liver
- MCF-7– Breast Cancer (+ve)
- MDA-MB-231– Breast Cancer (–ve)
- CCD-841– Normal Colon
- HT-29– Colon cancer
- JURKAT– Leukaemia

'–', inactive.
IC50 < 5.0 μg/ml – strongly active,
IC50 5.0 < 10.0 μg/ml –moderately active,
IC50 10.0 < 25.0 μg/ml – weakly active,
IC50 >25.0 l μg/ml – not active.

IC50 (μg/ml) = Cytotoxic dose at 50%, i.e.the concentration to reduce growth of cancer cells by 50%.

Based on this results, indicates that ligand of L^1H exhibit strong active against MCF-7, breast cancer cell line and HT-29, colon cancer cell line. L^1H ligand shows stronger activity against breast cancer cells with positive estrogen receptor (MCF-7) as compared to breast cancer cells with negative estrogen receptor (MDA-MB-231). In addition, L^1H reveal inactive to normal liver cells (WRL-68) implying the ligand is nontoxic to the normal cell lines. Whereas, the L^2H ligands appears to be moderately active against MDA-MB-231 cell lines but slightly toxic to normal liver cells. Schiff base ligand, L^2H inhabits moderate activity against colon cancer cells (HT-29) and also less toxic to normal colon cell lines (CCD-841). This ligand also displays a moderately active against leukaemia disease (JURKAT).

Furthermore, $[Zn(L^1)Cl]$ complex exhibit moderate active against breast cancer cell line (MCF-7) and appears nontoxic to the normal liver cells. This is the only complex that reveals anticancer properties. All the other Schiff base complexes have low or no activity against the cancer cell lines.

In conclusion, these results demonstrate that L^1H ligand is a good inhibitor for both colon and breast cancer cells with IC_{50} of 1.10 and 0.86 μg/ml respectively.

4.3.2 **Antioxidant - Ferric Reducing Antioxidant Power (FRAP)**

The antioxidant activities of the synthesized compounds were determined by using reducing power assay. This assay was carried out in triplicates and average reading was recorded. The figure 4.26 shows FRAP assay standard curve at absorbance 593 nm and figure 4.27 illustrates the FRAP value of the ligands and complexes in comparison to butylated hydroxytoluene (BTH), quercetin, trolox and ascorbic acid (vitamin C) as the standard.

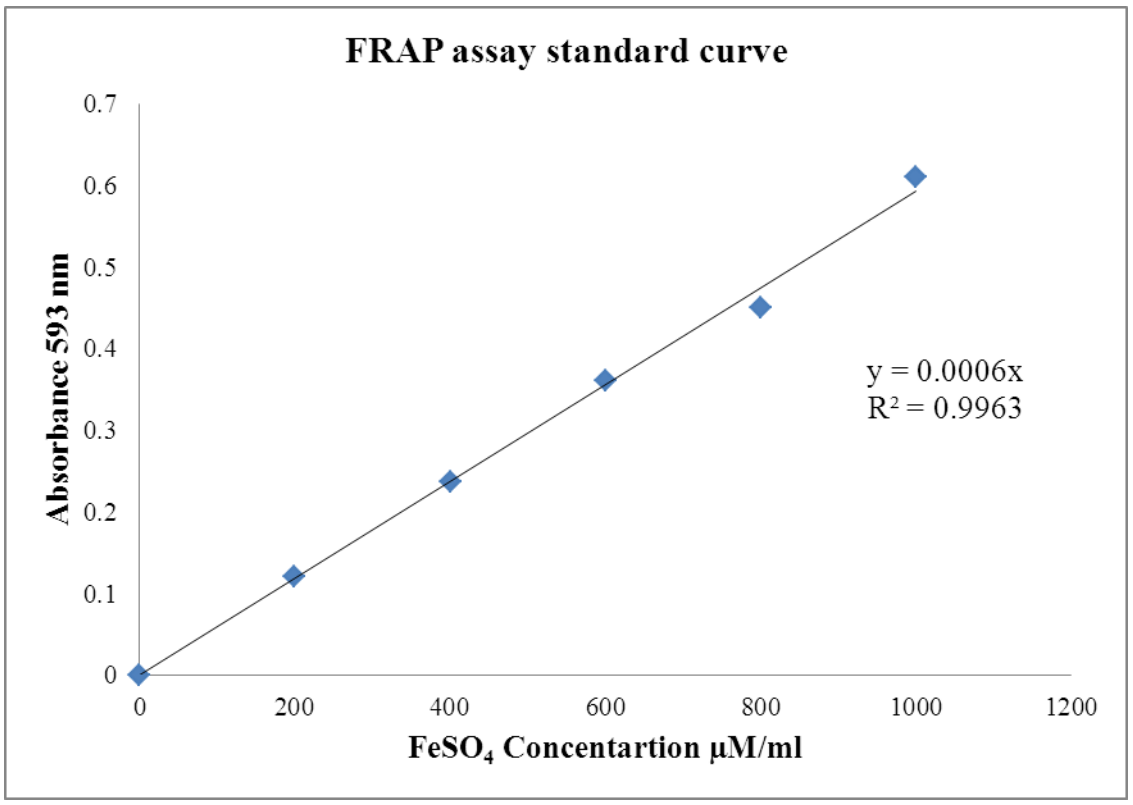

Figure 4.26: FRAP assay standard curve at absorbance 593 nm.

From the data evaluation, ligand L^1H has the highest FRAP value as compared to the other synthesized compounds. The L^1H ligand has higher ferric reducing efficiency than the standard BTH and trolox. However, this ligand reducing ability is similar or slightly lower than the standard quercetin and ascorbic acid. Meanwhile, upon complexation of L^1H has led to decreasing of FRAP value. On the other hand, L^2H shows

inferior reducing ability than L^1H may be due the chloride substituted aromatic ring. The L^2 complexes do not show any increase in the reducing power.

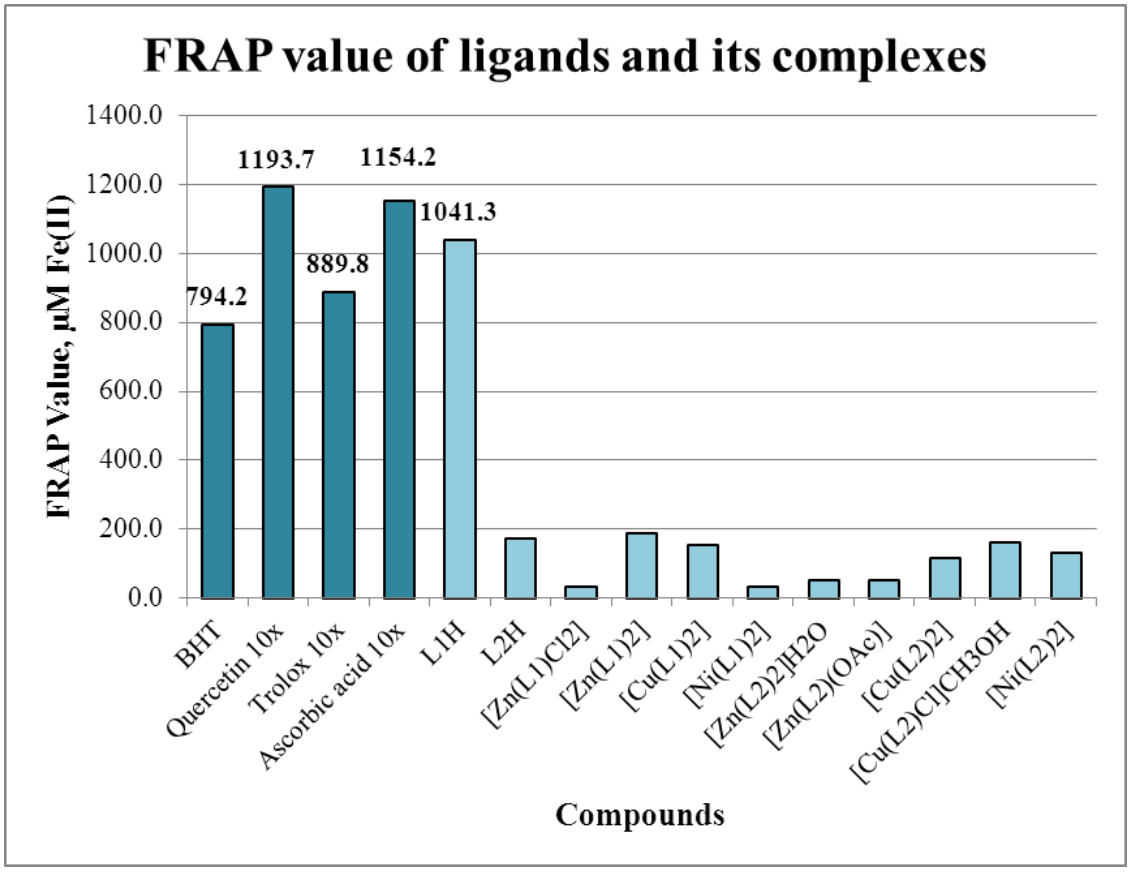

Figure 4.27: FRAP value of ligands and its complexes.

In summary, the L^1H Schiff base ligand has the strongest potential of antioxidant activity.

5.0 CONCLUSION

L^1H and L^2H may show ambidentate behavior in coordination to metal ions. Upon reactions of the Schiff bases with metal salts in a 2 : 1 ratio (ligand : metal), the ligands deprotonate and chelate through phenolate and imine to form the di-ligated metal complexes. In these complexes, morpholine nitrogen and oxygen stay away from the coordination spheres. Structures of the products obtained from reactions of L^2H with metal salts in a 1 : 1 ratio show involvement of the morpholine nitrogen in coordination. In the latter complexes, L^2 is tridentate, forming two chelate rings with the metal centres. Coordination environments of the metal complexes vary from square-planar to tetrahedral to square-pyramidal.

The cytotoxic and antioxidant screening show that the Schiff base, L^1H is the best inhibitor. Based on the IC_{50} results, this ligand are active against MCF-7 cells as well as, nontoxic to the normal liver cell lines. L^1H also show very strong activity against HT-29 cells but slightly toxic to the normal colon cells. Furthermore, the L^1H have highest FRAP value compared to other synthesized compounds. As a conclusion, L^1H have high potential as anticancer drugs and potent antioxidant activity.

Further research on the biological application of L^1H can be extended to *in vivo* studies. Moreover, the comprehensive studies on antioxidant application can be done by DPPH radical scavenging activity assay.

The promising characteristics of the compounds as both remarkable flexidentate structures and biologically active have encouraged further extension into formation of other compound.

REFERENCES:

Adams, A. K., Wermuth, E. O., & McBride, P. E. (1999). Antioxidant vitamins and the prevention of coronary heart disease. *Am. Fam. Physician, 60,* 895-904.

Addison, A. W., Rao, T. N., Reedijk, J., Rijn, V. J., & Verschoor, G. C. (1984). Synthesis, structure, and spectroscopic properties of copper(II) compounds containing nitrogen–sulphur donor ligands; the crystal and molecular structure of aqua[1,7-bis(N-methylbenzimidazol-2′-yl)-2,6-dithiaheptane]copper(II) perchlorate. *J. Chem. Soc., Dalton Trans.*, 1349-1356.

Adsule, S., Barve, V., Chen, D., Ahmed. F., Dou. Q. P., Padhye, S., & Sarkar, F. H. (2006). Novel Schiff base copper complexes of quinoline-2 carboxaldehyde as proteasome inhibitors in human prostate cancer cells. *J. Med. Chem., 49*, 7242-7246.

Agarwala, B. V., Hingorani, S., Puri, V., Khetrapal, C. L., & Naganagowda, G. A. (1994). Physicochemical studies of (o-vanillin thiosemicarbazonato)-nickel(ii) chelate. *Trans. Met. Chem., 19,* 25-27.

Ali, H. M., Abdul Halim, S. N., Subramaniam, P., Zain, S. M., & Ismail, E. (2006). Synthesis and biological activities of Nickel(II) and Cadmium(II) complexes of chlorohydroxyacetophenone-nitrobenzoylhydrazone: Mechanism for formation of the Nickel(II) complex. *Malaysian J. Sci., 25*, 99-105.

Aminabhavi, T .M., Biradar, N. S., Patil, S. B., & Roddabasanagoudar, V .L. (1985). Amino acid schiff base complexes of dimethyldichlorosilane. *Inorg. Chim. Acta, 107*, 231-234.

Aranha, P. E., dos Santos, M. P., Romera, S., & Dockal, E. R. (2007). Synthesis, characterization and spectroscopic studies of tetradentate Schiff base chromium(III) complexes *Polyhedron, 26,* 1373-1382.

Ardestani, M. S., Mehrab, H. & Sadeghzadeh, N. (2007). Effects of dexamethasone and betamethasone as COX-2 gene expression inhibitors on rigidity in a rat model of Parkinsons disease. *Ind. J. Pharmacol., 39,* 235-239.

Balasubramanian, K. P., Parameswari, K., Chinnusamy, V., Prabhakaran, R., & Natarajan, K. (2006). Synthesis, characterization, electro chemistry, catalytic and biological activities of ruthenium(III) complexes with bidentate N, O/S donor ligands. *Spectrochim. Acta A, 65,* 678–683.

Barbour, L. J. (2001). X-Seed-A Software Tool for Supramolecular Crystallography. *J. Supramol. Chem., 1,* 189-191.

Benzie, I. F., & Strain, J. J. (1996). The ferric reducing ability of plasma (FRAP) as a measure of "antioxidant power": The FRAP assay. *Anal. Biochem., 239,* 70-76.

Bocâ, M., Valigura, D. & Linert, W. (2000). NMR study of new ligands as products of condensation of 2-pyridinecarboxaldehyde-N-oxide with polyamines. *Tetrahedron, 56,* 441-446.

Broekkamp, C. L., Leysen, D., Peeters, B. W., & Pinder, R. M. (1995). Prospects for improved antidepressants. *J. Med. Chem., 38,* 4615-4633.

Bruker APEX2 and SAINT, Bruker AXS Inc., Madison, WI, USA, 2007.

Bu, X. R., Jackson, C. R., VanDerveer, D., You, X. Z., Meng, Q. J., & Wang, R. X. (1997). New copper(II) complexes incorporating unsymmetrical tetradentate ligands with

cis-N_2O_2 chromophores: synthesis, molecular structure, substituent effect and thermal stability. *Polyhedron, 16*, 2991-3001.

Calligaris, M., Nardin, G., & Randaccio, L. (1972). Structural aspects of metal complexes with some tetradentate Schiff bases. *Coord. Chem. Rev., 7*, 385.

Casellato, U., & Vigato, P. A. (1977). Transition metal complexes with binucleating ligands. *Coord. Chem. Rev., 23*, 31-117.

Castro, F. G., & Hernandez-Aaron, E. (2002). Integrating cultural variables into drug abuse prevention and treatment with racial/ethnic minorities. *J. Drug, 32*, 783-810.

Chandra, S., Jain, D, & Sharma, A. K. (2009). EPR, mass, electronic, IR spectroscopic and thermal studies of bimetallic copper(II) complexes with tetradentate ligand, 1,4-diformyl piperazine bis(carbohydrazone). *Spectrochim. Acta Part A, 71*, 1712-1719.

Chandra, S., Kumara, R., Singh, R., & Jain, A. K. (2006). Coordination stability between metal/ligands interaction by modern spectroscopic studies: IR, electronic, EPR and cyclic voltammetry of cobalt(II) complexes with organic skeleton containing cyclic ligands. *Spectrochim. Acta Part A, 65*, 852-858.

Chen, Q., & Kristallogr, Z. (2005). Crystal structure of bis[N-cyclohexyl-4-nitrosalicylaldiminato]copper(II), Cu($C_{13}H_{15}N_2O_3$)(2). *New Cryst. Struct., 220*, 635-636.

Cozzi, P. G. (2004). Metal–Salen Schiff base complexes in catalysis: Practical aspects. *Chem. Soc. Rev.*, *33*, 410-421.

Cukurovali, A., Yilmaz, I., & Kirbag, S. (2006). Spectroscopic characterization of salicylaldehyde thiazolyl hydrazone ligands and their metal complexes. *Transition Met. Chem.*, *31*, 207-213.

Denisov G. S., Golubev, N. S., Schreiber, V. M., Shajakhmedov, S. S., & Shurukhina, A. V. (1997). Effect of intermolecular hydrogen bonding and proton transfer on fluorescence of salicylic acid. *J. Mol. Struct., 436-437,* 153-160.

Deshmukh, P. S., Yaul, A. R., Bhojane, J. N., & Aswar, A. S. (2010). Synthesis, characterization and thermogravimetric studies of some metal complexes with N_2O_2 Schiff base ligand. *World J. Chemistry, 5*, 57-61.

Dey, K., Biswas, A. K., & Roy, A. (1981). Metallic complexes as ligands .2. nickel(II) complex of the schiff-base derived from 3-formylsalicylic acid and ethylenediamine as ligand for Ti, Zr, Sn, P and B. *Ind. J. Chem. A, 20,* 848-851.

Dhar, S., Senapati, D., Das, P. K., Chattopadhyay, P., Nethaji, M., & Chakravarty, A. R. (2003). Ternary copper complexes for photo-cleavage of DNA by red light: direct evidence for sulfur to copper charge transfer and *d-d* band involvement. *J. Am. Chem. Soc.,125*, 12118-12124.

Dilović I., Rubcić M., Vrdoljak V., Kraljević P. S., Kralj M., Piantanida I., & Cindrić M. (2008). Novel thiosemicarbazone derivatives as potential antitumor agents: Synthesis, physicochemical and structural properties, DNA interactions and antiproliferative activity. *Bioorg. Med. Chem., 16,* 5189-5198.

Eichhorn, G. L. & Marzilli, L. G. (1994). *Advances in inorganic biochemistry models in inorganic chemistry*. PTR prentice-Hall Inc.

El-Sonbati, A. Z. (1991). Polymer Complexes. XX. Stability Studies in Relation to IR Data and Structural Chemistry of Polychelate from Poly (5-Vinylsalicylidene Semicarbazone) with Some Transition Metal Acetates. *Synth. React. Inorg. Met.-Org. Chem., 21,* 977-990.

Fernandez-G, J. M., Xochitiotzi-Flores, J., Hernandez-Ortega, S., Gomez-Vidales, V., & Patino- Maya, M. D. R. The crystal structures of some Schiff base copper(II) complexes derived from -p-benzylamines. (2010). *J. Coord. Chem., 63*, 2132-2145.

Fessenden, R. J., & Fessenden, J .S. (1998). *Organic Chemistry*. California, USA: Brooks/Cole.

Gaballa, A. S., Asker, M. S., Barakat, A. S, & Teleb, S. M. (2007). Synthesis, characterization and biological activity of some platinum(II) complexes with Schiff bases derived from salicylaldehyde, 2-furaldehyde and phenylenediamine. *Spectrochim. Acta Part A, 67*, 114-121.

Galli, F., Piroddi, M., Annetti, C., Aisa, C., Floridi, E., & Floridi, A. (2005). Oxidative stress and reactive oxygen species. *Contrib. Nephrol., 149*, 240-260.

Geeta, B., Shravankumar, K., Reddy, P. M., Ravikrishna, E., Sarangapani, M., Reddy, K. K., & Ravinder, V. (2010). Binuclear cobalt(II), nickel(II), copper(II) and palladium(II) complexes of a new Schiff-base as ligand: Synthesis, structural characterization, and antibacterial activity. *Spectrochim. Acta Part A, 77*, 911-915.

Golcu, A., Tumer, M., Demirelli, H. & Wheatley, R. A., (2005). Cd(II) and Cu(II) complexes of polydentate Schiff base ligands: synthesis, characterization, properties and biological activity. *Inorg. Chim. Acta, 358*, 1785-1797.

Golcu, A., Tumer, M., Demirelli, H., & Wheatley, R. A. (2005). Cd(II) and Cu(II) complexes of polydentate Schiff base ligands: synthesis, characterization, properties and biological activity. *Inorg. Chim. Acta, 358*, 1785-1797.

Greenwald, R. A. (1990). Superoxide dismutase and catalase as therapeutic agents for human diseases. A critical review. *Free Radic. Biol. Med., 8*, 201-209.

Guillonneau, B., el-Fettouh, H., Baumert, H., Cathelineau, X., Doublet, J. D., Fromont, G., & Vallancien, G. (2003). Laparoscopic radical prostatectomy: oncological evaluation after 1,000 cases a Montsouris Institute. *J. Urol., 169*, 1262-1266.

Guha, A., Banu, K. S., Das, S., Chattopadhyay, T., Sanyal, R., Zangrando, E., & Das, D. (2013). A series of mononuclear nickel(II) complexes of Schiff-base ligands having N,N,O- and N,N,N-donor sites: Syntheses, crystal structures, solid state thermal property and catecholase-like activity. *Polyhedron, 52*, 669-678.

Gupta, S. P. (1994). Quantitative structure-activity relationship studies on anticancer drugs *Chemical reviews, 94*, 1507-1551.

Hine, J., & Yeh, C. Y. (1967). Equilibrium in formation and conformational isomerization of imines derived from isobutyraldehyde and saturated aliphatic primary amines. *J. Am. Chem. Soc., 89*, 2669.

Hisham, N. A. I., Ali, H. M., Ng, S. W. (2009). Chlorido{4-chloro-2-[(2 morpholinoethyl)iminomethyl] phenolato-kappa N-3,N ',O}copper(II). *Acta Cryst., E65*, m870.

Howard-Lock, H. H. & Lock, C. J. L. (1987). *Medicinal properties of organometallic compounds: In: Comprehensive Coordination Chemistry*. Pergamon: Oxford.

Hughes, M. N., (1984). *The inorganic chemistry of biological processes, 2nd edition*. Wiley: New York.

Hughes, R. A. C., Gregson, N. A., Hadden, R. D. M., & Smith, K. J. (1999). Pathogenesis of Guillain-Barré syndrome. *J. Neuroimmunol., 100*, 74-97.

Kalanithia, M., Rajarajan, M., Tharmaraj, P., & Sheela, C. D. (2012). Spectral, biological screening of metal chelates of chalcone based Schiff bases of N-(3-aminopropyl) imidazole. *Spectrochim. Acta Part A, 87*, 155-162.

Kelley, J. L., Musso, D. L., Boswell, G. E., Soroko, F. E., & Cooper, B. R. (1996). (2S,3S,5R)-2-(3,5-difluorophenyl)-3,5-dimethyl-2-morpholinol: a novel antidepressant agent and selective inhibitor of norepinephrine uptake. *J. Med. Chem., 39*, 347-349.

Latour, J. -M., Tandon, S. S., Leonard, G. A., & Povey, D. C. (1989). Structure of chloro{N-[2-(4-imidazolyl)ethyl]salicylideneaminato}copper(II) monohydrate. *Acta Cryst., C45*, 598-600.

Leovac, V. M., Jevtovic´, V. S., Jovanovic´, L. S., & Bogdanovic´, G. A. (2005). Metal complexes with Schiff-base ligands-pyridoxal and semicarbazide-based derivates. *J. Serb. Chem. Soc., 70*, 393-422.

Li, W.-H., & Huaxue, J. (2007). Synthesis and Structure of a Novel Copper (II) Dinuclear Complex with 4,4′-Dipyridyl as the Bridge. *Chin. J. Struct. Chem., 26*, 1053.

Lim, G. C. C., & Halimah, Y. (2004). *Second report of the National Cancer Registry.Cancer incidence in Malaysia 2003*. Kuala Lumpur: National Cancer Registry.

Liu, G. -l., He, S. -f., Zhang, S., & Li, H. (2012). *In situ* ligand and complex transformation of an iron(III) Schiff base complex: structural evidence and theoretical calculations. *Dalton Trans., 41*, 6256-6262

Lovejoy, D. B. & Richardson, D. R. (2002). Novel "hybrid" iron chelators derived from aroylhydrazones and thiosemicarbazones demonstrate selective antiproliferative activity against tumor cells. *Blood, 100,* 666-676.

Lu, Z. -L., Xiao, W., Kang, B. -S., Su, C. -Y., & Liu, J. (2000). Chemistry of aroylhydrazones: bis-bipyridine ruthenium(II) complexes with aroylhydrazone ligands containing ferrocenyl moiety. *J. Mol. Struct., 523,* 133-141.

Mahmood, I, & Sahajwalla, C. (1999). Clinical pharmacokinetics and pharmacodynamics of buspirone, an anxiolytic drug. *Clin. Pharmacokinet., 36,* 277-287.

Martin, M. G., Gili, P., Zarza, P. M., Medina, A., & Diaz, M. C.(1986). Complexes of Cu(II), Ni(II) and Co(II) with the shiff base: 1H-indole-3-ethylensalicylaldimine as ligand. *Inorg. Chim. Acta, 116,* 153-156.

Mikhaylova, Y., Adam, G., Haussler, L., Eichhorn, K. J., & Voit, B. (2006). Temperature-dependent FTIR spectroscopic and thermoanalytic studies of hydrogen bonding of hydroxyl (phenolic group) terminated hyperbranched aromatic polyesters. *J. Mol. Struct., 788,* 80-88.

Mills, G. C. (1957). Hemoglobin catabolism. I. Glutathione peroxidase, an erythrocyte enzyme which protects hemoglobin from oxidative breakdown. *J. Biol. Chem., 229,* 189-197.

Mishra, A. K., Manav, N., & Kaushik, N. K. (2005). Organotin(IV) complexes of thiohydrazones: synthesis, characterization and antifungal study. *Spectrochim. Acta, Part A, 61,* 3097-3101.

Mishra, A. P., & Soni, M.(2008). Synthesis, structural, and biological studies of some Schiff bases and their metal complexes. *Met.-Based Drugs, 2008,* 1-7.

Mosmann, T. (1983). Rapid colorimetric assay for cellular growth and survival: application to proliferation and cytotoxicity assays. *J. Immunol. Methods, 65*, 55-63.

Mukhopadhyay, S., Mandal, D., Ghosh, D., Goldberg, I., & Chaudhury, M. (2003). Equilibrium studies in solution involving nickel(II) complexes of flexidentate Schiff base ligands: Isolation and structural characterization of the planar red and octahedral green species involved in the equilibrium. *Inorg. Chem., 42*, 8439-8445.

Mustafa, I. M, Ali, H. M, Abdulla, M. A, & Ward, T. R. (2009). Synthesis, structural characterization, and anti-ulcerogenic activity of schiffbase ligands derived from tryptamine and 5-chloro, 5- nitro, 3,5-ditertiarybutyl salicylaldehyde and their nickel(II), copper(II), and zinc(II) complexes. *Polyhedron, 28*, 3993-3998.

Muzykantov, V. R. (2001). Targeting of superoxide dismutase and catalase to vascular endothelium. *J. Control. Release, 71,* 1-21.

Nakamoto, K. (1986). *Infrared spectra of inorganic and coordination compounds*. New York: Wiley and Sons.

Nelson, S. M., Knox, C. V., McCann, M., & Drew, M. G. B. (1981). Metal-ion-controlled transamination in the synthesis of macrocyclic Schiff-base ligands. Part 1. Reactions of 2,6-diacetylpyridine and dicarbonyl compounds with 3,6-dioxaoctane-1,8-diamine. *J. Chem. Soc. Dalton Trans.*, 1669-1677.

Ning, Y. -C. (2011). *Interpretation of Organic Spectra: Interpretation of ^{13}C NMR Spectra.* Asia: John Wiley & Son

Oki, T., Masuda, M., Furuta, S., Nishiba, Y., Terahara, N., & Suda, I. (2002). Involvement of anthocyanins and other phenolic compounds in radical-scavenging activity of purplefleshed sweet potato cultivars. *J. Food Sci., 67*, 1752-1756.

Osowole, A. A., Ott, I., & Ogunlana, O. M. (2012). Synthesis, spectroscopic, anticancer and antimicrobial properties of some metal(II) complexes of 2-[(2,3- dihydro-1H-inden-4-ylimino) methyl]-5-nitrophenol. *Inter. J. Inorg. Chem., 2012*, 1-6.

Otto, P., Ladik, J., & Szent-Gyorgyi, A. (1978). Internal charge transfer in proteins to the Schiff bases of their lysine side chains. *Proc. Nat. Acad. Sci., 75*, 3548.

Pandeya, S. N., Sriram, D., Nath, G., & Clercq, E. (2000). Synthesis, antibacterial, antifungal and anti-HIV evaluation of Schiff and Mannich bases of isatin and its derivatives with triazole. *Arzneimittel Forsch., 50*, 55.

Panneerselvam, P., Nair, R. R., Vijayalakshmi, G., Subramanian, E. H., & Sridhar, S. K. (2005). Synthesis of Schiff bases of 4-(4-aminophenyl)-morpholine as potential antimicrobial agents. *Eur J Med Chem, 40*, 225-229.

Panneerselvam, P., Priya, M. G., Kumar, N. R. & Saravanan, G. (2009). Synthesis and pharmacological evaluation of schiff bases of 4-(2-aminophenyl)-morpholines. *Indian J Pharm Sci., 71*, 428-432.

Paschke, R., Liebsch, S., Tschierske, C., Oakley, M. A., & Sinn, E. (2003). Synthesis and mesogenic properties of binuclear copper(II) complexes derived from salicylaldimine Schiff bases. *Inorg. Chem., 42*, 8230-8240.

Pastor, M. F., Whitehorne, T. J. J., Oguadinma, P. O., & Schaper, F. (2011). Zinc complexes of chiral ligands obtained from methylbenzylamine. *Inorg. Chem. Commun.*, *14*, 1737-1741.

Percy, G.C., & Thornton, J. (1973). Infrared spectra of N-aryl salicylaldimine complexes substituted in both aryl rings. *J. Inorg. Nucl. Chem., 35*, 2319

Poirier, V., Roisnel, T., Carpentier, J. -F., & Sarazin, Y. (2009). Versatile catalytic systems based on complexes of zinc, magnesium and calcium supported by a bulky bis(morpholinomethyl)phenoxy ligand for the large-scale immortal ring-opening polymerisation of cyclic esters. *Dalton Trans.* (44), 9820-9827.

Polishchuk , A. P., Antipin, M. Y., Timofeeva, T. V., Struchkov, Y. T., Galyametdinov, Y. G., & Ovchinnikov, I. V.(1986). Structure of crystalline predecessors of mesophases - x-ray-investigation and energy calculation of bis[4-normal-heptyloxy)-n-(para-methoxyphenyl)benzaldimino-2-olate] copper(2+) crystal. *Kristallografiya (Russ.)[Crystallogr. Rep.]*, *31*, 466-473.

Prasad, K. S., Kumar, L. S., Prasad, M., & Revanasiddappa, H. D. (2010). Novel organotin(IV)-Schiff base complexes: synthesis, characterization, antimicrobial activity, and dna interaction studies. *Bioinorg. Chem. Applic*., *2010*, 1-9.

Prelog, V., & Driza, G. (1933). Sur la N-phénylpipérazine. *J. Collect. Czech. Chem. Commun., 5*, 497-502.

Qiu, X. -Y. (2006). {4-Bromo-2-[3-(dimethylamino)propyliminomethyl]phenolato}-dichlorozinc(II). *Acta Cryst., E62*, m2173-m2174.

Rang, H.P., Dale, M.M., & Ritter, J.M. (1995). *Pharmacology 3rd Edition*. (pp. 835) Churchill Livingstone: Edinburgh

Rawls, R. L. (1998). Puzzling promise of protein prenylation. *Chem. Eng. News, 76,* 67-69.

Rezaeifard, A., Jafarpour, M., Nasseri, M. A., & Haddad R. (2010). Pronounced catalytic activity of manganese(III)–Schiff base complexes in the oxidation of alcohols by tetrabutylammonium peroxomonosulfate. *Helv. Chim. Acta, 93*, 711-717

Rossen, K., Weissman, S. A., Sager, J., Reamer, R. A., Askin, D., Volante, R. P., & Reider, P. J. (1995). Asymmetric hydrogenation of tetrahydropyrazines: Synthesis of (S)-piperazine-2-tert-butylcarboxamide, an intermediate in the preparation of the HIV protease inhibitor indinavir. *Tetrahedron Lett., 36*, 6419-6422.

Sang, Y. L., & Lin, X. S. (2010). Synthesis and crystal structures of two Schiff base copper(II) complexes derived from 4-chloro-2-[(2-morpholin-4-ylethylimino)methyl]-phenol and 4-chloro-2-(cyclohexyliminomethyl)phenol. *Synt. Cryst. Struct., 36*, 475-479.

Sang, Y. L., & Lin, X. S. (2009). Synthesis, crystal structures, and antibacterial activities of two copper(II) complexes derived from 1-[(2-morpholin-4-ylethylimino)methyl]-naphthalen-2-ol. *Transition Met. Chem., 34*, 931-936.

Sarkar, B., Drew, M. G. B., Estrader, M., Diaz, C., & Ghosh, A. (2008). Cu^{II} acetate complexes involving *N,N,O* donor Schiff base ligands: Mono-atomic oxygen bridged dimers and alternating chains of the dimers and $Cu_2(OAc)_4$. *Polyhedron, 27*, 2625-2633.

Schon, E., Plattner, D. A., & Chen, P. (2004). Defect-induced acceleration of a solid-state chemical reaction in zinc alkoxide single crystals. *Inorg. Chem., 43*, 3164.

Selvakumar, K., & Vancheesan, S. (1995). Synthesis and characterization of cyclopalladated binuclear complexes of benzylamines. *Polyhedron, 14*, 2091-2097.

Shamspur, T., Mashhadizadeh, M. H., & Sheikhshoaie, I. (2003). *J. Anal. At. Spectrom., 18*, 1407-1410.

Sheldrick, G. M. (2008). A short history of SHELX. *Acta Cryst., A64*, 112-122.

Shnulin, A.N., Struchkov, Y.T., Mamedov, K.S., Mezhidov, A.A., & Kutovaya, T.M. (1977). Stereochemistry of the copper atom in salicylaldiminate complexes. *J. Struct. Chem., 18,* 799-805.

Singh, B. K., Jetley, U. K., Sharma, R. K., & Garg, B. S. (2007). Synthesis, characterization and biological activity of complexes of 2-hydroxy-3,5-dimethyl-acetophenoneoxime (HDMAOX) with copper(II), cobalt(II), nickel(II) and palladium(II). *Spectrochim. Acta Part A, 68*, 63-73.

Sladojevich, F., Trabocchi, A., & Guarna, A. (2008). Stereoselective cyclopropanation of serine- and threonine-derived oxazines to access new morpholine-based scaffolds. *Org. Biomol. Chem., 6*, 3328-3336.

Sultana, R., Banks, W. A., & Butterfield, D. A. (2010). Decreased Levels of PSD95 and Two Associated Proteins and Increased Levels of BCl2 and Caspase 3 in Hippocampus from Subjects with Amnestic Mild Cognitive Impairment: Insights into Their Potential Roles for Loss of Synapses and Memory, Accumulation of A beta, and Neurodegeneration in a Prodromal Stage of Alzheimer's Disease. *J. Neurosci. Res., 88*, 469-477.

Sun, Y. -X., Kong, D. -S., Yang, G., & You, Z. -L. (2006). Synthesis, crystal structures and antibacterial activities of a pair of isostructural dinuclear Schiff base nickel(II) and copper(II) complexes. *Polish J. Chem., 80*, 1457-1463.

Syamal, A. & Maurya, M. R. (1989). Coordination chemistry of Schiff base complexes of molybdenum. *Coord. Chem Reviews, 95,* 183-238.

Szlyk, E., Surdykowski, A., Barwiolek, M., & Larsen, E. (2002). Spectroscopy and stereochemistry of the optically active copper(II), cobalt(II) and nickel(II) complexes with Schiff bases *N*,*N*′-(1R,2R)-(−)-1,2-cyclohexylenebis(3-methylbenzylidene-iminato) and *N*,*N*′-(1R,2R)-(−)-1,2-cyclohexylenebis(5-methylbenzylideneiminato). *Polyhedron, 21*, 2711-2717.

Tai, X., Yin, X., Chen, Q., & Tan, M. (2003). Synthesis of some transition metal complexes of a novel Schiff base ligand derived from 2,2′-bis(p-methoxyphenylamine) and salicylicaldehyde. *Molecules, 8,* 439-443.

Tai, X. -S., Feng, Y. -M., & Zhang, H. -X. (2008). {2,2'-[4-Methyl-4-azaheptane-1,7-diylbis(nitrilomethylidyne)]diphenolato}zinc(II). *Acta Cryst., E64,* m502.

Tamizh, M. M., Mereiter, K., Kirchner, K., Bhat, B. R., & Karvembu, R. (2009). Synthesis, crystal structures and spectral studies of square planar nickel(II) complexes containing an ONS donor Schiff base and triphenylphosphine. *Polyhedron, 28,* 2157-2164.

Tarafder, M. H., Saravanan, N., Crouse, K. A. & Ali, A. M. (2001).Coordination chemistry and biological activity of Ni(II)and Cu(II) ion complexes with nitrogen-sulphur donor ligands derived from S-benzyldit. *Trans. Met. Chem., 26,* 613-618.

Tas, E., Kilic, A., Durgun, M., Kupecik, L., Yilmaz, I., & Arslan, S. (2010). Cu(II), Co(II), Ni(II), Mn(II), and Fe(II) metal complexes containing N,N′-(3,4-diaminobenzo-phenon)-3,5-But2-salicylaldimine ligand: Synthesis, structural characterization, thermal properties, electrochemistry, and spectroelectrochemistry. *Spectrochim. Acta A, 75,* 811-818.

Torzilli, M. A., Colquhoun, S., Doucet, D., & Beer, R. H. (2002). The interconversion of dichlorobis(N-n-propylsalicylaldimine)zinc(II) and bis(N-n-propylsalicylaldiminato)-zinc(II). *Polyhedron, 21*, 697-708.

Turan-Zitouni, G., Kaplancikli, Z. A., Özdemir, A., & Chevallet, P. (2007). Studies on 1,2,4-triazole derivatives as potential anti-inflammatory agents. *Arch. Pharm. Chem. Life Sci., 340*, 586.

Ustynyuk, Y.A., Chertkov, V.A., & Barinov, I.V. (1971). *J. Organomet. Chem., 29*, C53-C54.

Valko, M., Leibfritz, D., Moncol, J., Cronin, M. T., Mazur, M. & Telser, J. (2007). Free radicals and antioxidants in normal physiological functions and human disease. *Int. J. Biochem. Cell. Biol.,39*, 44-84.

Vanco, J., Marek, J., Trávnícek, Z., Racanská, E., Muselík, J., & Švajlenová, O. (2008). Synthesis, structural characterization, antiradical and antidiabetic activities of copper(II) and zinc(II) Schiff base complexes derived from salicylaldehyde and β-alanine. *J. Inorg. Biochem., 102*, 595-605.

Vogel, V.G. (2008). Epidemiology, genetics, and risk evaluation of postmenopausal women at risk of breast cancer. *Menopause, 15*, 782-789.

Wang, C. Y. (2010). Synthesis and Crystal Structures of Cobalt(III) and Zinc(II) Complexes Derived From 4-Chloro-2-[(2-Morpholin-4-Ylethylimino)Methyl]Phenol with Urease Inhibitory Activity. *Russ. J. Coor. Chem., 32*, 177-182.

Wang, P. H., Keck, J. G., Lien, E. J., & Lai, M. M. (1990). Design, synthesis, testing, and quantitative structure-activity relationship analysis of substituted salicylaldehyde Schiff bases of 1-amino-3-hydroxyguanidine tosylate as new antiviral agents against coronavirus. *J. Med. Chem., 33,* 608-614.

Wilkinson, G., Gillard, R. D., & McCleverty, J. A. (1987). *Comprehensive coordination chemistry: The synthesis, reactions, properties & applications of coordination compounds*. United Kingdom: Wiley.

Woollins, J. D. (2010). *Inorganic experiments* (pp. 124). New York: Wiley-Vch.

Ye, L. -J. & You, Z. (2008). {(E)-2-Bromo-4-chloro-6-[3(dimethylammonio)-propylimino methyl]phenolato}dichloridozinc(II). *Acta Cryst., E64*, m869.

Yin, H., Hong, M., Xu, H., Gao, Z., Li, G., & Wang, D. (2005). Self-assembly of organotin(IV) moieties with the Schiff-base ligands pyruvic acid isonicotinyl hydrazone and pyruvic acid salicylhydrazone: Synthesis, characterization, and crystal structures of monomeric or polymeric complexes. *Eur. J. Inorg. Chem., 2005*, 4572-4581.

You, Z. -L., & Chi, J. -Y. (2006). Syntheses and structures of 2,4-dichloro-6 (cyclopropyl-iminomethyl)phenol and its copper(II) complex. *J. Coord. Chem., 59,* 1999-2004.

You, Z.-L., Shi, D. -H., & Zhu, H. –L. (2006). The inhibition of xanthine oxidase by the Schiff base zinc(II) complex. *Inorg. Chem. Commun., 9,* 642-644.

Zhu, X. -W. (2008). Dichlorido{2-[3(dimethylammonio)propyliminomethyl]-phenolato}zinc(II) hemihydrate. *Acta Cryst., E64*, m1456-m1457.

Zishen, W., Zhiping, L., & Zhenhuan, Y. (1993). Synthesis, characterization and antifungal activity of glycylglycine Schiff base complexes of 3d transition metal ions. *Trans. Met. Chem., 18,* 291-294.

Zumdahl, S. S., & Zumdahl, S. A. (2008). *Chemistry 8th Edition*. United State of America: Charles Hartford.

APPENDICES

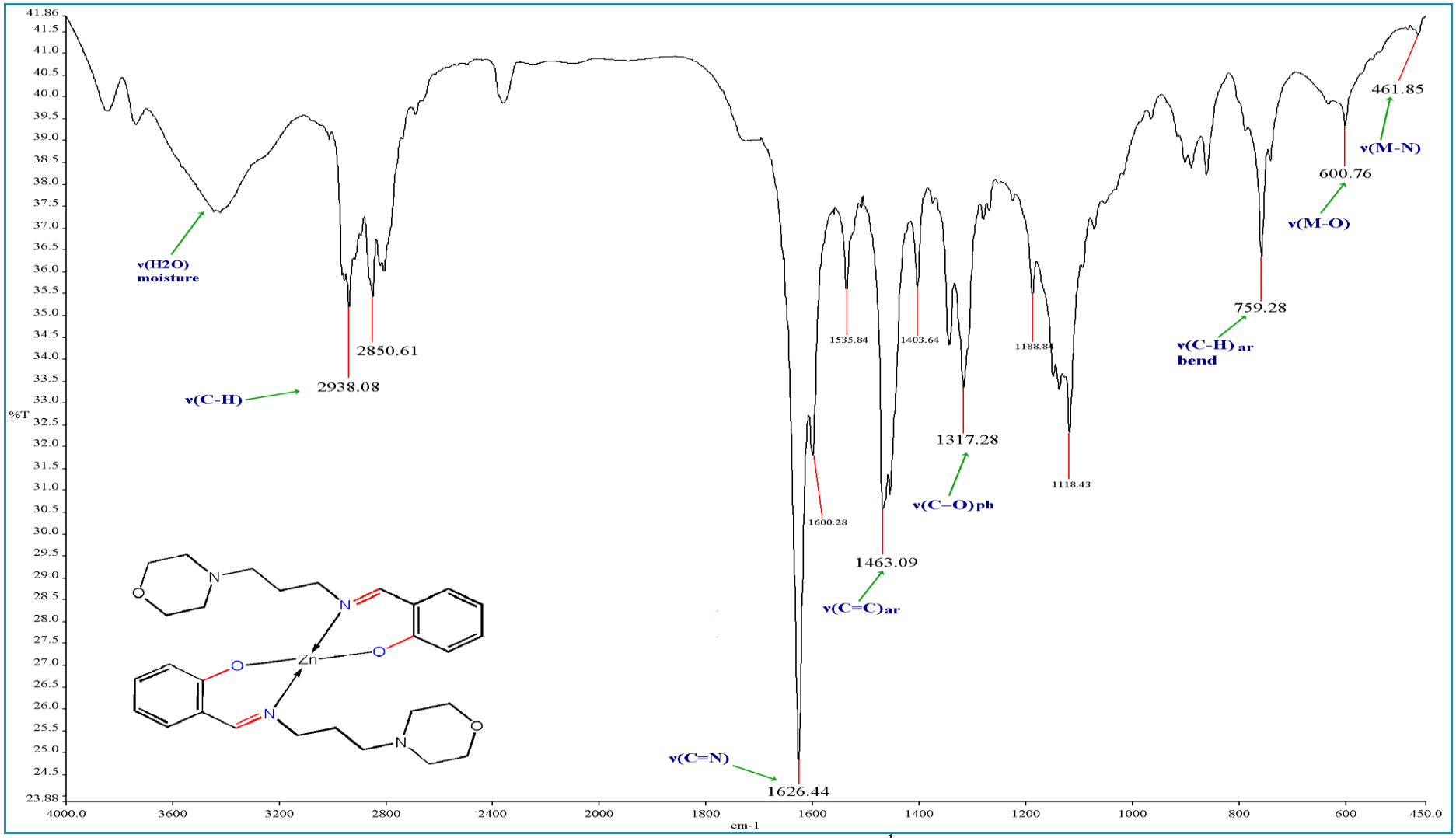

Appendix A.1: IR spectra for $[Zn(L^1)_2]$.

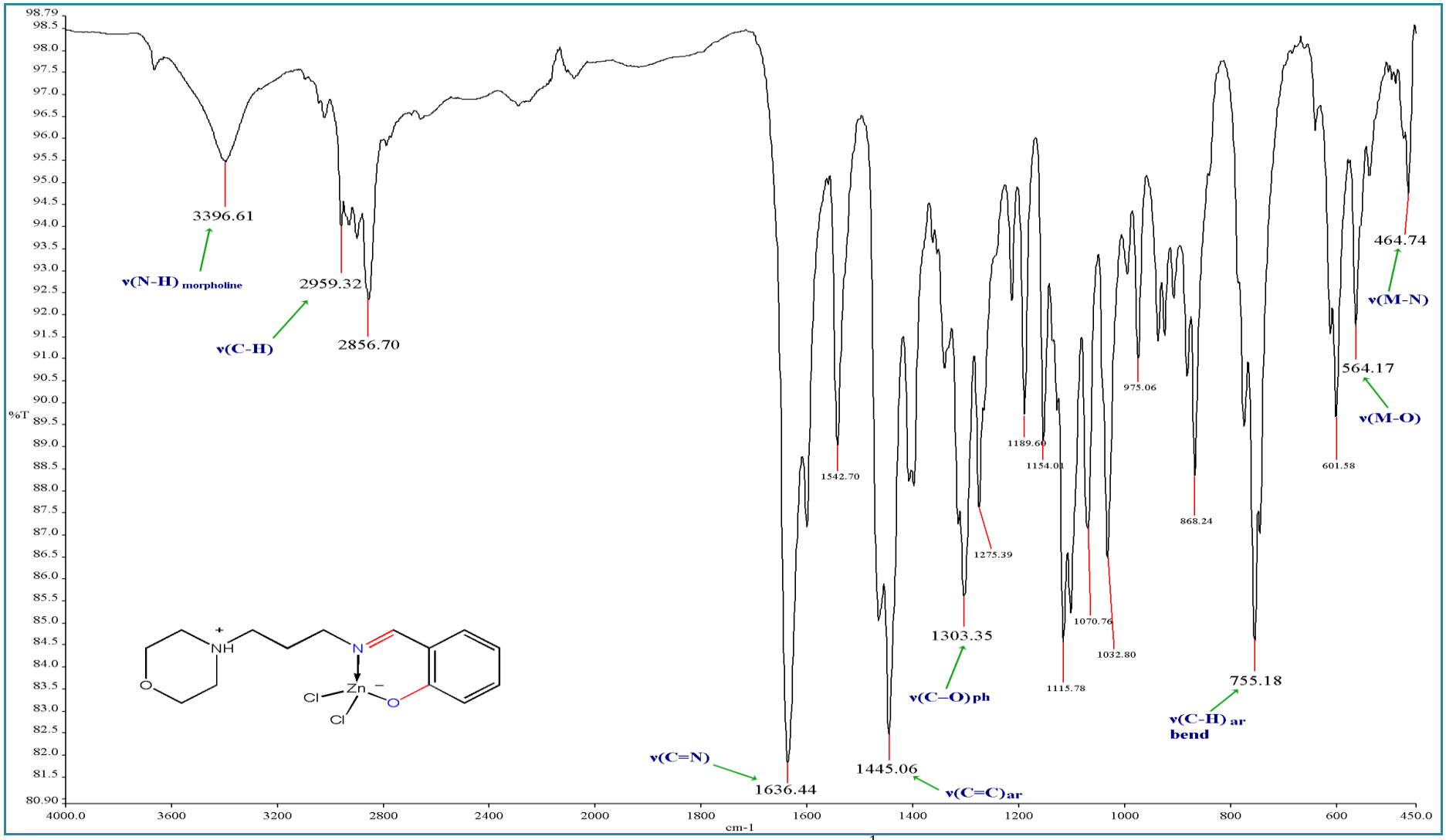

Appendix A.2: IR spectra for $[Zn(L^1)Cl_2]$.

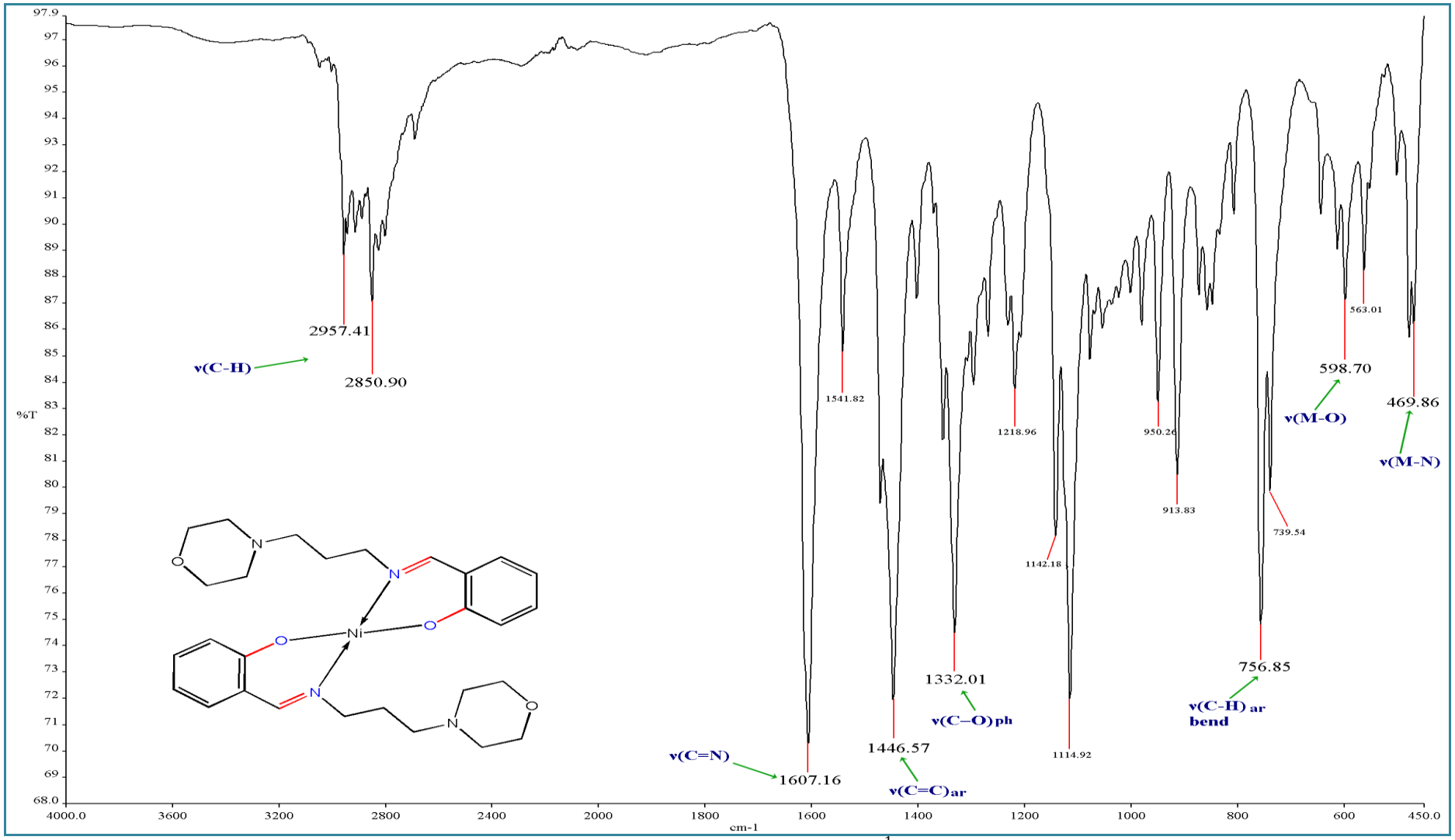

Appendix A.3: IR spectra for $[Ni(L^1)_2]$.

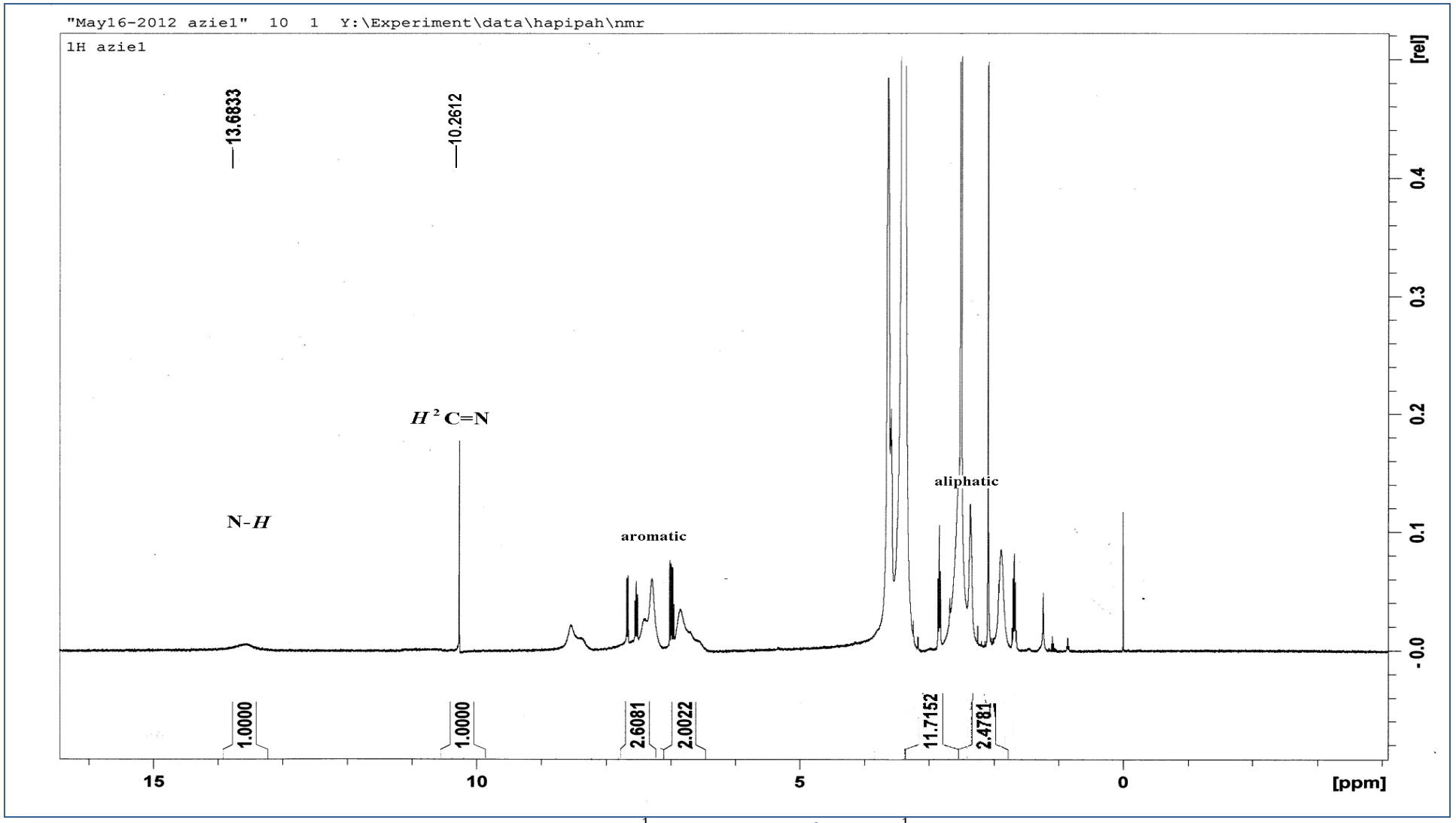

Appendix A.4: ^{1}H-NMR spectra for $[Zn(L^{1})Cl_2]$.

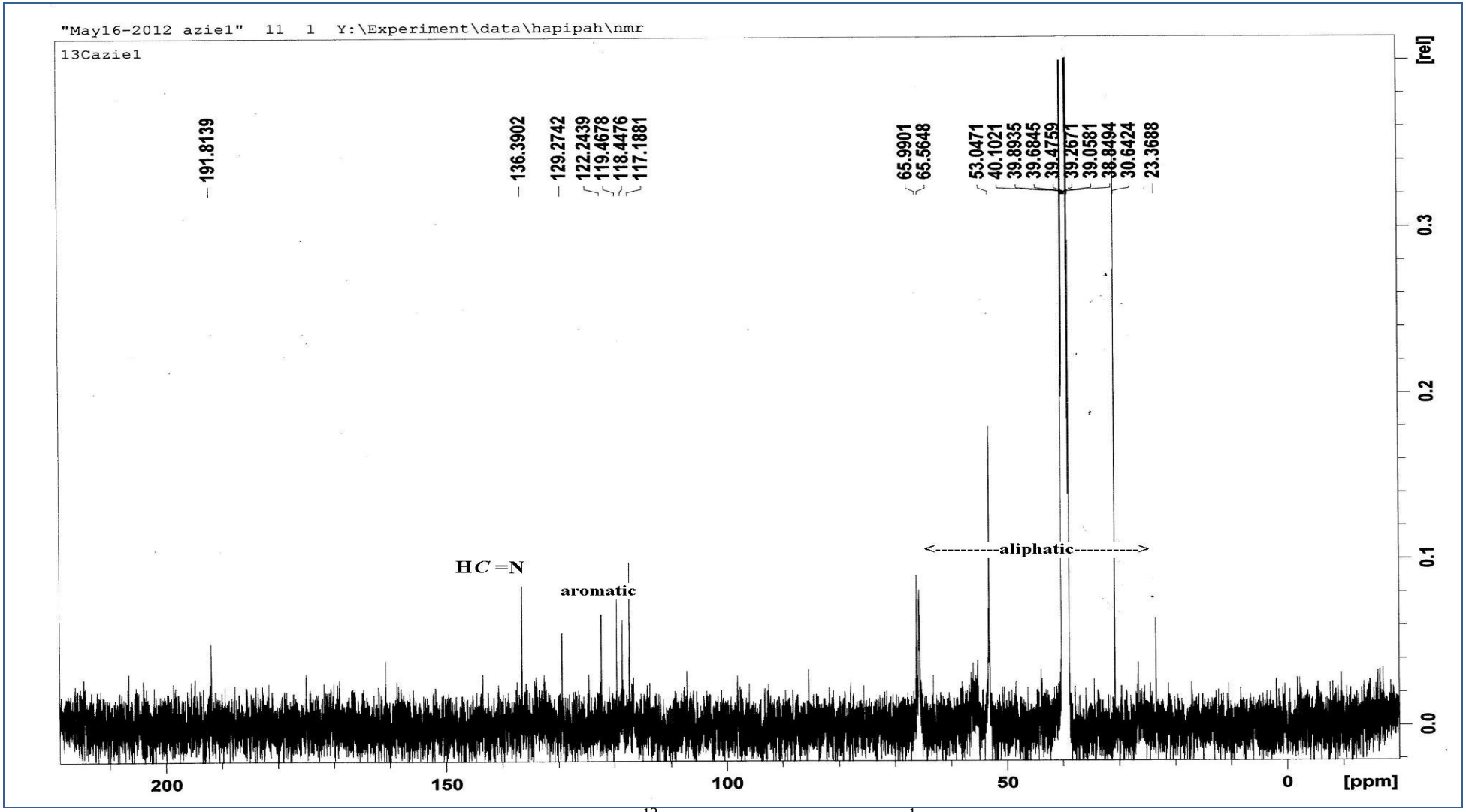

Appendix A.5: ^{13}C-NMR spectra for [Zn(L^1)Cl_2].

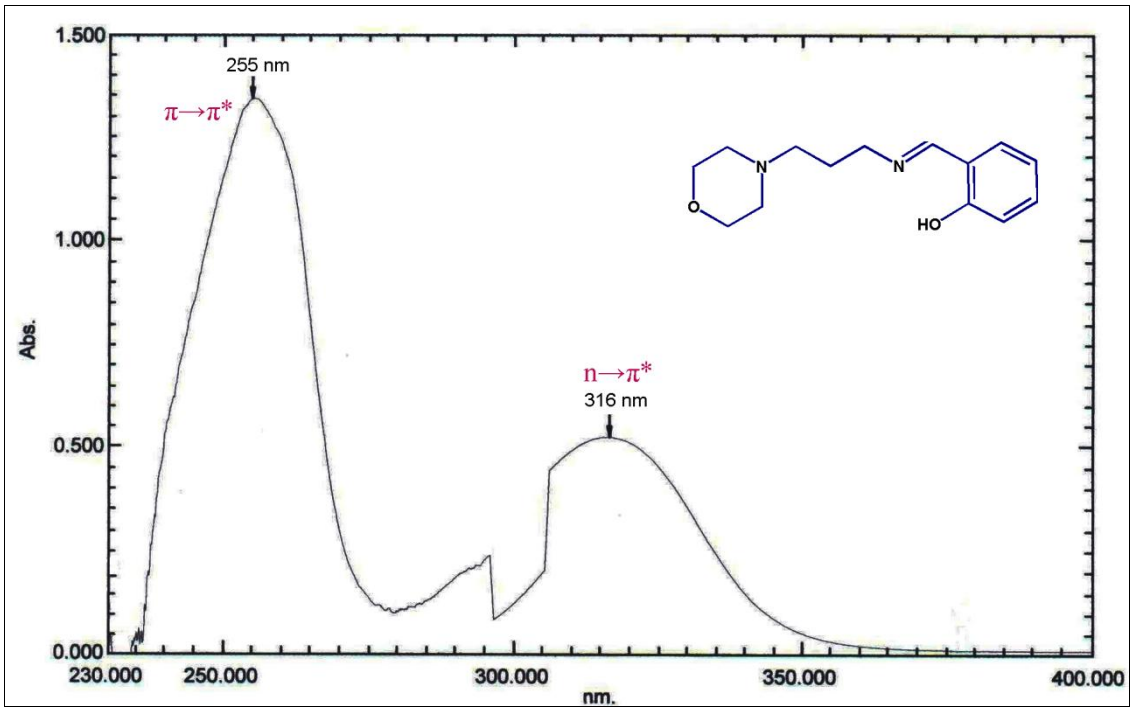

Appendix A.6: UV-Vis spectra for L^1H.

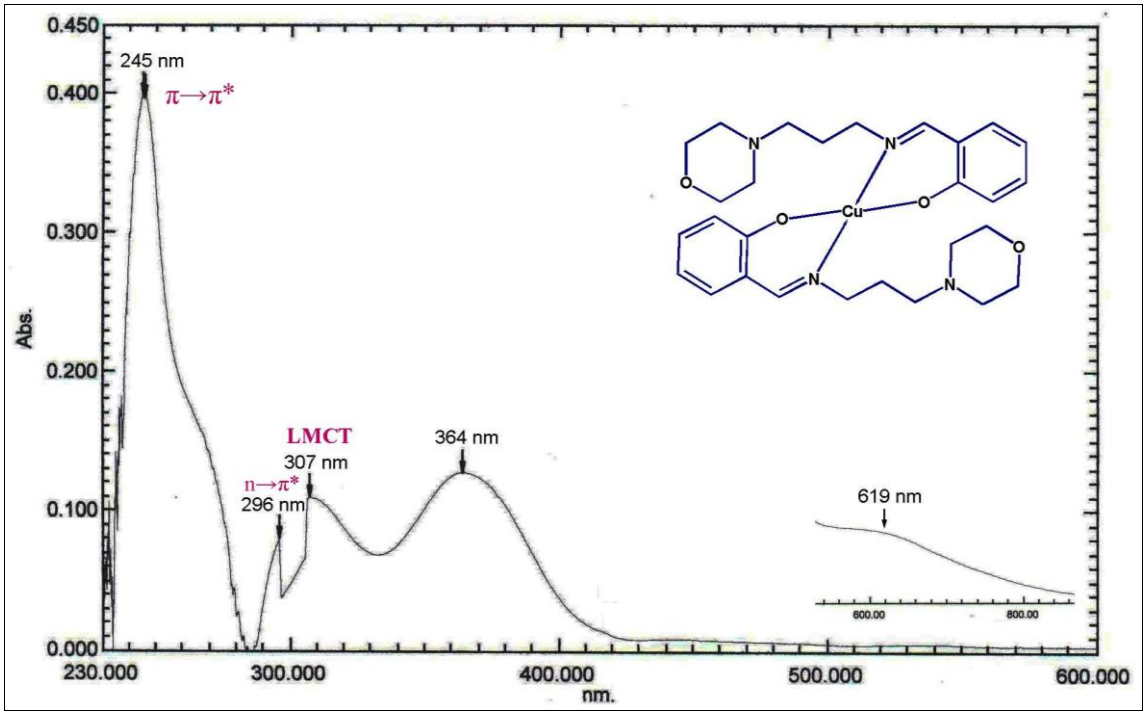

Appendix A.7: UV-Vis spectra for $[Cu(L^1)_2]$.

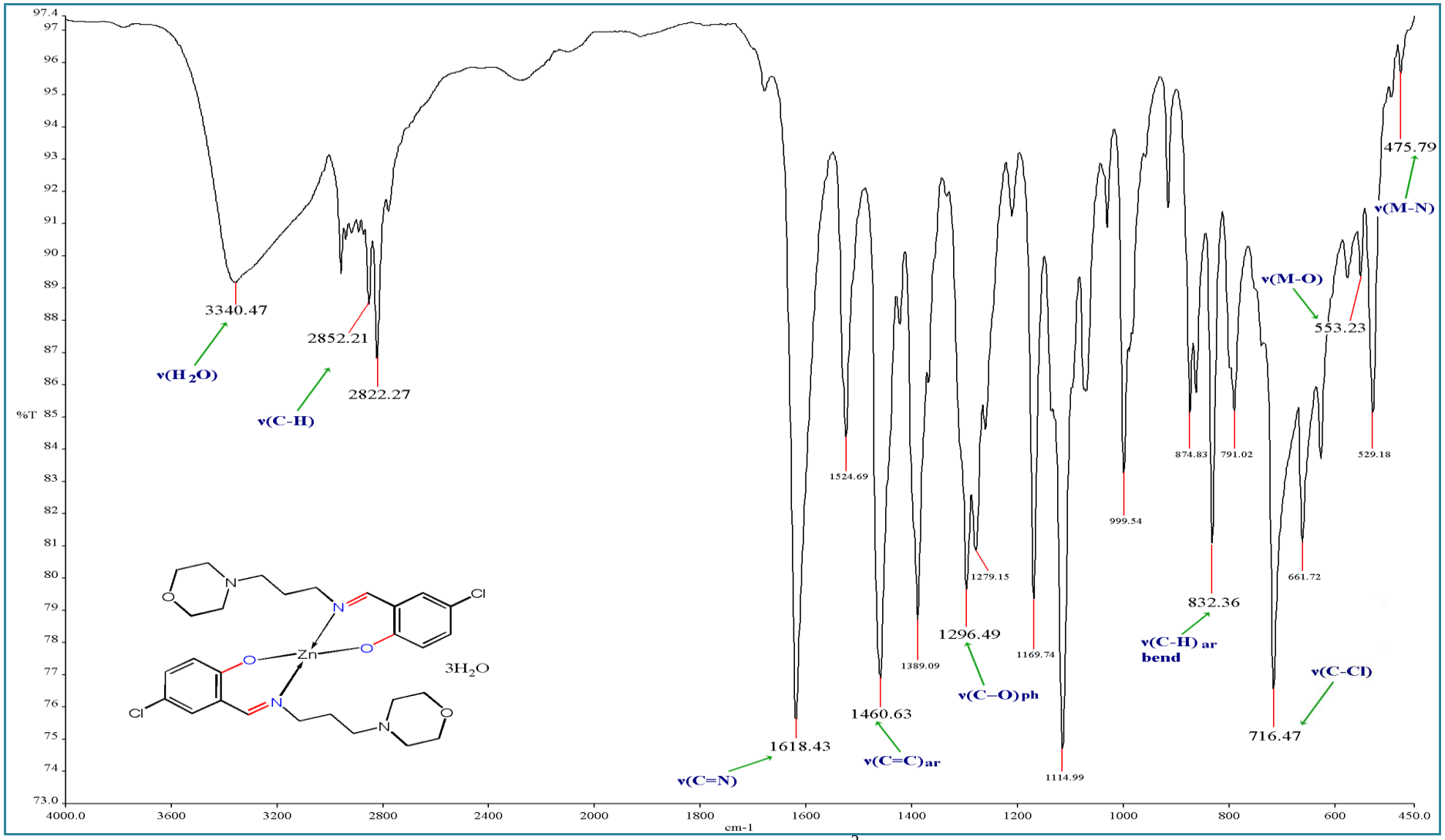

Appemdix B.1: IR spectra for $[Zn(L^2)_2]\cdot 3H_2O$.

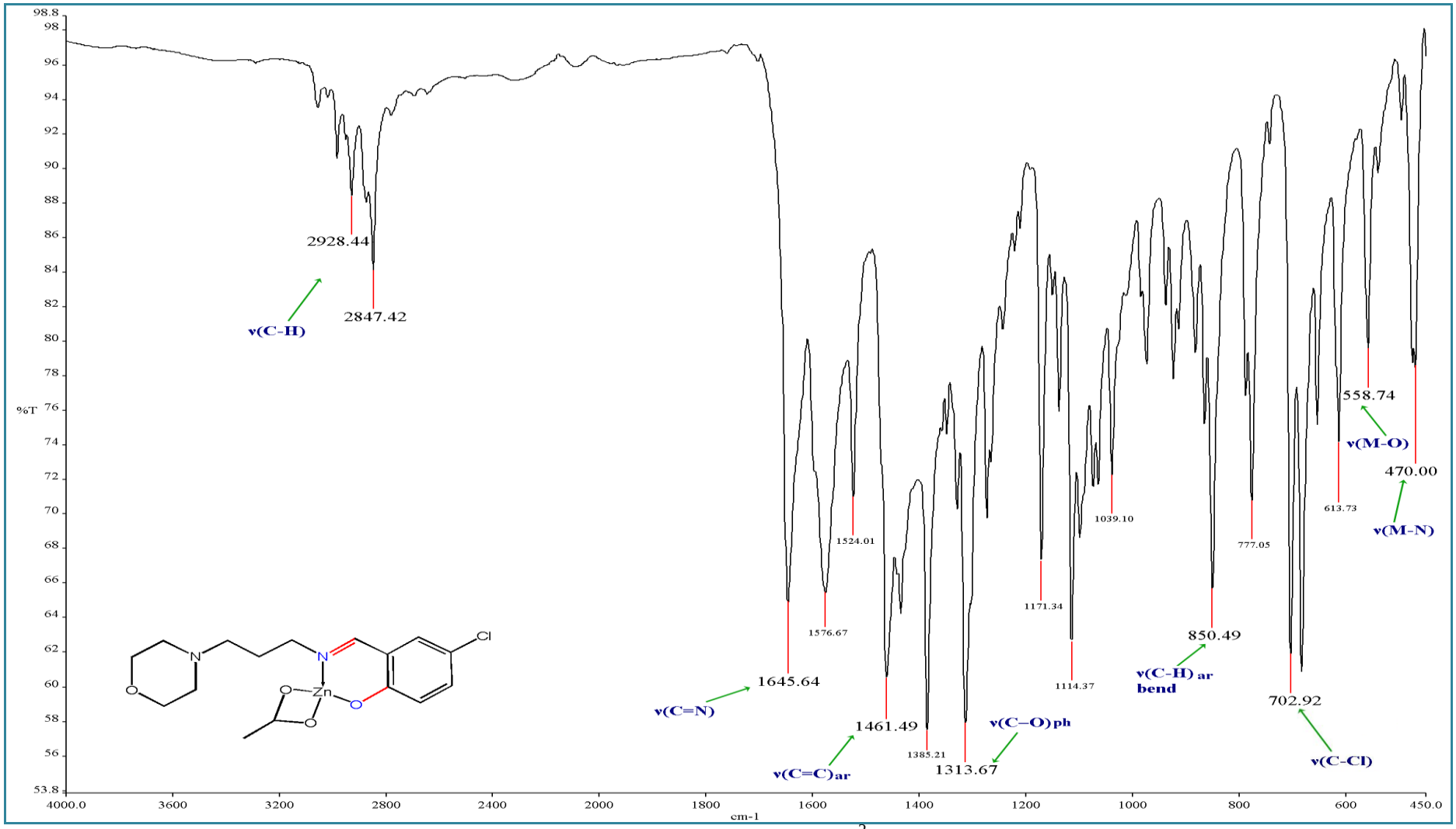

Appendix B.2: IR spectra for $[Zn(L^2)(OAc)]$.

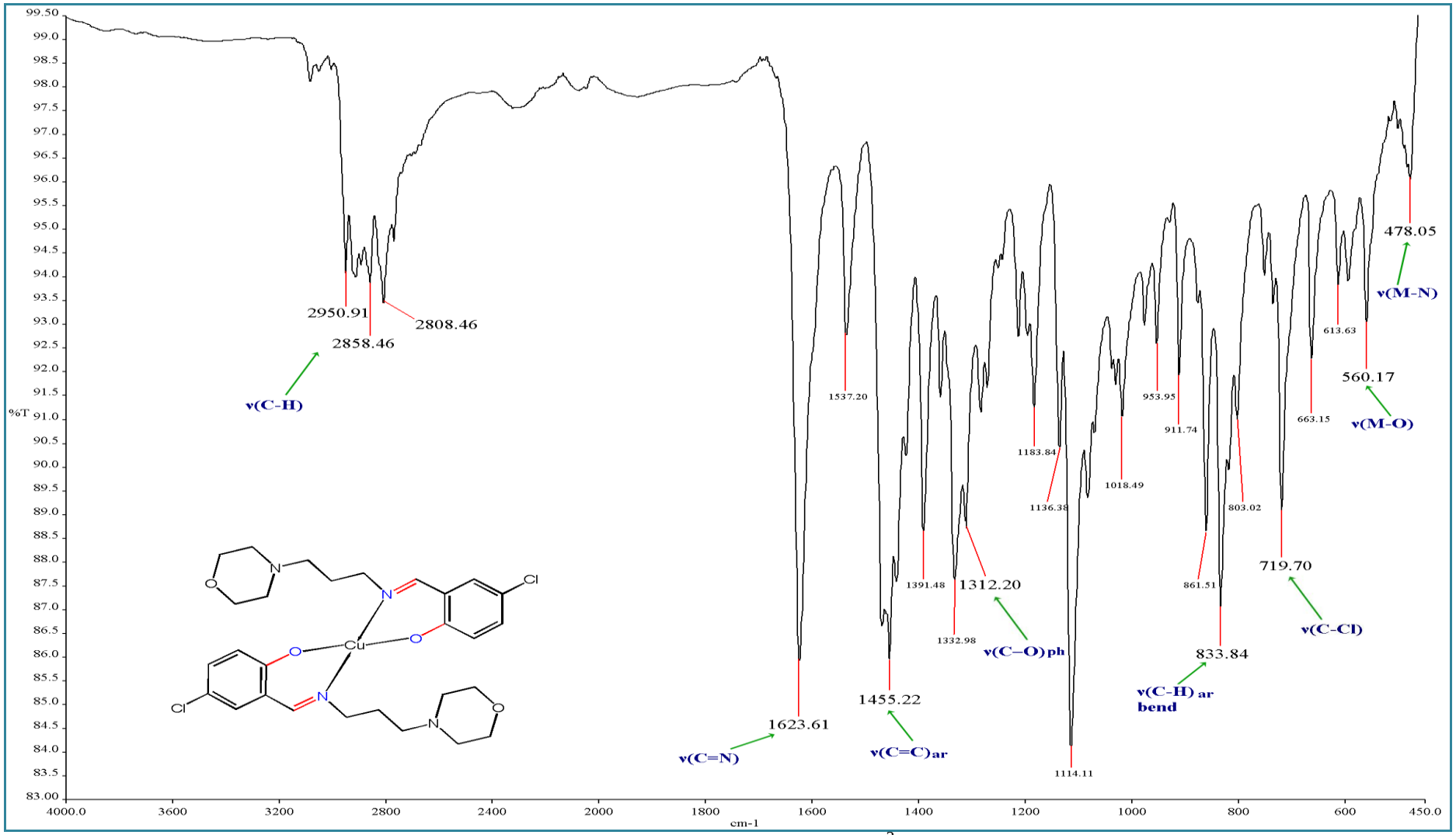

Appendix B.3: IR spectra for $[Cu(L^2)_2]$.

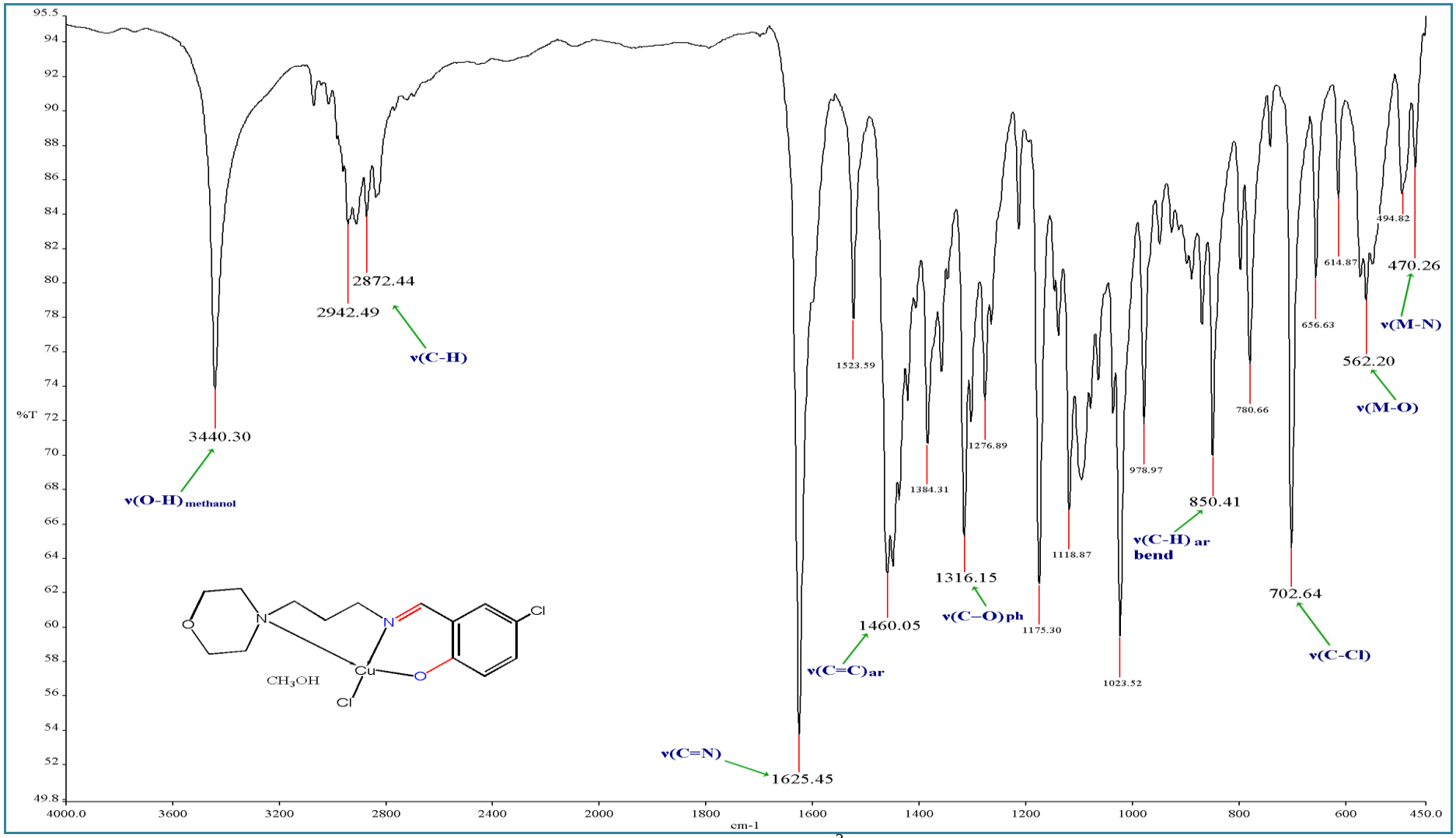

Appendix B.4: IR spectra for $[Cu(L^2)Cl]\bullet CH_3OH$.

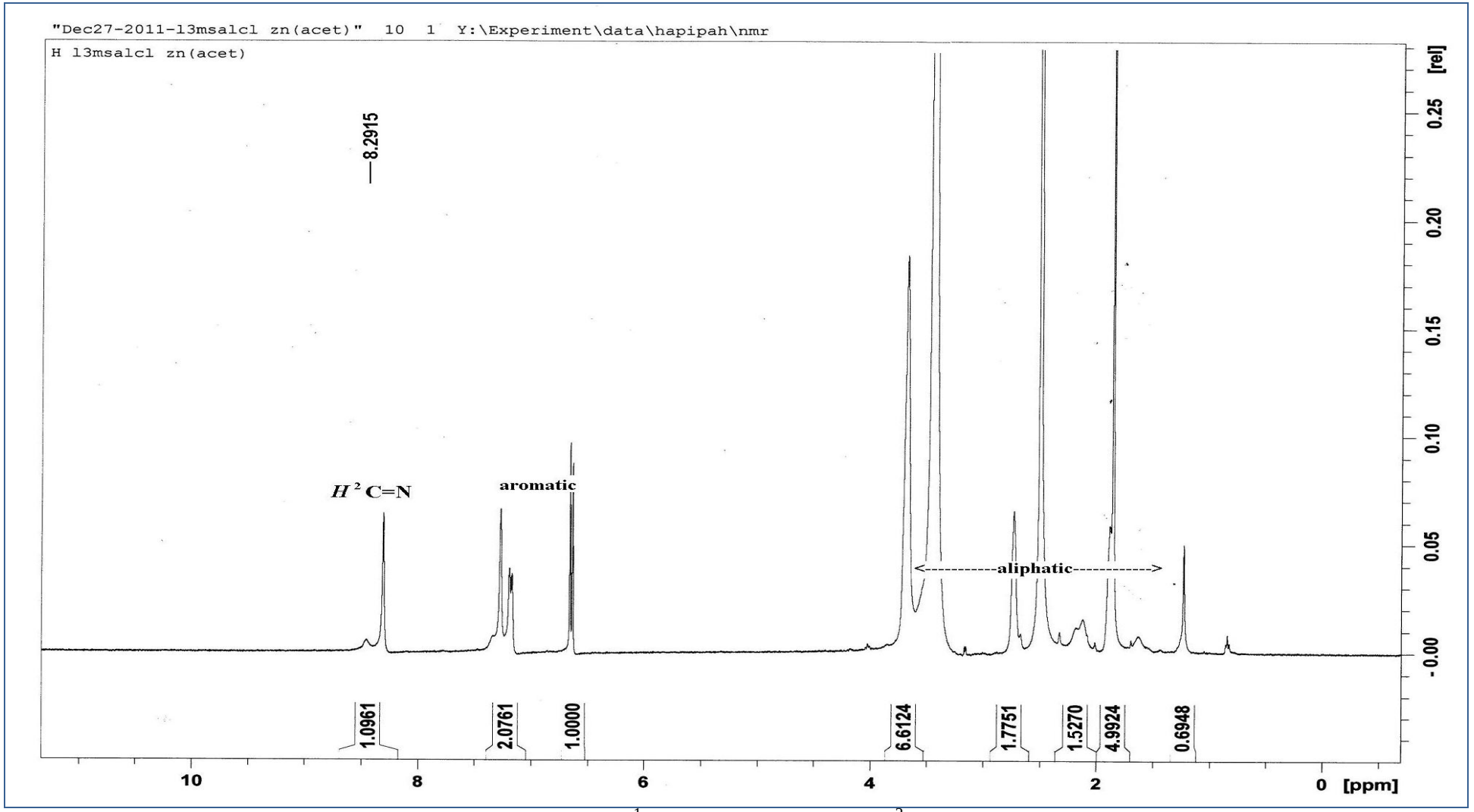

Appendix B.5: ^{1}H-NMR spectra for [Zn(L^{2})(OAc)].

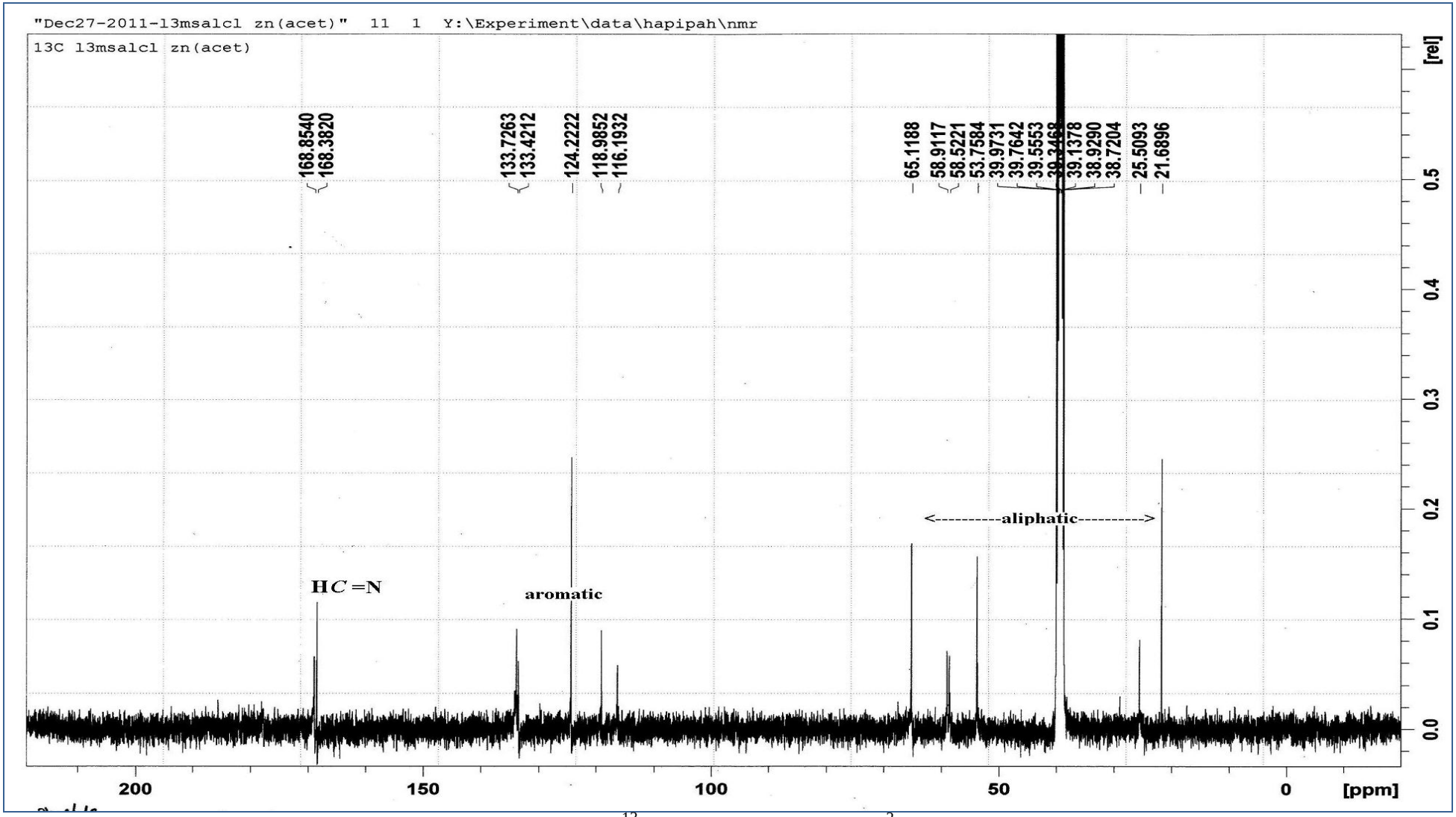

Appendix B.6: ^{13}C-NMR spectra for [Zn(L^2)(OAc)].

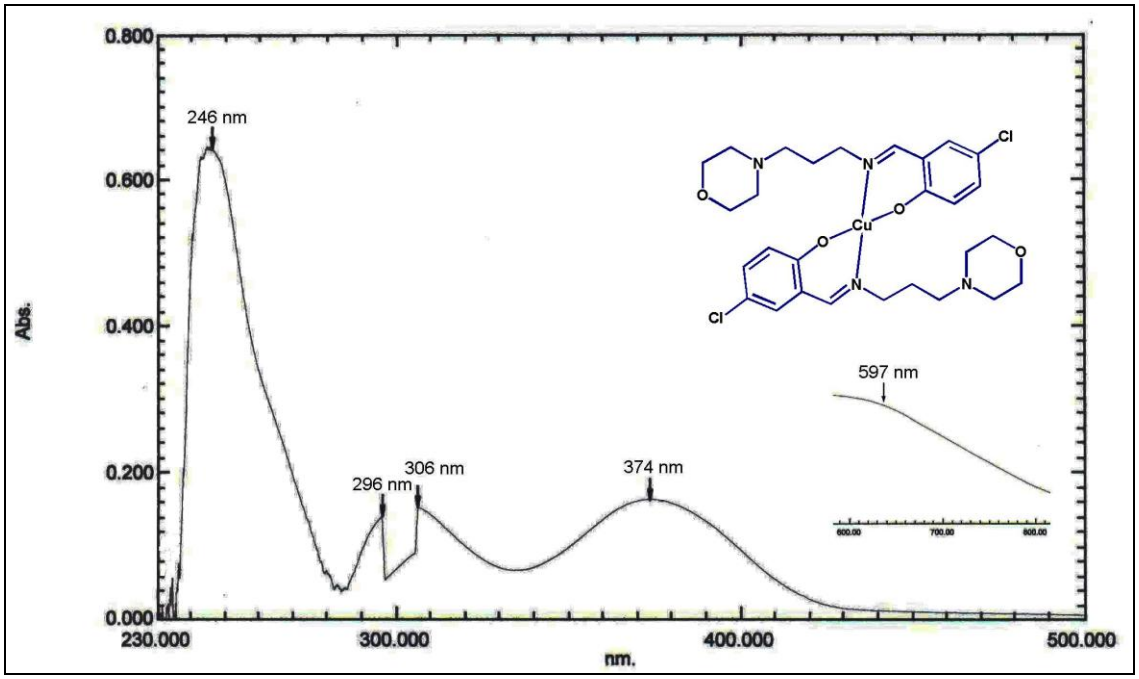

Appendix B.7: UV-Vis spectra for $[Cu(L^2)_2]$.

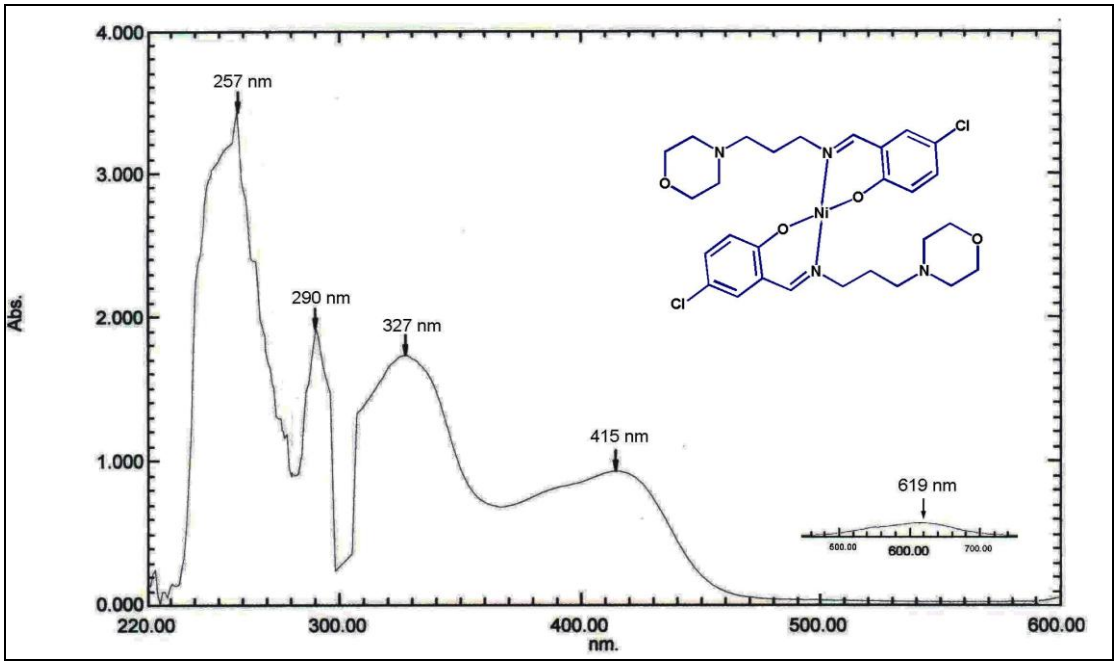

Appendix B.8: UV-Vis spectra for $[Ni(L^2)_2]$.

LIST OF PUBLICATION

1) .A. Ikmal Hisham, H. Khaledi , H.M. Ali, and H.A. Hadi. Coordination modes of two flexidentate salicylaldimine ligands derived from N-(3 aminopropyl)morpholine toward zinc and copper . *J. Coord. Chem*. (2012). 65, 2992-3006.

2) . A. Ikmal Hisham, H. Khaledi and H. Mohd Ali. *Acta Cryst*. (2011). E67, m932.

3) . A. Ikmal Hisham, H. Khaledi and H. Mohd Ali. *Acta Cryst*. (2011). E67, m1044-m1045.

4) . A. Ikmal Hisham, N. Suleiman Gwaram, H. Khaledi and H. Mohd Ali. *Acta Cryst*. (2011). E67, m229.

5) . A. Ikmal Hisham, N. Suleiman Gwaram, H. Khaledi and H. Mohd Ali. *Acta Cryst.* (2011). E67, m57.

6) . A. Ikmal Hisham, N. Suleiman Gwaram, H. Khaledi and H. Mohd Ali. *Acta Cryst.* (2011). E67, m41.

7) . A. Ikmal Hisham, N. Suleiman Gwaram, H. Khaledi and H. Mohd Ali. *Acta Cryst.* (2011). E67, m55.

8) . Suleiman Gwaram, N. A. Ikmal Hisham, H. Khaledi and H. Mohd Ali. *Acta Cryst.* (2011). E67, m205.

9) . Suleiman Gwaram, N. A. Ikmal Hisham, H. Khaledi and H. Mohd Ali. *Acta Cryst*. (2011). E67, m251.

10) . Suleiman Gwaram, N. A. Ikmal Hisham, H. Khaledi and H. Mohd Ali. *Acta Cryst.* (2011). E67, m131.

11)

. Suleiman Gwaram, N. A. Ikmal Hisham, H. Khaledi and H. Mohd Ali. *Acta Cryst*. (2011). E67, m58.

12)

. Suleiman Gwaram, N. A. Ikmal Hisham, H. Khaledi and H. Mohd Ali. *Acta Cryst.* (2011). E67, m108.

13)

. Ikmal Hisham, N. Suleiman Gwaram, H. Khaledi and H. Mohd Ali. *Acta Cryst.* (2010). E66, m1471.